



Abstract Volume

10th Swiss Geoscience Meeting

Bern, 16th – 17th November 2012

2. Structural Geology, Tectonics and Geodynamics

sc | nat 

Swiss Academy of Sciences
Akademie der Naturwissenschaften
Accademia di scienze naturali
Académie des sciences naturelles

u^b

^b
**UNIVERSITÄT
BERN**

2. Structural Geology, Tectonics and Geodynamics

Neil Mancktelow, Guido Schreurs, Paul Tackley

Swiss Tectonics Studies Group of the Swiss Geological Society

TALKS:

- 2.1 Bauville, A., Schmalholz, S.: Thermo-mechanical model for the finite strain distribution in kilometer-scale shear zones
- 2.2 Beltrán-Triviño, A., Einkler, W., Bussien, D., von Quadt, A.: Early Mesozoic rift-related sandstones of the Southern Alpine Tethys margin characterised by detrital zircons: U-Pb dating and Hf-isotopes analysis
- 2.3 Ben Slama, M., Ghanmi, M., Ben Youssef, M., Zargouni, F.: Early Cretaceous Triassic salt extrusion rates at Jebel Ech Cheid (N. Tunisia, southern Tethyan passive margin)
- 2.4 Cardello, G.L., Mancktelow, N.S.: Oblique normal faulting in carbonates at different crustal levels: examples from the SW Helvetics and Central Apennines
- 2.5 Fischer, R.: Self-consistent modelling of planetary differentiation and onset of mantle convection on Mars. A comparative study in 2D and 3D
- 2.6 Frehner, M., Reif, D., Grasemann, B.: Mechanical versus kinematical shortening reconstructions of the Zagros High Folded Zone (Kurdistan Region of Iraq)
- 2.7 Gerya, T.: Tectono-magmatic crustal convection produces novae and coronae on Venus
- 2.8 Gonzalez, L., Pfiffner, O.A.: Structure and evolution of the Central Andes of Peru
- 2.9 Heuberger, S., Naef, H.: The St.Gallen Fault Zone (NE Switzerland): A long-lived, multiphase structure in the North Alpine Foreland - Insights from high-resolution 3D seismic data
- 2.10 Madritsch, H., Birkhäuser, P., Heuberger, S., Malz, A., Meier, B., Schnellmann, M.: Thin- vs. Thick-skinned tectonics in the Alpine foreland of central northern Switzerland: New perspectives based on reprocessed and new reflection seismic data
- 2.11 Robyr, M., Banerjee, S., El Korh, A.: New time-constraints on the prograde metamorphism in the High Himalaya of NW Lahul (NW India)
- 2.12 Ruh, J., Gerya, T., Burg, J.-P.: Towards 4D modeling of transpressional fold-and-thrust belts
- 2.13 Sala, P., Pfiffner, O.A., Frehner, M.: Alpine fold and thrust structures: a 3-D model of the Säntis area (Switzerland)
- 2.14 Scheiber, T., Pfiffner, O.A., Schreurs, G.: The nature of the “Frilihorn nappe” (Valais, Switzerland)
- 2.15 Schmid, S.M., Scharf, A., Handy, M.R., Rosenberg, C.L.: The Tauern Window (Eastern Alps, Austria) – A new tectonic map, cross-sections and tectonometamorphic synthesis
- 2.16 Ueda, K., Willett, S., Gerya, T.: Coupling of landscape evolution and rheologically layered thermomechanical models in three dimensions
- 2.17 Villiger, A., Geiger, A., Marti, U., Brockmann, E., Schlatter, A.: Swiss 4D: Determination of strain rates from GNSS campaign and levelling data
- 2.18 Wehrens, P., Baumberger, R., Herwegh, M.: Deformational evolution of the Aar Massif (Central Alps): From macro- to micro-scale
- 2.19 Zhu, G., Gerya, T., Tackley, P., Kissling, E.: 4-D Numerical Modeling of Crustal Growth at Active Continental Margins

POSTERS:

- P 2.1 Thielmann, M., Rozel, A., Kaus, B.J.P., Ricard, Y.: Dynamic recrystallization and shear heating in numerical models of lithospheric-scale shear zones
- P 2.2 Rolf, T., Coltice, N., Tackley, P.J.: Dynamic origin of Wilson cycles in mantle convection with self-consistent plate tectonics and continental drift
- P 2.3 Liao, J., Gerya, T.: 3D numerical modeling of continental extension to oceanic spreading
- P 2.4 Crameri, F., Tackley, P., Meilick, I., Gerya, T., Kaus, B.: Implications of single-sided subduction in global self-consistent models of mantle convection
- P 2.5 Ueda, K., Gerya, T.: Exhumation of HP to UHP-HT rocks during delamination in orogenic settings - distribution of P-T paths from numerical modelling
- P 2.6 Golabek, G., Gerya, T., Morishima, R., Tackley, P., Labrosse, S.: Towards combined modelling of planetary accretion and differentiation
- P 2.7 May, D.: A 3D Marker-In-Cell Finite Element based Discretisation for Lithospheric Scale Geodynamics: Theory and Applications
- P 2.8 von Tscharner, M., Schmalholz, S.: 3D FEM modeling of fold nappe formation in the Western Swiss Alps
- P 2.9 Frehner, M., Exner, U.: Do foliation refraction patterns around buckle folds represent finite strain?
- P 2.10 Collignon, M., Kaus, B., Frehner, M., Fernandez, N., Castellort, S., Simpson, G., Burg, J.-P.: Modeling interactions between tectonic and surface processes in the Zagros Mountain, Iran
- P 2.11 Bahiraie, S., Abbasi, M.: Kinematic Investigation of the Central Alborz Mountain belt
- P 2.12 Bagheri, S., Damani, G.S., Jafari, S.: Cenozoic deformation of Mount Birk: A key to restoring of Iranian Baluchestan tectonic history
- P 2.13 Mohammadi, A., Winkler, W., Burg, J.-P.: Sandstone detrital mode and heavy mineral study in the Makran accretionary wedge, southeast Iran: implication for the tectonic setting
- P 2.14 Heredia, B.D., Hilgen, F., Gaylor, J.R., Kuiper, K., Mezger, K.: The Cretaceous-Palaeogene (K/Pg) boundary: cyclostratigraphic and U-Pb zircon geochronological constraints
- P 2.15 Peybernes, C., Martini, R., Chablais, J.: The breccias of Sambosan Accretionary Complex (southwestern Japan): tectonic vs depositional origin
- P 2.16 Abdelfettah, Y., Mauri, G., Kuhn, P., Schill, E., Vuataz, F.-D.: Investigation of deep geological structures in the north-west part of Canton of Neuchatel using a combination of gravity and 3D geological model
- P 2.17 Arndt, D., Jordan, P., Madritsch, H.: The Born Engelberg Anticline (Eastern Jura Mountains): New insights from balanced cross sections and 3D modelling
- P 2.18 Malz, A., Madritsch, H., Meier, B., Heuberger, S., Navabpour, P., Kley, J.: To what extent have inherited normal faults influenced thrust propagation at the front of the easternmost Jura fold-and-thrust belt?
- P 2.19 Mauri, G., Negro, F., Abdelfettah, Y., Schill, E., Vuataz, F.-D.: Deep geothermal exploration of low enthalpy reservoir in the Neuchâtel Jura (GeoNE project) – Use of gravity survey to validate and improve 3D geological models.

- P 2.20 Negro, F., Mauri, G., Vuataz, F.-D., Schill, E.: Exploration of deep low enthalpy geothermal reservoirs in the Neuchâtel Jura (GeoNE project) – 3D geological and thermal modeling of potential aquifers.
- P 2.21 Giroud, N., Vuataz, F.-D., Schill, E.: Permeable Fault Detection in Deep Geothermal Aquifer Exploration by Soil Gas Measurement
- P 2.22 Abedgno, M., Vouillamoz, N., Deichmann, N., Husen, S., Wust-Bloch, H.G., Mosar, J.: Cross-correlation and location error assessment of nano-earthquakes on the Fribourg Lineament - Switzerland
- P 2.23 Peters, M., Weber, C.: The application of titanium-in-quartz geothermometry in recrystallized quartz - a methodological discussion
- P 2.24 Poilvet, J.-C., Goncalves, P., Oliot, E., Marquer, D.: Role of brittle deformation and fluid-rock interaction on the formation of ductile shear zone under blueschist facies conditions
- P 2.25 Moulas, E., Podladchikov, Y., Vrijmoed, J., Tajcmanova, L., Simon, N., Burg, J.-P.: Transient Temperature and Pressure variations in crustal shear zones – numerical modelling using local-thermodynamic equilibrium and a conservative approach
- P 2.26 Moulas, E., Burg, J.-P., Kostopoulos, D., Schenker, F.: Chemical zoning and ductility of natural garnet at lower crustal conditions: An example from the Rhodope Massif
- P 2.27 Antić, M., Kounov, A., Trivić, B., Peytcheva, I., von Quadt, A., Gerdjikov, I.: Fission-track constraints on the thermal evolution of the Serbo-Macedonian Massif (south Serbia, southwest Bulgaria and east Macedonia)
- P 2.28 Schenker, F.L., Forster, M., Burg, J.-P.: The Eastern Pelagonian metamorphic core complex: insight from the $^{40}\text{Ar}/^{39}\text{Ar}$ dating of white micas
- P 2.29 Ladeb, M.F., Zargouni, F.: Inversion tectonique d'une zone de relais extensive adjacente à un diapir salifère: terminaison orientale du J. Chambi (Atlas central tunisien).
- P 2.30 Egli, D., Mancktelow, N., Spikings, R.: $^{40}\text{Ar}/^{39}\text{Ar}$ dating of Alpine shear zones in the Mont Blanc area
- P 2.31 Pleuger, J., Mancktelow, N., Spikings, R.: Structural and $^{40}\text{Ar}/^{39}\text{Ar}$ geochronological data from different mylonite belts along the Canavese Fault
- P 2.32 Cavargna-Sani, M., Epard, J.-L., Bussy, F., Ulianov, A.: Basement lithostratigraphy of the Adula nappe: implications for alpine kinematics
- P 2.33 Ziegler, M., Loew, S., Moore, J.R.: Distribution and inferred ages of exfoliation joints in the Aar Granite (Central Alps, Switzerland)
- P 2.34 Almqvist, B.S.G., Misra, S.: Seismic properties and anisotropy in melt-generating metapelites
- P 2.35 Hetényi, G., Kissling, E., Husen, S., Clinton, J. and the AlpArray Working Group: AlpArray – the next generation seismology initiative
- P 2.36 Houlié, N.: Deformation of flat areas by using InSAR. Application to the Geneva (CH) and la Faute-sur-mer (FR) areas

2.1

Thermo-mechanical model for the finite strain distribution in kilometer-scale shear zones

Arthur Bauville¹, Stefan Schmalholz¹¹ Institute of Geology and Paleontology, University of Lausanne, Switzerland

We present a one-dimensional shear zone model which considers a power-law flow law and a temperature dependent viscosity. The analytical solution for the velocity profile across the shear zone depends on the single dimensionless parameter β . β depends on the activation energy of the applied flow law, the temperature at the base of the shear zone and the temperature difference across it. We then derive the analytical solution of the ellipticity of strain ellipses along the shear zone. We perform a systematic parameter search over 1) the rheological parameter β , 2) the mean finite strain γ_m of the shear zone and 3) the shear zone thickness. We thus determine the parameters that provide the best fit between sets of strain ellipses measured in natural kilometer scale shear zones and our model (Figure 1). The estimates of β from the fitting are consistent with the ones based on temperature estimates from field data and laboratory derived activation energies of crustal rocks. Our simple 1D analytical solution can predict the nonlinear distribution of finite strain across natural kilometer-scale shear zones as a function of temperature and rheological parameters. Our results for several kilometer-scale shear zones worldwide suggest that temperature increase across shear zones controls to first order the observed nonlinear increase of finite strain towards the base of the shear zone. In the lowermost tens of meters natural shear zones often exhibit a stronger increase of finite strain (often expressed by mylonitic texture) than predicted by our simple model. This deviation from our model is likely caused by processes not considered in the model, such as for example, grain-size reduction, effects of fluids or viscous shear heating.

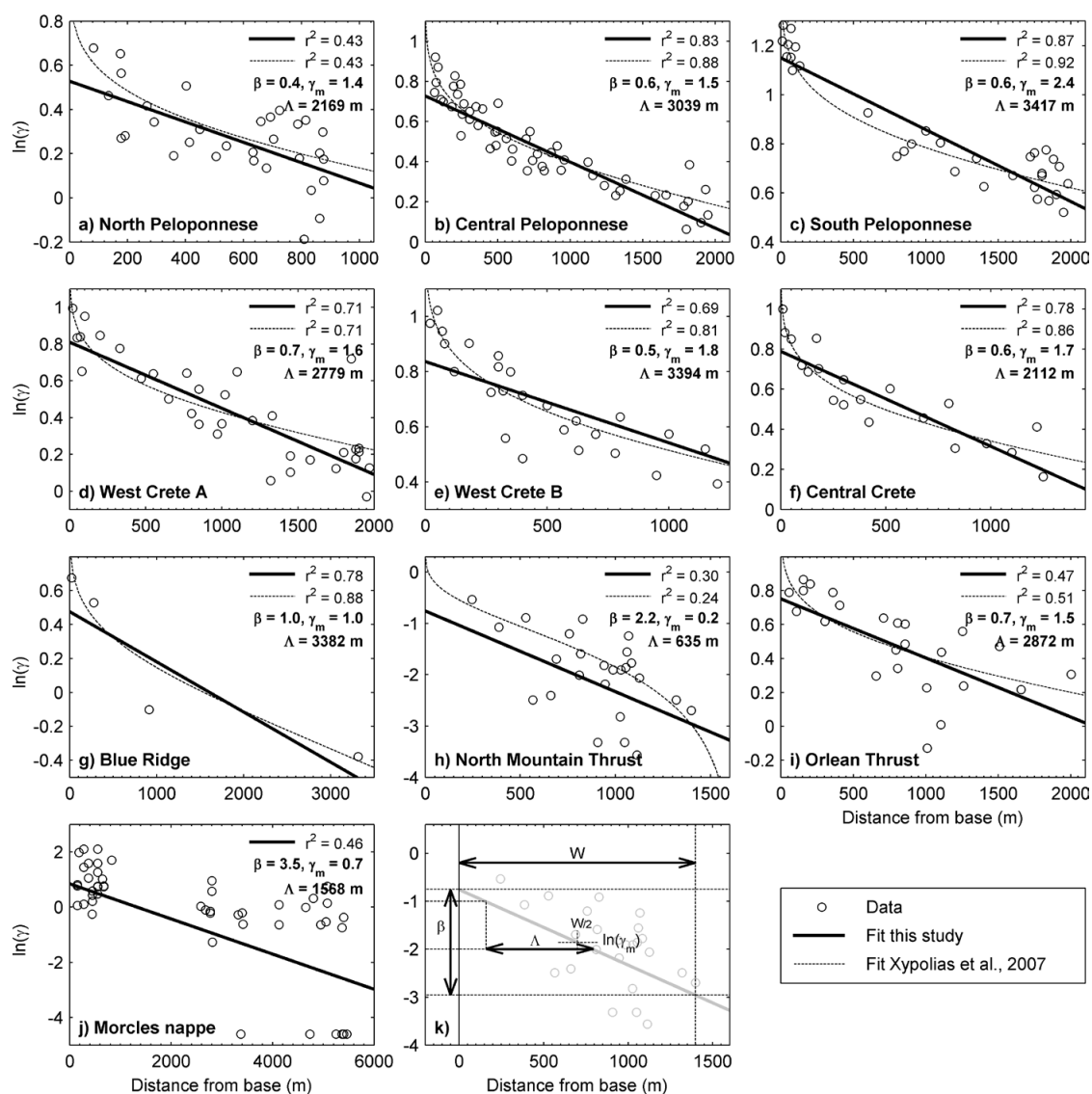


Figure 1. Model results showing the influence of the parameter β on a) velocity, b) strain rate and c) ellipticity profiles across the shear zone. The influence of the mean finite strain γ_m on the finite deformation is illustrated in d). Strain ellipses have been calculated by deforming small initial circles, which have been scaled up, with the analytical velocity profile.

REFERENCES

Xypolias, P., Chatzaras, V., and Koukouvelas, I. K., 2007, Strain gradients in zones of ductile thrusting: Insights from the External Hellenides: *Journal of Structural Geology*, v. 29, p. 1522-1537.

2.2

Early Mesozoic rift-related sandstones of the Southern Alpine Tethys margin characterised by detrital zircons: U-Pb dating and Hf-isotopes analysis

Alejandro Beltrán-Triviño¹, Wilfried Winkler¹, Denise Bussien¹ & Albrecht von Quadt²

¹ *Geologisches Institut, ETH Zentrum, Sonneggstrasse 5, CH-8092 Zürich (alejandro.beltran@erdw.ethz.ch)*

² *Institut für Geochemie und Petrologie, ETH Zentrum, Clausiusstrasse 25, CH-8092 Zürich*

Detrital zircons from Triassic and Jurassic rift-related sandstones from the southern margin of the Alpine Tethys (SMAT) were analysed in order to characterise the age of the sources and the origin of the magmas in which the zircons have crystallised. We present results from: (1) The Fuorn Formation in the Upper Austroalpine Silvretta nappe, which represents tidally influenced shallow marine deposits of Early Triassic age (e.g. Furrer et al., 2008). (2) The Middle Jurassic Saluver Fm, which is situated in the Lower Austroalpine Err nappe and represents an example of turbiditic sandstones and breccias deposited during protracted rifting along the SMAT (Finger et al., 1982). (3) Two volcanoclastic layers within the Middle Triassic (Ladinian) carbonates of the Upper Austroalpine Silvretta nappe; the lower layer is interbedded in the Prosanto Fm (called Ducan-I) and the upper one is interbedded in the Altein Fm (Ducan-II) (Furrer et al., 2008). (4) The Carnian Val Sabbia sandstone located in the South Alpine domain, which is considered a continental terrigenous-volcanoclastic sequences with palaeocurrents from the south (Crisci et al., 1984).

The U-Pb zircon ages of the Fuorn Fm show a population spanning from 310 to 260 Ma with a peak at ca 292 Ma. Thus, the Fuorn Fm was mainly sourced in Permian igneous rocks and volcanoclastics, which obviously were exhumed and eroded at the SMAT during the Triassic. Schaltegger and Brack (2007) suggest that Permian magmatism and associated basin formation occurred during major post-Variscan extensional and strike-slip movements between ca 285 - 275 Ma, which is in line with our results. The calculated epsilon-Hf values of the Permian detrital zircons between +5 to -5 indicate contamination of mantle magmas with crustal material and depict probably two different sources of similar age.

U-Pb ages of detrital zircons from Saluver Fm have a dominant population from ca 320 to 250 Ma with a peak at ca 300 Ma and other minor populations from 460 - 420 Ma and from 1 - 0.95 Ga. The calculated epsilon-Hf values of the eroded Variscan and late-Variscan (Permian and Carboniferous) zircons lie between -3 to +7, indicating contamination of the magma source with crustal material. The present Saluver Fm sandstone was mainly sourced in Variscan and post-Variscan magmatic and volcanoclastic rocks, whereas no Triassic magmatic rocks were exposed in the source areas.

Detrital zircons from the volcanoclastic layer Ducan-I show a U-Pb age spectrum spanning from 268 to 228 Ma with a peak at ca 252 Ma. The calculated epsilon-Hf values range between -1 to +8, indicating magmas with high contribution of juvenile mantle sources with slight contamination by crustal material. The U-Pb ages of detrital zircons from the second volcanoclastic layer Ducan-II shows a range from 264 to 238 Ma with a peak at ca 247 Ma. The calculated epsilon-Hf values range between -4 to +4, which point to contamination of mantle magmas by crustal material. The differences of the measured Hf - isotope ratios between these two volcanoclastic layers can be explained by two scenarios: (i) The two volcanoclastic layers were sourced by two different magma reservoirs; one more contaminated by crustal material sourced Ducan-II and the other one with more influence of juvenile material sourced Ducan-I. (ii) The evolution of a single source where the reservoir first was dominated by juvenile mantle material (Ducan-I) and subsequently more contaminated by crustal material (Ducan-II).

The U-Pb age population of detrital zircons from the Val Sabbia sandstone covers the time span from 257 to 220 Ma with a peak at ca 240 Ma. The younger age spectrum (240-220 Ma) correlates with other Ladinian and Carnian volcanic and volcanoclastic formations in the Austroalpine domain. The epsilon-Hf values (-6 to -3) suggest a mantle source highly mixed with crustal material.

There are contrasting models proposed to explain the Triassic Alpine magmatism, either within an extensional environment (e.g. Crisci et al., 1984) or in a subduction-related setting (e.g. Castellarin, 1988). The results from Triassic detrital zircons corroborate the model of Crisci et al. (1984). These authors suggest the origin of the magmas through partial melting of an upper mantle, which was deeply modified during the previous Variscan orogeny. The rising melts included crustal material during early stages of rifting along the SMAT.

REFERENCES

- Castellarin, A., Lucchini, F., Rossi, P. L. & Simboli, G. 1988: The Middle Triassic magmatic-tectonic arc development in the Southern Alps. *Tectonophysics*, 146, 79-89.
- Crisci, C. M., Ferrara, G., Mazzuoli, R. & Rossi, P. M. 1984: Geochemical and geochronological data on Triassic volcanism of the Southern Alps of Lombardy (Italy): Genetic implications. *Geologische Rundschau*, 73, 279-292.
- Finger, W., Mercolli, I., Kündig, R., Stäubli, A., de Capitani, Ch., Nievergelt, P., Peters, T. & Trommsdorff, V. 1982: Bericht über die gemeinsame Exkursion der Schweizerischen Geologischen Gesellschaft und der Schweizerischen Mineralogischen und Petrographischen Gesellschaft ins Oberengadin vom 21. bis 24. September 1981. *Eclogae Geol. Helv.*, 75, 199-222.
- Furrer, H., Schaltegger, U., Ovtcharova, M. & Meister, P. 2008: U-Pb zircon age of volcanoclastic layers in Middle Triassic platform carbonates of the Austroalpine Silvretta nappe (Switzerland). *Swiss J. Geosci.*, 101, 595–603.
- Schaltegger, U. & Brack, P. (2007) Crustal-scale magmatic systems during intracontinental strike-slip tectonics: U, Pb and Hf isotopic constraints from Permian magmatic rocks of the Southern Alps. *Int. J. Earth Sci.*, 96, 1131-1151.

The project is supported by the ETH Zurich internal grant no. 04 09-1.

2.3

Early Cretaceous Triassic salt extrusion rates at Jebel Ech Cheid (N. Tunisia, southern Tethyan passive margin)

Mohamed-Montassar BEN SLAMA¹, Mohamed GHANMI¹, Mohamed BEN YOUSSEF², Fouad ZARGOUNI¹

¹ *Unité de recherche Géologie structurale et Appliquée, Faculté des Sciences de Tunis, 2092 Tunis, Tunisie.*

² *Laboratoire Géoressources, Centre de recherches et Technologies des eaux, BP 273, 8020 Soliman, Tunisie.*

E-mail : mohamedmontassar.benslama@fst.rnu.tn

We apply the logic of (Talbot and Jarvis, 1984) to calculate the extrusion rates and likely heights reached by Triassic salt at Jebel Ech Cheid during Barremian-Aptian, Late Aptian, Late Cenomanian and middle Turonian times (Ben Slama, 2011; Ben Slama et al., 2012). The results allow us to reconstruct the movements of the Triassic salt during its Early Mesozoic history. The extrusion rate may have exceeded 55mm year⁻¹ and the salt fountain reached higher than 600 m in the Early Cretaceous sea if its vent was then narrower than its current maximum width.

REFERENCES

- Ben Slama, M.-M. (2011). "Mécanismes de mise en place du matériel salifère en Tunisie septentrionale : exemples du Jebel Ech Cheid et des structures voisines." Unpubl. PhD Thesis, Tunis Univ. Tunis., URL: <http://tel.archives-ouvertes.fr/tel-00626246/fr/>.
- Ben Slama, M.-M., Ghanmi, M., Ben Youssef, M., and Zargouni, F. (2012). Early Cretaceous extrusion rates and heights of Triassic salt at Jebel Ech Cheid (NE Moghrebian Atlas, Tunisia) (submitted manuscript). *Swiss j. geosci.*
- Talbot, C. J., and Jarvis, R., J. (1984). Age, budget and dynamics of an active salt extrusion in Iran. *Journal of structural geology* 6, 521-533.

2.4

Oblique normal faulting in carbonates at different crustal levels: examples from the SW Helvetics and Central Apennines

G. Luca Cardello¹ & Neil S. Mancktelow¹

¹Geological Institut, ETH-Zürich, Sonneggstrasse 5, CH-8092 Zürich (luca.cardello@erdw.ethz.ch)

For the same general boundary conditions, oblique normal faults can generate crustal earthquakes of larger magnitude than those generated on dip-slip normal faults of similar size (Ranalli, 1987). In order to provide constraints on the processes involved in fault slip accumulation on oblique normal faults, the current study describes the fault architecture in field exposure of such faults exhumed from different crustal levels. Fault length (12-20 km), accumulated displacement (1-2 km) and lithology (carbonate rich passive margin sequences) are comparable for the examples from the SW Helvetics and the Gran Sasso (Central Apennines). However faults from the SW Helvetics show an interplay between brittle and ductile structures whereas those from Gran Sasso were entirely brittle during seismic faulting. Most large crustal earthquakes are triggered on faults at the brittle-ductile transition, which in the continental crust commonly occurs in sedimentary rocks buried to depths of 8 to 13 km, depending on the geothermal gradient and the tectonic regime (in particular, whether faults are dominantly normal, thrust or strike-slip). In the SW Helvetics, oblique normal faults that developed during Neogene time under very low metamorphic grade and cross-cut the Alpine nappe-stack are currently exposed at the surface. Some of these faults were probably seismogenic when active at depth and represent exhumed “fossil” structures comparable to currently active faults in this active seismic area north of the Rhône Valley. The fossil fault structures developed at the brittle-ductile transition and experienced little significant late brittle overprint during exhumation. Locally, it is possible to establish a transition from mylonitic to cataclastic fabrics (e.g. on the Rezli fault), with a complex interplay of processes including pressure solution, veining, mineralization on fault planes and repeated brecciation. Generally, the fault architecture, as well as the vein distribution and composition, changes with the lithology, and therefore varies both along and across major faults. Where fault displacement is large and different formations are juxtaposed across a fault, the fault core and damage zones develop a complex architecture involving more important fluid circulation, veining and fluid-rock interaction, whereas faults with minor displacement (a few metres) are generally simpler and narrower, with veining concentrated close to the fault. This implies that the damage zone tends to broaden with increased displacement, rather than the fault increasingly localizing on a narrower zone. However, there are also many examples of fault localization on a late discrete surface. Veining and pressure solution are apparently always related to the initial stages of faulting. Mode 1 extensional veins, commonly developed in an en-echelon pattern, are locally dissolved by stylolites, which are themselves later crosscut by later veins and, finally, also by discrete fault planes. This implies multiple and interrelated processes of dissolution, crack opening, and mineralization during intermittent and repeated faulting. In the Gran Sasso, the outcropping faults were exhumed from depths of < 2 km and therefore provide information on the near-surface development. The fault-core is characterized by fault gouge and crusts of ultracataclasite preserved in the hanging wall of the main oblique normal WNW-ESE- and E-W-striking fault planes of Gran Sasso. Such faults displace Quaternary breccias and soils, showing recent activity. Ultracataclasite and very rare deformed veins infill cracks with an opening direction parallel to fault slip. Coarse grained porous cataclasites are cross-cut by Riedel planes defining book-shelf domino-type structures. This indicates fluidization of the fine grained cataclastic material and preferential slip on the main fault surface and gouge. The damage zone ranges from 5-10 m in the foot wall and up to 20 m in the hanging wall, whereas the fault-core is concentrated within a few metres of the fault plane. Repeated brecciation is also shown by reworking of cataclasites and the truncation of faulted breccias, suggesting a continuous rejuvenation of the fault plane and fault zone thickening. Between the fault-core and the damage zone, lenses of cataclasites are cross-cut by NW-striking normal faults which terminate on the cataclasites belonging to the main oblique slip planes. This geometry suggests that internal fragmentation of the fault structure was related to the regional stress orientation (i.e., SW-directed extension) whereas the main oblique faults remained preferential surfaces for reactivation and slip accumulation. The NW-striking normal faults can be interpreted as having formed in foreshock sequences of very low magnitude within the WNW-ESE striking fault zones, before the final activation of the main fault plane during the main shock. During the L'Aquila earthquake of 2009 (Mw = 6.3), purely normal faults were activated whereas contiguous oblique normal main faults in the Gran Sasso (e.g. Assergi and Campo Imperatore Faults) were not, despite their well established Quaternary activity. Considering that fault structures and boundary conditions of the Gran Sasso faults are similar to the ones involved during the L'Aquila earthquake, the termination of epicentres on NW-striking normal faults at the western tip of the Assergi Fault suggests that this fault could be seismically activated in the future. Generally, the fault damage zone is narrower in the SW Helvetics compared to the Apennines, implying that near the brittle-ductile transition there is less damage zone broadening with increasing displacement, possibly due to higher confining stress and pore pressure. In conclusion, fluid circulation, pressure-solution and veining are the most important processes that contribute to fault localization near the brittle-ductile transition. Closer to the surface, grain size reduction, fluidization and gouge formation become the most important factors promoting slip.

REFERENCES

Ranalli, G. 1987: Rheology of Earth. Allen and Unwin, Winchester, MA (1987), p. 248

2.5

Self-consistent modelling of planetary differentiation and onset of mantle convection on Mars. A comparative study in 2D and 3D

Fischer Ria¹

¹ *Institute of Geophysics, ETH Zürich, Sonneggstrasse 5, CH-8092 Zürich (fischeri@ethz.ch)*

The exact mechanism of core-mantle differentiation and the formation of the crustal dichotomy and the Tharsis rise on Mars, are still unresolved problems. I, therefore, investigate a hypothesis which numerically combines both exogenic and endogenic processes, where a giant impact event and subsequent vigorous mantle convection are building the southern highland crust. I focus on the effect, various initial factors have on core and crustal formation. Key factors of interest are the impactor core temperature, the initial planetary iron and silicate temperature, as well as the initial setup and the impactor size.

A hemispherical magma ocean can be observed at the impact site which spreads over the planet's surface and finally builds one large patch of thicker crust. In the special case of very hot iron diapirs or a hot protocore, an additional magma ocean at the depth of the core-mantle boundary develops. In the case of a very hot impactor and cool protocore, the impactor core will form a hot liquid outer core, surrounding a solid inner core and enable dynamo generation.

2.6

Mechanical versus kinematical shortening reconstructions of the Zagros High Folded Zone (Kurdistan Region of Iraq)

Marcel Frehner¹, Daniel Reif² and Bernhard Grasemann³

¹ *Geological Institute, ETH Zurich, Switzerland (marcel.frehner@erdw.ethz.ch)*

² *Institute for Earth Sciences, Karl-Franzens-University, Graz, Austria*

³ *Department for Geodynamics and Sedimentology, University of Vienna, Austria*

This work (Frehner et al., 2012) compares kinematical and mechanical techniques for the palinspastic reconstruction of folded cross sections in collision orogens. The studied area and the reconstructed NE–SW trending, 55.5 km long cross section is located in the High Folded Zone of the Zagros fold-and-thrust belt in the Kurdistan region of Iraq. The present-day geometry of the cross section has been constructed from field as well as remote sensing data (Figure 1a). In a first step, the structures and the stratigraphy are simplified and summarized in eight units trying to identify the main geometric and mechanical parameters. In a second step, the shortening is kinematically estimated using the dip domain method to 11%–15%. Then the same cross section is used in a numerical finite element model (Figure 1b) to perform dynamical unfolding simulations (Schmalholz, 2008; Lechmann et al., 2010) taking various rheological parameters into account.

The main factor allowing for an efficient dynamic unfolding is the presence of interfacial slip conditions between the mechanically strong units (Figure 2a). Other factors, such as Newtonian versus power law viscous rheology (Figure 2a) or the presence of a basement (Figure 2b), affect the numerical simulations much less strongly. If interfacial slip is accounted for, fold amplitudes are reduced efficiently during the dynamical unfolding simulations, while welded layer interfaces lead to unrealistic shortening estimates (Figure 2). It is suggested that interfacial slip and decoupling of the deformation along detachment horizons is an important mechanical parameter that controlled the folding processes in the Zagros High Folded Zone (Frehner et al., 2012). A similar conclusion has recently been found by Yamato et al. (2011) for the Iranian part of the Zagros fold-and-thrust belt using numerical forward modeling.

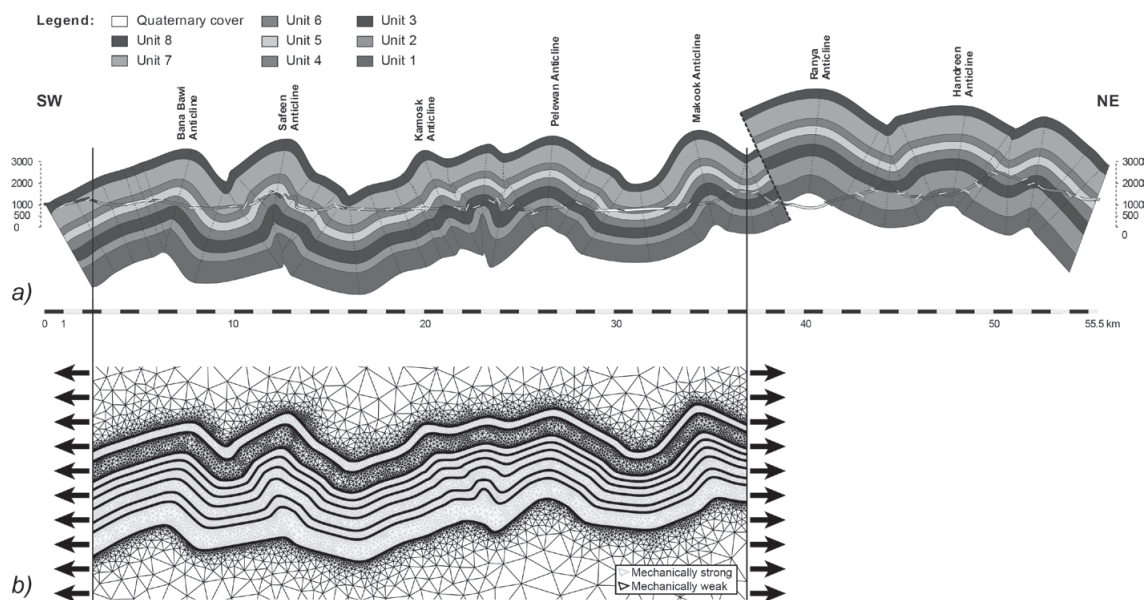


Figure 1. a) Geological cross-section through the Zagros Simply Folded Belt in NE Iraq constructed from field- and remote sensing data. b) Finite-element mesh of the SW part of the same cross-section used for numerical unfolding simulations.

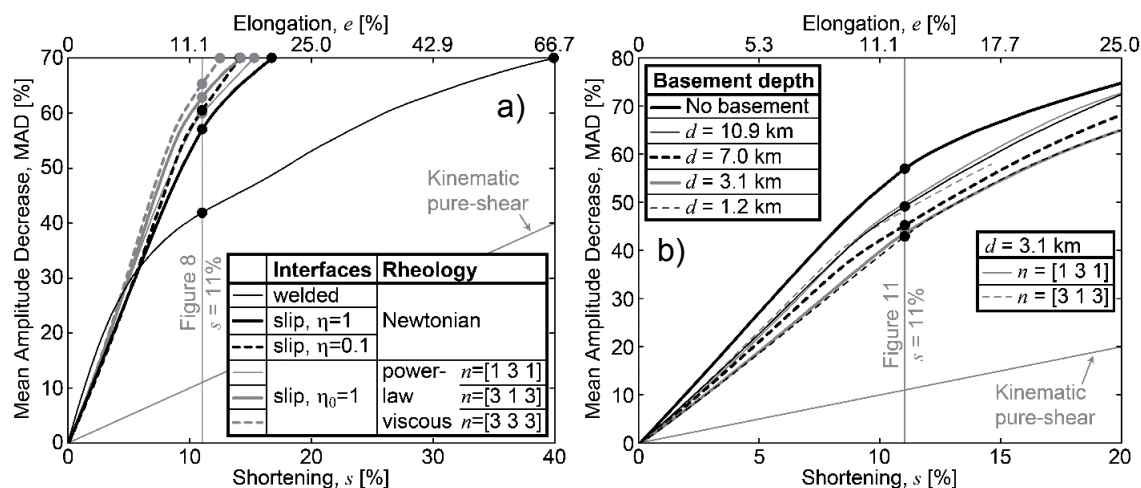


Figure 2. Mean amplitude decrease during the different progressive dynamical unfolding simulations without basement (a) and including a basement at depth d (b). The thick black line is the same in both subfigures. The legend in the top left corner in b) corresponds to simulations using a Newtonian rheology. The second legend corresponds to simulations using power law viscous rheologies. Kinematical pure shear is equivalent to a dynamical unfolding simulation with no mechanical difference between the layers ($MAD = s$).

REFERENCES

- Frehner, M., Reif, D. & Grasemann, B. 2012: Mechanical versus kinematical shortening reconstructions of the Zagros High Folded Zone (Kurdistan Region of Iraq). *Tectonics*, 31, TC3002.
- Lechmann, S. M., Schmalholz, S. M., Burg, J.-P. & Marques, F. O. 2010: Dynamic unfolding of multilayers: 2D numerical approach and application to turbidites in SW Portugal. *Tectonophysics*, 494, 64–74.
- Schmalholz, S. M. 2008: 3D numerical modeling of forward folding and reverse unfolding of a viscous single-layer: Implications for the formation of folds and fold patterns. *Tectonophysics*, 446, 31–41.
- Yamato, P., Kaus, B. J. P., Mouthereau, F. & Castelltort, S. 2011: Dynamic constraints on the crustal-scale rheology of the Zagros fold belt, Iran. *Geology*, 39, 815–818.

2.7

Tectono-magmatic crustal convection produces novae and coronae on Venus

Taras Gerya

Institute of Geophysics, Swiss Federal Institute of Technology (ETH-Zurich), Sonneggstrasse 5, 8092 Zurich, Switzerland.

Novae and coronae are characteristic surface features on Venus but their origin and relationship remain enigmatic. Several competing hypotheses were proposed for both coronae and novae based on variability of their sizes, shapes, internal structures and topography, yet little work has been done for quantitative testing of these hypotheses.

Here we demonstrate based on new high-resolution three-dimensional thermomechanical numerical model that formation of medium sized (50-300 km) novae and coronae can be explained by tectono-magmatic interaction of mantle plume with hot and thin lithosphere, which has thick low-viscosity lower-middle crust and thin brittle upper crust characterized by elevated surface temperature. According to this model, decompression melting of hot plume material produces large amount of magma, which intrude into the ductile lower crust, and triggers crustal melting and convection.

The crustal convection cell exists for up to several tens of millions years where plume magma and partially molten lower-middle crustal rocks interact and mechanically mix causing gradual thinning of the brittle upper crustal lid. The long time span of the convection cell is maintained by the plume heat, which causes gradual warming and melting of crustal rocks. Novae forms at the initial stage of the process by radial fracturing of the uplifted region above the convection cell center.

At the later stage, such novae can be converted into coronae by concentric fracturing of thinned upper crustal lid and subsequent overthrusting of partially molten lower-middle crustal rocks over the surface of the down-bending brittle upper crust. Concentric normal faults form in the extensional outer rise region of the bending crust. In contrast, concentric thrust faults form in the advancing front of the advancing overriding crustal wedge. Deep trench-like depression forms in between these two contrasting tectonic regions.

The process resembles subduction with important difference been that no slab is formed and subducted cold upper-crustal lid warms up rapidly and recycles into the convection cell. Model further suggests that coronae and novae fracture pattern and topography evolve with time with different stages been corresponding to various types of these patterns observed on Venus.

2.8

Structure and evolution of the Central Andes of Peru

Gonzalez Laura¹, Pfiffner O. Adrian¹

¹Institut für Geologie, Universität Bern, Baltzerstr. 1+3, CH-43012 Bern (Adrian.pfiffner@geo.unibe.ch)

Based on fieldwork the structural style and the kinematic evolution of the Peruvian Andes are analyzed. A quantitative estimate of the shortening of the orogeny was obtained from the construction of two transects that run from the Pacific coast to the undeformed Amazon foreland. The Coastal Belt consists of a Late Jurassic – Early Cretaceous volcanic arc sequence that was accreted to the South American craton. The volcanoclastic deposits are characterized by relatively open folds which were intruded by the Coastal Batholith in Late Cretaceous times. The Mesozoic strata of the adjacent Western Cordillera represent an ENE-verging fold-and-thrust belt.

Tight symmetrical folds developed above a detachment horizon. In contrast, steeply dipping reverse faults and open folds are observed in the Neoproterozoic crystalline basement and the Paleozoic sediments of the Eastern Cordillera. The reverse faults are in part of transpressive nature and uplifted large blocks of basement rocks.

The Central Highlands between the two cordilleras forms a transition zone. Here, late Paleozoic and, restricted to the western part, Mesozoic strata display open folds. In the Subandean Zone, Paleozoic and Cenozoic strata are affected by mainly NE-verging imbricate thrusting. Total shortening of the two transects is 120 – 150 km (24 –27%), most of which is taken up by the Western and Eastern Cordilleras.

Three major deformation phases can be recognized in the study area. The earliest, the Mochica Phase corresponds to the open folding of the Coastal Belt and is sealed by the Coastal Batholith. The tight folding and thrusting in the Western Cordillera and the neighboring Central Highlands and Eastern Cordillera is attributed to the Inca Phase. This phase is sealed by the unconformity at the base of the Paleogene volcanics. The last phase, called Quechua Phase, can be subdivided into several episodes and accounts for the imbricate thrusting in the Subandean zone involving Neogene and even Pliocene sediments. The Central Highlands were uplifted as a block in the process. Post-Eocene thrusting in the Western Cordillera uplifted this mountain range relative to the Central Highlands. The most recent episode can be correlated with unconsolidated Pleistocene sediments that are folded in the Central Highlands and cut by a steep reverse fault bordering the Cordillera Blanca.

Highlights:

- Two balanced sections yield a total shortening of 120 – 150 km across the Andes of Peru.
- The structural style is governed by NE-verging thrusts and various detachment horizons.
- Neogene deformation was responsible for the uplift of the entire orogen.
- A late fault system raised the Western Cordillera relative to the Central Highlands.

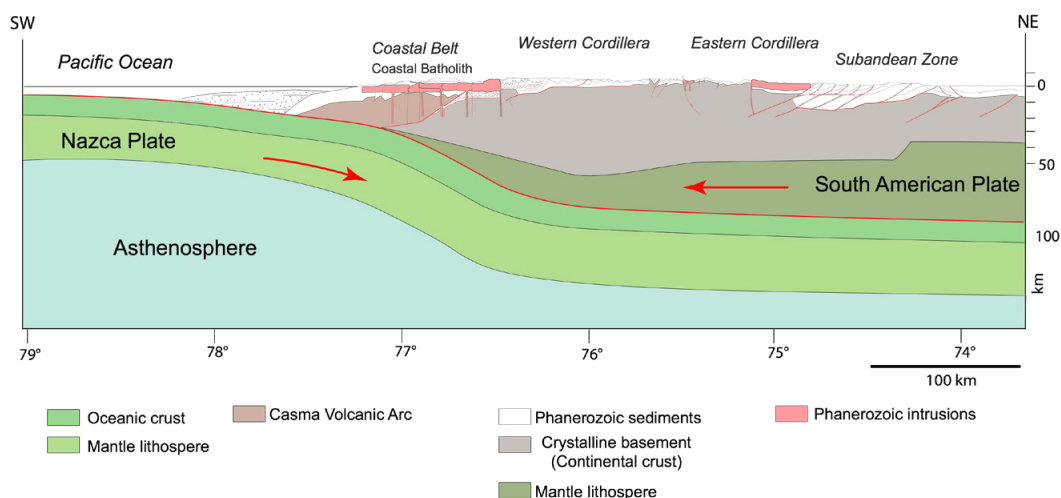


Figure 1. Cross-section showing the geometry of the subduction zone and the general structure of the Central Andes of Peru.

2.9

The St.Gallen Fault Zone (NE Switzerland): A long-lived, multiphase structure in the North Alpine Foreland - Insights from high-resolution 3D seismic data

Heuberger Stefan¹ & Naef Henry¹

¹ *geosfer ag, Glockengasse 4, CH-9000 St.Gallen (stefan.heuberger@geosfer.ch)*

Surface geology and reflection seismic data in NE Switzerland show that the Mesozoic and Cenozoic formations of the North Alpine Foreland are widely lacking large extensional faults (Nagra 2008). The only existing large structures are represented by either the NW-SE striking normal faults of the Freiburg-Bonndorf-Hegau-Bodensee half graben or by the WSW-ENE striking Baden-Irchel-Herdern lineament. Furthermore, there is a NNE-SSW striking fault zone, cross-cutting almost the entire Molasse Basin between the Bodensee and the city of St.Gallen (Nagra 2008; Sommaruga 2011). This zone, termed here St.Gallen Fault Zone (SFZ), is more than 30 km long and consists of normal faults interpreted from 2D seismic data. It offsets the complete Mesozoic sedimentary cover by several decametres up to approximately 200 m. Offsets of the Tertiary Molasse units are known from a few seismic sections in the northernmost part of the SFZ near the Bodensee. There, the uppermost Tertiary unit, the Upper Freshwater Molasse (OSM) seems to be faulted up to the Base Quaternary. However, the SFZs topmost (Tertiary to Quaternary) extent is vastly unknown as faults are difficult to seismically identify due to the laterally very variable Molasse lithologies and because the fault's potential surface expression is obliterated by young glacial landforms.

To precisely locate the individual faults of the SFZ and the target aquifers (Upper Malm, Upper Muschelkalk) for the St.Gallen Geothermal Power Plant Project, a 270 km² 3D seismic survey was performed in 2010. Here we present first results of the stratigraphic and structural interpretation of this new 3D seismic data set. The SFZ is defined by an up to 1 km wide zone mainly comprising 70-80° ESE-dipping normal faults and local reverse faults. The northern part strikes N-S to NNE-SSW and delimits a Late Paleozoic to Tertiary graben to its east. The eastern edge of this graben is represented by the Roggwil Fault Zone (RFZ) consisting of NW-dipping normal faults. The southern part of the SFZ strikes NNE-SSW and exhibits significantly less faults throw. Here, the SFZ rather represents a flexure zone with only small segments of normal faults offsetting mainly the lower Mesozoic units.

Seismic stratigraphy analyses indicate at least three synsedimentary normal faulting events during the Mesozoic. Furthermore, faulted OSM marker horizons indicate continued normal faulting until at least the mid-Miocene. Additionally, the SFZ and the RFZ seem to root in extensional pre-Mesozoic basement structures that may border comparatively small Permo-Carboniferous troughs. Although a detailed seismic stratigraphy analysis on the Mesozoic and Permo-Carboniferous has not yet been performed we are able to postulate a multiphase tectonic activity along the SFZ.

Geological mapping along the Sitter valley in the area of Bernhardzell revealed indications of normal faults in the OSM (e.g. Hofmann 1951) that might be genetically linked to the faults of the SFZ. Schrader (1988) analysed deformed pebbles in conglomeratic Molasse (mainly OSM) units in the North Alpine Foreland Basin. He postulated for the St.Gallen-Bodensee region that this post-OSM deformation must have taken place in a strike-slip to normal faulting regime with compression in NNW-SSE direction and extension in WSW-ENE direction. The same principal stress directions were derived from fault plane solutions of recent seismic events in NE Switzerland (Kastrup et al. 2004). Thus, the overall stress field does not seem to have changed significantly since the Late Miocene. With this stress field it is obvious that the faults of the SFZ are ideally oriented (at an angle of about 30°) to have been reactivated in a transtensional mode. From a geothermal exploration point of view, this is an important finding indicating that these faults might exhibit an increased permeability.

REFERENCES

- Hofmann, F. 1951: Zur Stratigraphie und Tektonik des st.gallisch-thurgauischen Miozäns (Obere Süswassermolasse) und zur Bodenseegeologie, St.Gallische Naturwissenschaftliche Gesellschaft, 74, pp. 88.
- Kastrup, U., Zoback, M. L., Deichmann, N., Evans, K. F., Giardini, D. & Michael, A. J. 2004: Stress field variations in the Swiss Alps and the northern Alpine foreland derived from inversion of fault plane solutions, *Journal of Geophysical Research*, 109, B01402.
- Nagra 2008: Vorschlag geologischer Standortgebiete für das SMA- und das HAA-Lager - Geologische Grundlagen. Nagra Technical Report NTB 08-04.
- Schrader, F. 1988: Symmetry of pebble-deformation involving solution pits and slip-lineations in the northern Alpine Molasse Basin, *Journal of Structural Geology*, 10, 41-52.
- Sommaruga, A. 2011: From the central Jura Mountains to the Molasse Basin (France and Switzerland), *Swiss Bulletin for Applied Geology*, 16, 63-75.

2.10

Thin- vs. Thick-skinned tectonics in the Alpine foreland of central northern Switzerland: New perspectives based on reprocessed and new reflection seismic data

Madritsch, Herfried¹, Birkhäuser Philip¹, Heuberger Stefan², Malz Alexander³, Meier Beat⁴, Schnellmann Michael¹

¹ Nagra, Hardstrasse 73, 5430, CH 5430, Wettingen (herfried.madritsch@nagra.ch)

² geosfer-ag, Büro für angewandte Geologie, Glockengasse 4. CH-9000 St.Gallen

³ Friedrich Schiller Universität Jena Institut für Geowissenschaften, Burgweg 11, D-07749 Jena

⁴ Interoil Exploration & Production Switzerland AG Seefeldstrasse 287 8008 Zürich

The question whether the Late Miocene propagation of the Central Alpine deformation front far into the northern foreland of the collision zone was thin-skinned, thick-skinned or something in between (compare Pfiffner, 2006) is the matter of a long lasting scientific debate. It is considered of fundamental importance for a better understanding of the late stage and future evolution of the Alpine orogen (Rosenberg and Berger 2009) and for seismic hazard assessment in the Northern Alpine Foreland (e.g. Schmid & Slejko, 2009).

One of the key investigation areas in this regard is the Alpine foreland of central northern Switzerland (Laubscher, 1986). In this region, the Late Miocene to Early Pliocene Jura fold- belt - widely accepted to have been formed by thin-skinned distant push -was thrust onto a Permo-Carboniferous trough. The latter has been considered to be potentially reactivated in a thick-skinned manner by many authors ever since its identification.

As part of its exploration program of potential siting regions for deep geological repositories Nagra recently re-processed existing 2D- reflection seismic data across the eastern-most Jura fold-belt and the adjacent parts of the Swiss Molasse Basin. In addition, an extensive new dataset of more than 300km high resolution seismic profiles was acquired during the winter of 2011/12. We will present an overview and first insights into the ongoing interpretation of these new datasets. Critical aspects concerning the seismic interpretation of a thin-skinned, thick-skinned or combined tectonic scenario will be discussed.

REFERENCES

- Laubscher, H. 1986: The eastern Jura: Relations between thin-skinned and basement tectonics, local and regional, *Geologische Rundschau*, 75, 535–553.
- Pfiffner, A. (2006): Thick-skinned and thin-skinned styles of continental contraction. *Geological Society of America Special Paper* 414, 153-177.
- Rosenberg, C. L. and A. Berger, 2009: On the causes and modes of exhumation and lateral growth of the Alps, *Tectonics*, 28, TC6001, doi:10.1029/2008TC002442
- Schmid, S.M. & Slejko, D., 2009: Seismic source characterization of the Alpine foreland in the context of a probabilistic seismic hazard analysis by PEGASOS Expert Group 1 (EG1a). *Swiss J. Geosci.*, 102, 121–148.

2.11

New time-constraints on the prograde metamorphism in the High Himalaya of NW Lahul (NW India)

Robyr Martin¹, Banerjee Sriparna¹, El Korh Afifé¹

¹ Institut für Geologie, Universität Bern, Baltzerstrasse 1+3, CH-3012 Bern, Switzerland (robyr@geo.unibe.ch)

In the central parts of the Himalayas, the High Himalayan Crystalline (HHC) high-grade rocks are mainly exhumed in the frontal part of the range as a consequence of a tectonic exhumation controlled by combined thrusting along the Main Central Thrust (MCT) and extension along the South Tibetan Detachment System (STDS). In the NW Himalaya, however, the hanging wall of the MCT, in the frontal part of the range, consists mainly of low- to medium grade metasediments, whereas most of the amphibolite facies to migmatitic paragneisses of the HHC of Zaskar are exposed in a more internal part of the orogen as a large scale dome structure referred to as the Gianbul dome.

This Gianbul dome is cored by migmatitic paragneisses symmetrically surrounded by rocks of the sillimanite, kyanite ± staurolite, garnet, biotite, and chlorite mineral zones. The structural data from the Miyar-Gianbul Valley section reveal that the Gianbul dome is bounded by two major converging thrust zones, the Miyar Shear Zone (MSZ) and the Zanskar Shear Zone (ZSZ), which were reactivated as ductile zones of extension during early Miocene (Dèzes et al., 1999;).

Structural and metamorphic data indicate that the Barrovian metamorphism observed in the northern limb of the dome results from the northwestward underthrusting of the HHC of Zanskar beneath the sediments of the Tethyan Himalayan that occurred between 35 and 28 Ma (Vance and Harris 1999; Walker et al 1999). In contrast with the tight constraints on the timing of the tectonometamorphic evolution of the NE half of the Gianbul dome, the timing of the crustal thickening and subsequent extension on the southern limb of the dome is poorly constrained. On the southern limb of the dome, the Miyar Valley represents a natural cross-section through the southern half of the HHCZ of Zanskar. Moving northward along the valley, the metapelites of the HHCZ preserve a typical Barrovian metamorphism characterized by the succession of chlorite, biotite, garnet, kyanite + staurolite, sillimanite and migmatite zones.

The main tectonic structure in the Miyar valley corresponds to the SW-dipping Miyar Shear Zone. Sheath folds testify to an intense ductile deformation in this shear zone, and a clear top-to-the-NE shear sense is indicated by sigma clasts and shear bands. Sigmoidal inclusion trails in syntectonic garnets in the amphibolite facies paragneiss support a syntectonic growth associated with NE-directed movements. Across the Miyar Shear Zone, the contractional structures are superposed by SW-dipping extensional shear bands and sigma clasts indicating a top-to-the SW sense of shear. These observations reveal that the Miyar Shear Zone was reactivated as a ductile zone of extension (Steck et al., 1999).

One of the major features of the tectonometamorphic evolution of the HHC in the southern limb of the Gianbul dome is that the metamorphism and tectonism in this portion of the Himalaya relates to NE-directed thrusting. In order to bring geochronological constraints on the regional metamorphism observed on the southern limb of the dome, the prograde sequence of allanite and monazite has been investigated in detail.

Along the Miyar Valley, allanite appears to be the LREE-stable accessory phase at greenschist facies conditions. Its first occurrence coincides with the stability field of biotite suggesting a temperature of 430–450 °C for its growth. Moving upsection, the first metamorphic monazite forms at amphibolite facies conditions at the staurolite- in isograd. At these P-T conditions, allanite is preserved only as inclusion in garnet and staurolite indicating that allanite is replaced by monazite at ca.610-640°C.

In situ LA-ICPMS U-Th-Pb dating of the first metamorphic monazite occurring within the upper structural level of the staurolite-kyanite zone gives ages ranging between 42 and 37 Ma. These data indicate that the upper structural level of the staurolite-kyanite zone realized temperature conditions of 610-640°C during the middle Eocene. In contrast dating of monazites collected in the lower structural level of the staurolite-kyanite as well as in the structurally lower sillimanite zone provides ages ranging from 27-30 Ma. Coexisting allanite and monazite preserved in garnet porphyroblasts of the sillimanite zone give ages between 35 and 39 Ma for the allanites and between 29 and 30 Ma for the monazites. These data reveal a leap of about ten million years between monazite growth across the Miyar shear zone indicating that the contractional movements along the MSZ were active between 40 and 30 Ma. Furthermore these new data constrain the time elapsed between of 430–450 °C and 610-640°C which implies an average heating rate of ca 20-25 °C/m.y.

Combined with geochronological data from the migmatite zone (monazite, 26 Ma; Robyr et al., 2006) and from undeformed leucogranitic dykes in the centre of the dome, (monazite, 22-19 Ma; Dèzes et al., 1999; Robyr et al., 2006) the new data provided by this study allow the entire reconstruction of the tectonometamorphic evolution of the Gianbul dome.

REFERENCES

- Dèzes, P., Vannay J.-C., Steck A., Bussy F., and Cosca M., 1999, Synorogenic extension: quantitative constraints on the age and displacement of the Zanskar Shear Zone (NW Himalayas), *Geol. Soc. Am. Bull.*, 111, 364-374
- Robyr, M., Vannay, J.C., Epard, J.-L., and Steck, A., 2002, Thrusting, extension and doming during the polyphase tectonometamorphic evolution of the High Himalayan Crystalline Sequence in NW India. *Journal of Asian Earth Sciences*, v. 21, p. 221-239.
- Robyr, M., Hacker, B.R., and Mattinson, J., 2006, Doming in compressional orogenic settings: New geochronological constraints from the NW Himalaya. *Tectonics*, v. 25, TC2007, doi:10.1029/2004TC001774
- Steck, A., Epard, J.-L., and Robyr, M., 1999, The NE-directed Shikar Beh Nappe - a major structure of the Higher Himalaya. *Eclogae Geologicae Helveticae*, v. 92, p. 239-250.
- Vance, D. and Harris, N., 1999, Timing of prograde metamorphism in the Zanskar Himalaya. *Geology*, 27, 395-398.
- Walker, J. D., M. W. Martin, S. A. Bowring, M. P. Searle, D. J. Waters, and K. V. Hodges (1999), Metamorphism, melting, and extension : age constraints from the High Himalayan Slab of southeast Zanskar and northwest Lahul, *J. Geol.*, 107, 473-495.

2.12

Towards 4D modeling of transpressional fold-and-thrust belts

Ruh Jonas B.¹, Gerya Taras & Burg Jean-Pierre¹Department of Earth Science, ETH Zurich (jonas.ruh@erdw.ethz.ch)

Latest developments in computer power and computational solutions open new ways to envision complex natural systems. Advances in high-resolution 3D geodynamic modeling, in particular, allow investigating complex tectonic processes like the evolution of non-cylindrical fold-and-thrust belts. We demonstrate that implementing the 4 dimensions (space and time) provides and constrains new answers to long lasting discussions. Numerically simulating fold-and-thrust belts needs accurate treatment of brittle/plastic rheology with high resolution to produce spontaneously localizing narrow high strain rate shear bands. Thrusts and flats occur where stresses overcome the material yield stress. Therefore, a numerical approach must allow very high strain rates within the décollement and the “thrusts” while respecting the rigidity of the modelled wedge sediments. Effective viscosity variations across narrow shear bands often range six orders of magnitude. This poses a strong challenge for numerically solving the Stokes and continuity equations. For this purpose, we developed a three-dimensional, high-resolution, fully staggered grid, finite difference, marker in cell model with a visco-brittle/plastic rheology and an efficient OpenMP-parallelized multigrid solver.

As a case study, we chose the Zagros Simply Folded Belt in Iran. There, the recent shortening direction is oblique to the Main Zagros Thrust, which represents the suture between the Arabian and Central Iranian continental plates. This obliquity impels lateral backstop variations that can only be introduced in a three dimensional setup. Furthermore, along-strike structural variations are observed between the the Fars domain, in the SE, towards the Izeh domain, in the NW.

Results shows how a low-viscosity décollement becoming frictional towards the Dezful embayment influences the exposed fold patterns (Figure 1). They also emphasize the importance of an oblique backstop geometry to produce en-échelon arranged folds, where convergence-related and backstop-controlled folds are mingled in the transpressional orogen.

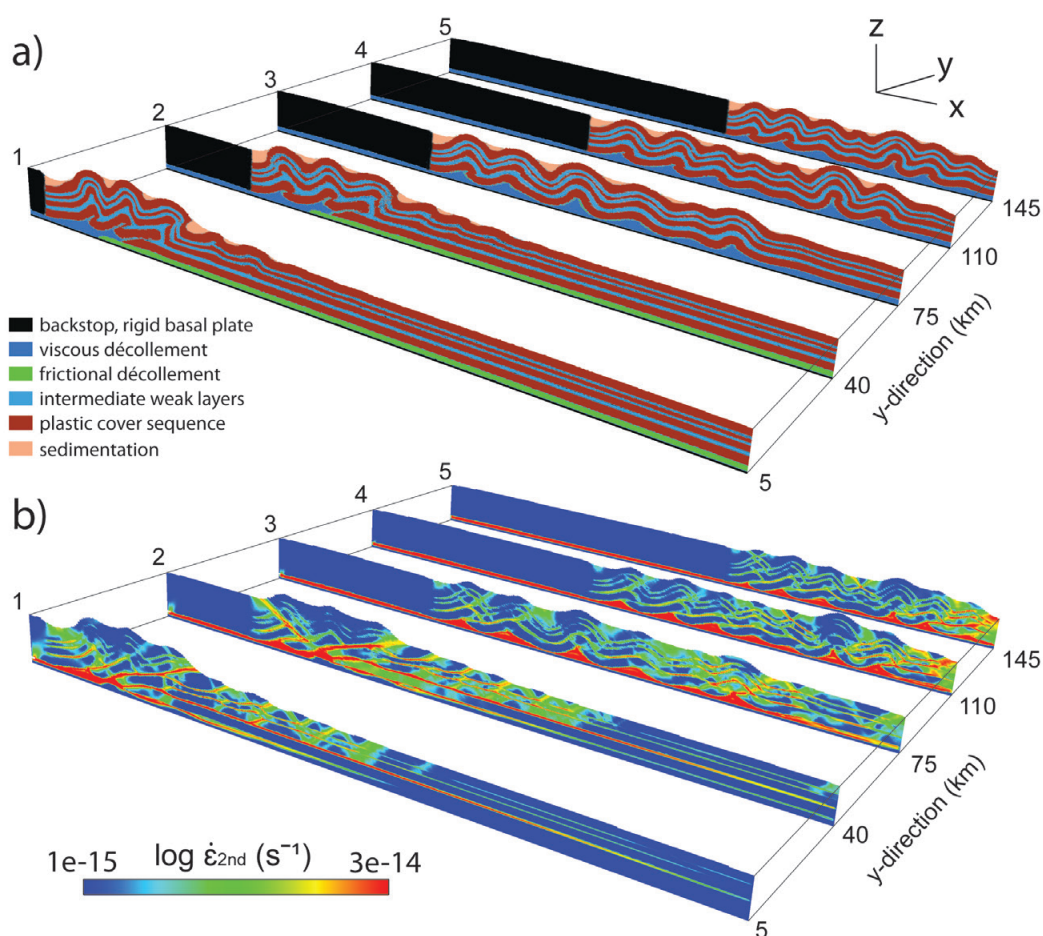


Figure 1. Profiles $y = 5, 40, 75, 110$ and 145 km after a simulation time of 3.4 Ma. a) Illustration of the rock type defined on markers. Profiles 1 and 2: Pinch-out of salt towards frictional décollement. b) Second invariant of strain rate tensor.

2.13

Alpine fold and thrust structures: a 3-D model of the Säntis area (Switzerland)

Sala Paola¹, Pfiffner O.Adrian. ¹, & Frehner Marcel²

¹ Institute of Geological Sciences, University of Bern, Baltzerstrasse 1, CH-3012 Bern Switzerland (sala@geo.unibe.ch)

² Geological Institute, ETH Zürich, Sonneggstrasse 5, CH-8092 Zürich

The Säntis area offers one of the most spectacular insights into the fold-and-thrust belt of the Helvetic nappes. The nearly perfect outcrop conditions, combined with the exemplary intersection of formation boundaries with topography, make it a natural laboratory for structural geology. Since the pioneering work of Heim (1905) at the beginning of 20th century, the area was mapped in detail (Eugster et al., 1982) and investigated in terms of deformation mechanisms (e.g. Groshong et al., 1984), structural evolution and fold-thrust interaction (Funk et al. 2000; Pfiffner 1982, 1993 & 2011). The proposed restorations are mostly 2 dimensional palinspastic reconstructions, either in map or in cross sectional view.

The main goal of this research is to better understand the geometrical relationships between folding and thrust faulting, investigating for example fault-propagation folds and analyzing the lateral changes of folds and thrust structures along strike. A three-dimensional model of the area is built using 3D MOVE, combining cross-sections from Schlatter (1941), Kempf (1966), Pfiffner (in Funk et al., 2000; 2011), the geological map 1:25.000 by Eugster et al (1982) and a digital elevation model (DEM) with a regular grid of 20X20 m.

Six main horizons are reconstructed, corresponding to the base of the Öhrli and Betlis Limestones, the Helvetic Kieselkalk, Schrattekalk and Garschella Fm and the Seewen Limestone. The main structural elements in the Säntis area, such as the Säntis Thrust or the Sax-Schwende Fault, are also implemented in the model. The 3-D model obtained highlights the shape of the main anticline-syncline pairs (e.g. Altmann-Wildseeli, Schafberg-Moor, Roslenfirst-Mutschén, Gulmen etc...); such fold trains vary in amplitude and wavelength along strike. The model also shows clearly the lateral extension, the trends and the variations in displacements of the principal faults. The reconstruction of 3-D horizons allows the geologists to investigate cross sections along any given directions. The 3-D model is useful to understand how the changes of the internal nappe structures, namely folds and thrust faults, change along strike. Such changes occur either across transverse faults or in a more gradual manner.

REFERENCES

- Eugster, H., Forrer, M., Fröhlicher, H., Kempf, Th., Schlatter, L., Blaser, R., Funk, H., Langenegger, H., Spoerri, M., & Habicht, K. 1982: Blatt 1115 Säntis. – Geol. Atlas Schweiz 1:25.000, Karte 78
- Funk, H., Habicht, J.K., Hantke, R., & Pfiffner, O.A., 2000: Blatt 1115 Säntis. – Geol. Atlas Schweiz 1:25.000, Erläuterungen 78.
- Groshong, R. H., Pfiffner, O. A. & Pringle, L. R. 1984: Strain partitioning in the Helvetic thrust belt of eastern Switzerland from the leading edge to the internal zone. *Journal of Structural Geology* 6/1, 5-18.
- Kempf, T.A. 1966: Geologie des westlichen Säntisgebirges. Beiträge geologische Karte der Schweiz N.F. 128.
- Heim, A. 1905: Das Säntisgebirge. Verhandlungen der Schweizerischen Naturforschenden Gesellschaft, Volume: 88
- Pfiffner, O. A. 1982: Deformation mechanisms and flow regimes in limestones from the Helvetic zone of the Swiss Alps. *Journal of Structural Geology* 4/4, 429-442
- Pfiffner, O.A. 1993: The structure of the Helvetic nappes and its relation to the mechanical stratigraphy. *Journal of Structural Geology*, 15/ 3-5, 511-521

2.14

The nature of the “Frilihorn nappe” (Valais, Switzerland)

Scheiber Thomas, Pfiffner O. Adrian & Schreurs Guido

Institute of Geological Sciences, University of Bern, Baltzerstrasse 1+3, CH-3012 Bern (scheiber@geo.unibe.ch)

The Penninic nappe system of western Switzerland comprises a stack of Briançon-derived basement and cover units, known collectively as the Bernard nappe complex. It is sandwiched between relics of N- and S- Penninic basin domains. The S- Penninic Tsaté nappe tectonically overlies the Bernard nappe complex and is mainly composed of Late Jurassic to Cretaceous metasedimentary rocks such as calcschists and black shales (“schistes lustrés”), and prasinites. Predominantly at the base of the Tsaté nappe, thin slices of metasedimentary continental constituents occur, which are attributed to the Frilihorn and Cimes Blanches nappes (Escher, 1997). Their internal stratigraphy resembles the one found in typical Briançonnais cover, but the paleogeographic origin of these fragments is still controversial.

In the model of Pleuger et al. (2007), for example, the Cimes Blanches and Frilihorn nappes are derived from the sedimentary cover of the Sesia-Dent Blanche nappe. They were emplaced along a major thrust zone and were themselves overthrust by the Tsaté nappe. In contrast, Marthaler et al. (2008) suggest that the Cime Blanches and Frilihorn nappes originate from the Briançonnais continental margin and represent possibly olistoliths, which slid into the S-Penninic oceanic basin. Subsequently, the development of an accretionary prism during subduction led to the incorporation of these margin sediments into a “tectono-sedimentary mélange zone”.

In this contribution we present field observations that support a tectonic model for the evolution of the Bernhard nappe complex, where stages of top-to-the N(NW) thrusting (Anniviers Phase) are followed by a phase of backfolding (Mischabel Phase). In the upper part of the Bernard nappe complex, where remnants of the Permo-Mesozoic and younger sedimentary cover sequence still rest on top of their crystalline substratum (parautochthonous Toûno and Barrhorn series after Sartori, 1987), backfolding is accompanied by strong top-to-the-S shearing. In the Le Boudri area (Figure 1) shear zones are localized in phyllitic calcschists of the Tsaté nappe. The footwall carbonates are folded into S-facing folds and disrupted fragments are incorporated into the shear zone. In the same area distinct shear planes cut through and detach several decameter-sized blocks of competent lithologies (carbonates and quartzites). Deformation in this tectonic mélange zone is highly complex. We propose that these blocks and lenses traditionally ascribed to the Frilihorn nappe are nothing else but fragments of the Toûno and Barrhorn series that were detached during strong top-to-the-S shearing along the upper limit of the Bernard nappe complex, a process which was severely underestimated so far.

The sequence and style of deformation is similar to the one observed in the Middle- and South-Penninic nappes of eastern Switzerland (i.e. Suretta and Avers nappes, Scheiber et al., 2012).

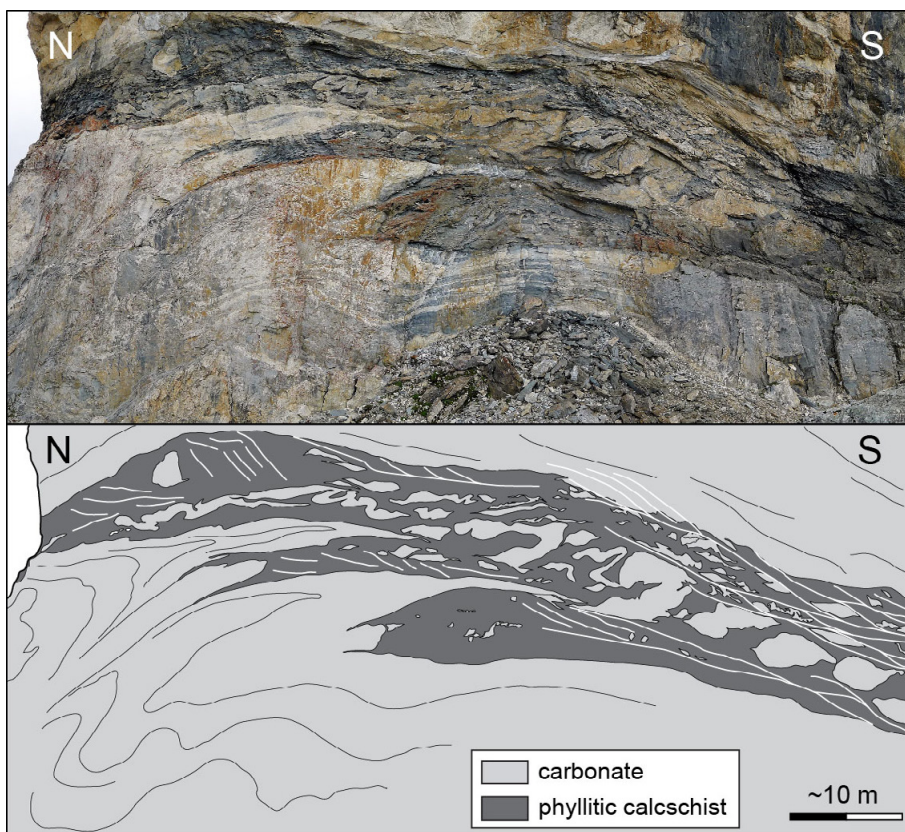


Figure 1. W-face of Le Boudri. S-vergent folding is accompanied by top-to-the S shearing, localized in minor competent lithologies. Fragments of both footwall and hangingwall carbonates are detached and incorporated into the (C'-type) shearband network (note scale!).

REFERENCES

- Sartori, M., 1987: Blocs basculés briançonnais en relation avec leur socle originel dans la nappe de Siviez-Mischabel (Valais, Suisse). C.R. Acad. Sci. Paris 305 (2), 999-1005.
- Escher, A., Hunziker, J.C., Marthaler, M., Masson, H., Sartori, M. & Steck, A. 1997: Geologic framework and structural evolution of the western Swiss-Italian Alps. In: Deep Structure of the Swiss Alps: Results of NRP 20 (Ed. by Pfiffner et al.). Birkhäuser Verlag, 205-221.
- Pleuger, J., Roller, S., Walter, J.M., Jansen, E. & Froitzheim, N. 2007: Structural evolution of the contact between two Penninic nappes (Zermatt-Saas zone and Combin zone, Western Alps) and implications for the exhumation mechanism and palaeogeography. International Journal of Earth Sciences 96 (2), 229-252.
- Marthaler, M., Sartori, M., Escher, A. & Meisser, N. 2008: Feuille 1307 Vissoie. Atlas géologique de la Suisse 1:25 000, Notice explicative 122.
- Scheiber, T., Pfiffner, O.A. & Schreurs, G. 2012: Strain accumulation during basal accretion in continental collision - A case study from the Suretta nappe (eastern Swiss Alps). Tectonophysics, doi:10.1016/j.tecto.2012.03.009.

2.15

The Tauern Window (Eastern Alps, Austria) – A new tectonic map, cross-sections and tectonometamorphic synthesis

Schmid Stefan M.¹, Scharf Andreas², Handy Mark R. &², & Rosenberg, Claudio L.³

¹ ETH-Zürich, Institut für Geophysik, Switzerland (stefan.schmid@erdw.ethz.ch)

² Freie Universität Berlin, Germany (scharfa@zedat.fu-berlin.de, mhandy@zedat.fu-berlin.de)

³ Université Pierre et Marie Curie Paris 6, France (claudio.rosenberg@upmc.fr)

We present a tectonic map of the Tauern Window and surrounding units, combined with a series of crustal-scale cross-sections parallel and perpendicular to the Alpine orogen. This compilation, largely based on literature data and completed by own investigations, reveals that the present-day structure of the Tauern Window is primarily characterized by a crustal-scale duplex, the Venediger Duplex (Venediger Nappe System), formed during the Oligocene, and overprinted by doming and lateral extrusion during the Miocene. This severe Miocene overprint was most probably triggered by the indentation of the Southalpine Units east of the Giudicarie Belt initiating at around 20 Ma and linked to a lithosphere-scale reorganization of the geometry of mantle slabs. A kinematic reconstruction shows that accretion of European lithosphere and oceanic domains to the Adriatic (Austroalpine) upper plate, accompanied by high-pressure overprint of some of the units of the Tauern Window has a long history, starting in Turonian times (around 90 Ma) and culminating in Lutetian to Bartonian time (45-37 Ma).

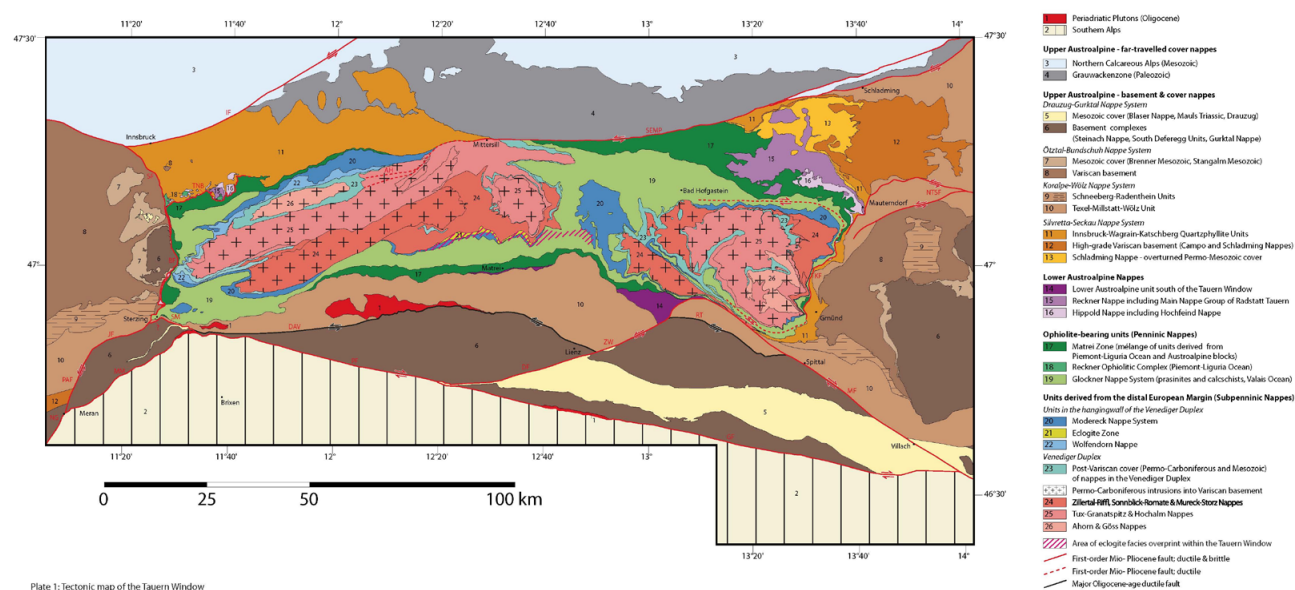


Figure 1. Tectonic Map of the Tauern Window

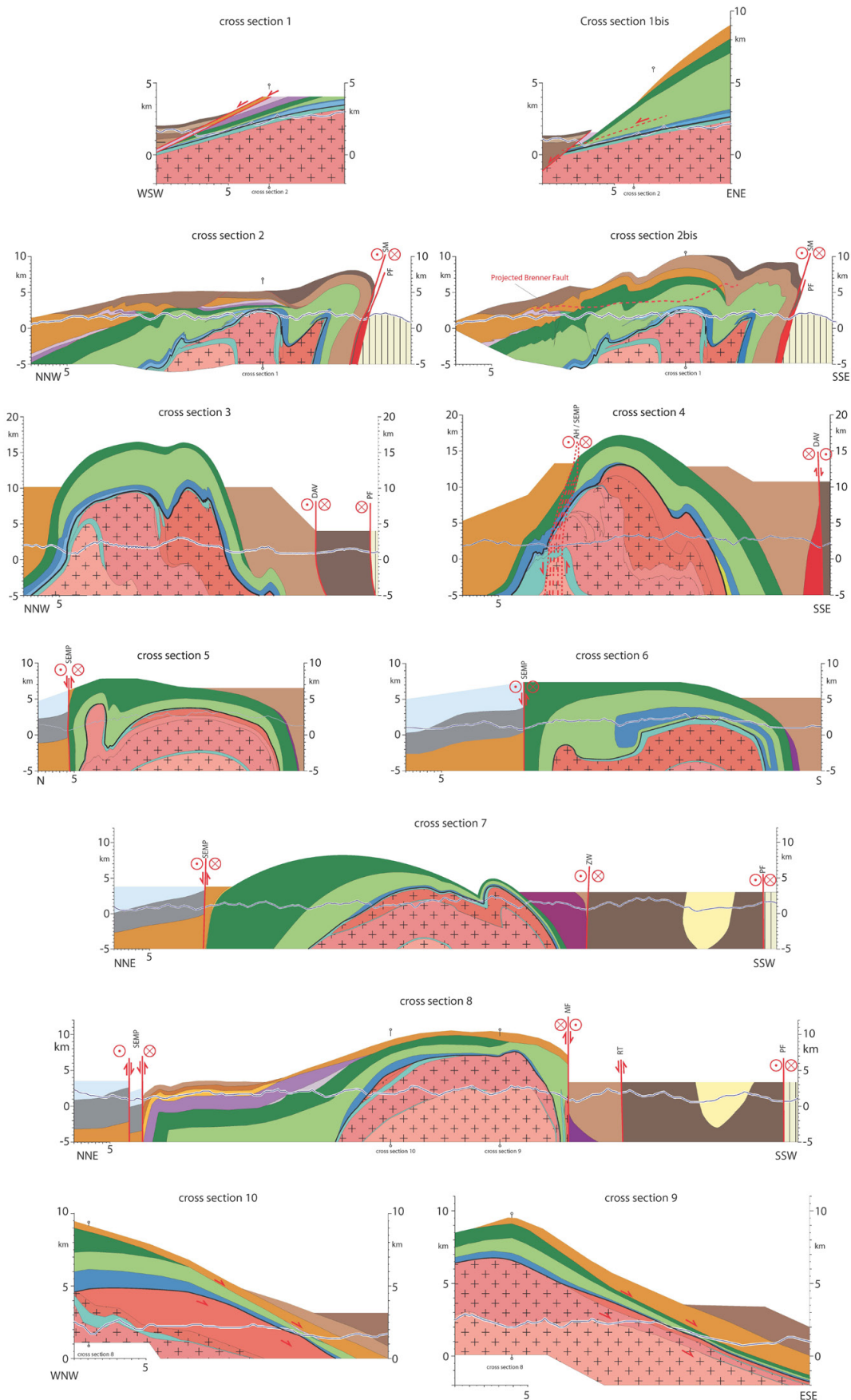


Fig. 2: Profiles across the Tauern Window. Cross sections 1,10 and 11 are orogen-parallel; cross sections 2 to 9 are orogen-perpendicular, arranged going from west to east. Sections 1bis and 2bis are alternative versions of 1 & 2.

2.16

Coupling of landscape evolution and rheologically layered thermomechanical models in three dimensions

Ueda Kosuke¹, Willett Sean¹, Gerya Taras¹

¹ *Departement Erdwissenschaften, ETH Zürich, Sonneggstrasse 5, 8050 Zürich*

Surface topography and drainage topology can contain copious information about tectonic deformation. Distinguishing a possible tectonic contribution from climate factors is however controversial, and limits the potential reconstruction of deformation histories from a first grade data set. From a different perspective on surface-lithosphere interaction, recent geodynamic studies have elucidated the strong dynamic influence of erosion and sedimentation on the evolution of convergent plate margins. In studying the interplay between tectonics and surface processes, various types of numerical models have been so far capable of providing valuable yet partial insights.

Landscape evolution models (LEM) capture the operation of an excerpt, according to scale and climate, of fluvial, glacial and hillslope processes. They are well suited to specific problems with simple, feedback-free kinematics to study the response of landscape to tectonics. In contrast, large-scale thermomechanical models incorporate simplified continuous surface functions that do not respect the scale-dependency of surface processes, and that do not reproduce landscape characteristics other than gross elevation. The coupled models that have been brought forward so far, aiming at combining each side's capabilities, have been subjected to limitations like two-dimensionality, lack of rheological layering, and computationally limited resolution, exacerbating the inaccuracy of discretized divide location. These models have successfully explored the sensitivity of topography and strain partitioning, on the efficiency of surface processes, but have not advanced to addressing the evolution of drainage patterns. Such research objectives are becoming more feasible as recent developments move towards coupling LEMs to three-dimensional, rheologically layered thermomechanical models at increasing resolution. In this contribution, we present results from coupling a scale-robust LEM with a full thermomechanical model.

The new LEM code DAC combines numerical-analytical modelling of fluvial and hillslope processes, and is capable of treating large model domains at feasible numerical resolution without loss of accuracy. First, location and migration of divides is not confined to the network discretization, and the channelization threshold can be honored on sub-grid scale. Second, the analytical accuracy of divide calculations and capture events provides a balance between dynamic reorganisation, and preservation of deformed river channels and drainage basins that do not adhere to instantaneous steepest-descent assumptions. These capabilities make the LEM suited to study the transient evolution of drainage patterns with full thermomechanical feedback. The LEM is coupled to a visco-plastic code - I3VIS - that models a rheologically layered lithosphere, and accounts for phase changes, melting, and hydration processes. The thermomechanical code employs a large number of markers, a component which is useful for prediction of Lagrangian (P)-T-t paths.

We present results from our coupled models applied to set-ups with isostatic compensation as well as convergent settings and indentation. We compare convergent, fully layered lithospheric plates to basally driven critical-wedge formulations. Using established scaling relationships, we compare characteristic measures of the fluvial network (spacing, length, drainage area) to natural analogues. Coupled models show a strong dynamical feedback between the maxima of fluvial erosion and tectonic uplift.

2.17

Swiss 4D: Determination of strain rates from GNSS campaign and levelling data

Villiger Arturo¹, Geiger Alain¹, Marti Urs², Brockmann Elmar², Schlatter Andreas²

¹ Institute of Geodesy and Photogrammetry, ETH Zurich, Schafmattstrasse 34, CH-8093 Zurich (villiger@geod.baug.ethz.ch)

² Federal Office of Topography swisstopo, Seftigenstrasse 264, CH-3084 Bern

In 2010 the federal office of topography, swisstopo, carried out a GNSS campaign for the CHTRF 2010. The measurements cover whole Switzerland and lead, in combination with former campaigns (1988-2010), to a set of velocity data at more than 230 points in the horizontal plane. Vertical velocities, derived from levelling data and covering a time span of more than 100 years, are an important additional data set because vertical velocities are not available from GNSS campaign data. The combination of both measuring methods allows to extract a velocity field consisting of East, North, and Up direction.

The provided velocities show only a very weak signal – in average 0.6 mm/yr in the horizontal and a little more significant in the vertical velocity (e.g. in the alpine areas). It is a major issue, to extract the deformation field. Therefore, an adaptive least-square collocation method (ALSC) (Egli et al. 2007) is developed assuming that tectonic deformations are affecting a wide region. The correlation between the points is based on their distance. During the iterative process the weighting is adapted to the magnitude of strain rates. In mathematical terms, this is realized by deforming the metric for the correlation length determination. This decorrelates points in areas with high strain rates.

The results are a velocity and strain field for the covered area. It can be seen that the collocation technique allows to separate a regional deformation from local effects and noise. The data shows, for some areas, similar trends as derived from seismic information (Kastrup et al. 2004).

REFERENCES

- Egli, R., Geiger, A., Wiget, A. & Kahle, H.-G. 2007: A modified least-squares collocation method for the determination of crustal deformation: first results in the Swiss Alps. *Geophysical Journal International*, 2007, 168, 1-12.
- Kastrup, U., Zoback, M., Deichmann, N., Evans, K., Giardini, D. & Michael A. 2004: Stress field variations in the Swiss Alps and the northern Alpine foreland derived from inversion of fault plane solutions. *J. Geophys. Res.*, 109.

2.18

Deformational evolution of the Aar Massif (Central Alps): From macro- to micro-scale

Wehrens Philip¹, Baumberger Roland¹ and Herwegh Marco¹

¹ Institut für Geologie, University of Bern, Baltzerstrasse 1+3, CH-3012 Bern (philip.wehrens@geo.unibe.ch)

The Aar massif belongs to the external massifs of the Alps and is mainly composed of granitoids and gneisses. Despite numerous detailed studies in the past decades, the overall exhumation history and the associated massif internal deformation (internal strain distribution and its evolution in time, kinematics etc.) are largely unknown at present. In this project, we aim to investigate the role of shear zones in the deformation history at a variety of scales. In this context it is important to understand their microstructural evolution, the involved deformation processes, kinematics and relative ages as well as the associated changes in rheology.

A GIS-based remote-sensing structural map, verified by fieldwork, (see Baumberger et al., this session) served as base for our investigations. Localization of strain takes place along lithological contacts between the units (Central Aare granite, ZAGr; Grimsel granodiorite, GrGr and gneisses). Furthermore, the initial magmatic differentiation in the granitoids locally controls the Alpine deformational overprint because of differences in effective viscosity during solid-state deformation. This behavior is illustrated by the increase of foliation intensity and the number of shear zones per rock volume from ZAGr to GrGr.

Preliminary results show that deformation at the N boundary of the Aar massif has to be distinguished from the central and the southern part. In the North steep NE-SW trending foliations and shear zones with subvertical lineations represent the major structures. The shear zones acted both as normal faults and as reverse faults, which mostly used pre-existing lithological boundaries between the different gneiss units. In a later stage, E-W trending shear zones and shear bands with moderate dipping angles cross cut the earlier structures. They always show a top to the North component and might be related to the late north directed movements of the Aar massif. Yet, no absolute age dating has been performed on such structures.

In the central and southern part strain localizes along aplitic dykes and inside lamprophyre dykes as well as in discrete zones in the Granitoid rocks. This region has NE-SW (dip azimuth 130°-180°) and NW-SE trending shear zones dissecting the Central Aar granite (ZAGr). The shear zones, mostly with steep lineations, are of ductile origin sometimes overprinted in a brittle manner. Again shear sense indicators of NE-SW structures show south block up and down movements for individual shear zones. In addition some of these shear zones have both subhorizontal and subvertical lineations. They may represent a late strike-slip reactivation of earlier vertical movements.

Crosscutting relationships indicate that the NW-SE shear zones are younger than the NE-SW ones, and acted as dextral strike slip zones (subhorizontal lineations).

2.19

4-D Numerical Modeling of Crustal Growth at Active Continental Margins

ZHu Guizhi , Gerya Taras, Tackley Paul and Kissling Eduard

Institute of Geophysics, Department of Earth Sciences, ETH-Zurich, Switzerland (guizhi.zhu@erdw.ethz.ch)

Crustal growth and topography development in subduction-related arcs are intimately related to magmatic processes and melt production above subducting slabs. Lateral and temporal variations in crust thickness and composition have been observed in nature, but until now no integrated approach is developed to comprehensively understand magmatic activities in subduction-related arcs. Here we aim at investigating the 4-D spatial, temporal and compositional character of continental crustal growth at active margins by using new 4-D (space-time) petrological-thermomechanical numerical model of a subduction-related magmatic arc.

Based on a series of numerical experiments we demonstrate that crustal growth inside the arc is inherently clustered in both space and time. The characteristic wavelength of crust thickness and topography variation along the arc is mainly defined by plate convergence velocity: faster subduction favors longer wavelength. The clusters of new crust are mainly contributed by basaltic composition episodically extracted from partially molten peridotite due to lateral variation of water release and movement in the mantle wedge. Melts derived from subducted oceanic crust and sediments could contribute up to 15-50 vol% to the arc crust growth and their relative proportion is maximal at the onset of subduction. Total amount of the newly formed crust correlates mainly with the amount of convergence since the beginning of subduction and is not strongly influenced by the plate convergence velocity. Indeed, slower subduction and lower melt extraction efficiency helps partially molten sediments and oceanic crust to be transported into the mantle wedge by hydrated, partially molten diapiric structures. Maximum of crust additional rate (25-40 km³/km/Myr) occurs when convergent amount reaches around 700 km. Mantle wedge structures developed in our models correlates well with available geophysical observations for Alaska subduction zone. In particular, partially molten mantle plumes found in our models could explain low seismic anomalies in the mantle wedge, whereas mobile water and water release patterns could reflect paths and sources for magmatic activities evidenced by seismic b-value analysis.

P 2.1

Dynamic recrystallization and shear heating in numerical models of lithospheric-scale shear zones

Marcel Thielmann¹, Antoine Rozel², Boris J.P. Kaus³, Yanick Ricard⁴

¹ Institute of Geophysics, ETH Zürich, Sonneggstrasse 5, CH- 8093 Zürich

² Dipartimento di Scienze Geologiche, Roma 3, Largo San Leonardo Murialdo 1, IT -00146 Roma

³ Institut für Geowissenschaften, Johannes Gutenberg-Universität Mainz, J.-J.-Becher-Weg 21, D-55099 Mainz

⁴ Laboratoire de Géologie de Lyon (LGLTPE), CNRS, Université de Lyon 1, ENSL, 2 rue Raphaël Dubois, F- 69622 Lyon

Shear zones are usually defined as regions inhomogeneous and localized deformation. Strain softening has been demonstrated to be a necessary prerequisite for localization. However, it is not clear which physical mechanisms are responsible for this weakening. In this study, we investigate the interplay between two mechanisms that have been proposed to govern the formation of lithospheric-scale shear zones: shear heating and grain size reduction.

Shear heating has been suggested to play an important role in i) creating deep focus as well as intermediate-depth earthquakes (Ogawa (1987), Kelemen and Hirth (2007)) and ii) creating lithospheric-scale shear zones (Kaus and Podlatchikov (2006), Cramer and Kaus (2010)).

Natural shear zones are typically characterized by a significantly reduced grain size. Dynamic recrystallization has therefore been put forward as a mechanism to provide the needed strain softening to localize deformation. With reducing grain size, the dominant deformation mechanism is thought to switch from dislocation to diffusion creep, thus requiring less stress to deform the rock. Recent work (Austin and Evans (2007), Rozel et al. (2011)) suggests that the amount of dynamic recrystallization is not – as previously suggested - only dependent on stress, but on deformational work.

In this study, we employ the grain size evolution law of Rozel et al. and use 1D viscoelastic numerical models of simple shear deformation to investigate the influence of both weakening mechanisms and their interaction. We find that grain size reduction in pure olivine does not localize very efficiently, as grain size very rapidly reaches a steady state and does not allow for further localization. Even when grain size reduction processes use a fraction of the deformational work, shear heating is the dominant weakening mechanism. Inside the shear zone, grain size is significantly increased due to the high temperature. This is not compatible with field observations and indicates that different mechanisms are required to create mylonitic shear zones and/or to reduce the temperature increase due to shear heating.

P 2.2

Dynamic origin of Wilson cycles in mantle convection with self-consistent plate tectonics and continental drift

Rolf Tobias¹, Coltice Nicolas^{2/3}, Tackley Paul J.¹

¹ Institute of Geophysics, ETH Zürich, Sonneggstrasse 5, CH-8092 Zürich (Tobias.Rolf@erdw.ethz.ch)

² Laboratoire de Géologie de Lyon, Université Claude Bernard Lyon 1, 43 Boulevard du 11 Novembre 1918, F-69622 Villeurbanne cedex

³ Institut Universitaire de France

The alternation of dispersed continent configuration and supercontinent assembly is part of the Wilson cycle. More and more evidence exist that continents have formed a supercontinent several times since the late Archaean. However, plate reconstruction techniques allow for looking back into Earth's tectonic history, but geologic evidence is hardly preserved for times prior to 200 Ma ago, such that only the existence of the last supercontinent, Pangaea, is well documented. Especially for the first supercontinents only poor constraints exist; among them is the episodic production rate of continental crust derived from analyzing the osmium decay system [1]. The peaks of crustal growth correlate with the proposed assembly times of some older supercontinents, which are derived from the argument that almost all cratons that stabilized at a certain time were located next to each other in Pangaea. This is very unlikely if they have not formed in a single continental block [2].

Supercontinents are thought to generate a large-scale thermal anomaly by insulation beneath them, which enhances melting processes and with that the growth of continental crust.

However, although the effects of supercontinents on tectonic history, head budget or climate have been debated, the dynamic origin of the Wilson cycle remains somewhat enigmatic. What causes the alternation of assembled and dispersed configuration?

Here we use fully dynamic models of mantle convection featuring self-consistently generated plate tectonics and buoyant, rheologically-distinct continents that eventually collide or split during their drift. In contrast to our previous models [3] the continents in this study consist of a strong core (representing Archaean cratons) surrounded by weaker belts (representing Proterozoic-Phanerozoic mobile belts). Using 2D and 3D models we investigate the key controls on the generation of a Wilson cycle and its period, in particular the rheological properties of the mobile belts and the properties of mantle flow (mode of heating, yield strength of the lithosphere). In order to generate a Wilson cycle a long-wavelength convection pattern is needed to assemble the continental fragments. During supercontinent break-up this long-wavelength pattern is disturbed due to the formation of new plate boundaries that cause the dispersal of continental fragments.

REFERENCES

- [1] D. G. Pearson, S. W. Parman, G. M. Nowell (2007), A link between large scale mantle melting and continent growth seen in osmium isotopes, *Nature*, 449, 202-205.
- [2] J. J. W. Rogers, M. Santosh (2003), Supercontinents in Earth History, *Gondwana Res.*, 6, 357-368.
- [3] T. Rolf, N. Coltice, P. J. Tackley (2012), Linking continental drift, plate tectonics and the thermal state of the Earth's mantle, *Earth Planet. Sci. Lett.*, 351-352, 134-146.

P 2.3

3D numerical modeling of continental extension to seafloor spreading

Jie Liao¹ & Taras Gerya¹

¹ *Institute of Geophysics, Department of Geosciences, Swiss Federal Institute of Technology (ETH-Zurich), CH-8093 (jie.liao@erdw.ethz.ch)*

The process of continental rifting to oceanic spreading is one of the most significant plate tectonics on the earth. There are many questions remained related to this whole process, most of which are poorly understood, such as how continental extension transforms into seafloor spreading? How the curved oceanic ridge developed from a straight continental rift? How the pre-existing weakness in either crust or lithospheric mantle individually influences the continental rifting and oceanic spreading? By employing the state-of-the-art three-dimensional thermomechanical-coupled numerical code (using Eulerian-Lagrangian finite-difference method and marker-in-cell technic)(Gerya and Yuen, 2007), which can model long-term plate extension and large strains, we investigated the continental extension to oceanic spreading based on two questions: (1) how the curved continental breakup/oceanic ridge formed? (2) Pre-existing lithospheric structure affects the continental rifting and oceanic spreading patterns, but where is the inheritance from, crust or lithospheric mantle?

We found that the continental rifting initiated geologically synchronous along the pre-existing weak zone, but the seafloor spreading develops in a propagation way. Curved ridge can form during the ridge propagation, and this process is related to the extension history, as the spreading ridge goes through the weakest spots in different places generated in the earlier extension stage.

REFERENCES

- Gerya, T. & Yuen, D. A. 2007: Robust characteristics method for modelling multiphase visco-elasto-plastic thermo-mechanical problems, *Phys. Earth Planet. Interiors*, 163, 83-105.

P 2.4

Implications of single-sided subduction in global self-consistent models of mantle convection

Fabio Crameri¹, Paul Tackley¹, Irena Meilick¹, Taras Gerya¹, Boris Kaus²

¹ Institute of Geophysics, ETH Zurich, Switzerland (fabio.crameri@erdw.ethz.ch)

² Institute of Geosciences, Johannes Gutenberg University Mainz, Germany

Previous global dynamical models using a visco-plastic rheology are able to reproduce some aspects of plate tectonics and mantle convection. However, these models still fail to reproduce some first-order features of plate tectonics, for example Earth-like one-sided subduction. The usual assumption these models make inhibits development of surface topography.

[1] and [2] showed that it is necessary to include a proper free surface in numerical models in order to reproduce laboratory results and to guarantee a physically accurate topographic evolution, respectively. According to these benchmark studies, mimicking a free surface by inserting a weak, zero density layer on top of the crust is an adequate approach if (a) it is sufficiently thick and (b) has a sufficiently low viscosity. As shown in [3], this model extension directly leads to single-sided subduction (Figure 1).

We here study the effect of the mode of subduction on Earth's interior dynamics using Cartesian 2-D to spherical 3-D global, fully dynamic mantle convection models with self-consistent plate tectonics. For this we use the finite volume multi-grid code STAGYY [4]. While in the mobile lid (plate tectonic like) regime, our model shows that single-sided subduction has strong implications on Earth's interior such as its rms. velocity and mantle flow distribution. Another feature caused by nature-like asymmetric subduction is the toroidal flow around the slab edges. This flow of mantle material is responsible for forming the slabs in the mantle and subsequently also the subduction trenches at the surface towards an arcuate shape.

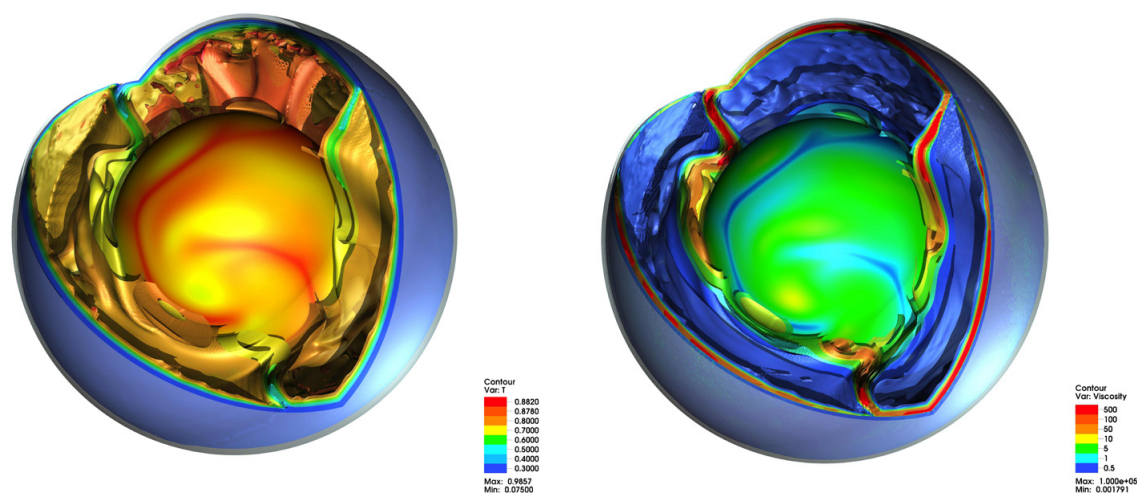


Figure 1. Single-sided subduction in a 3-D spherical, dynamically self-consistent global model of mantle convection and plate tectonics. Shown are temperature (left) and viscosity fields (right).

REFERENCES

- [1] Schmeling, H., Babeyko A., Enns A., Faccenna C., Funiciello F., Gerya T., Golabek G., Grigull S., Kaus B. J. P., Morra G., Schmalholz S. & van Hunen J. (2008): A benchmark comparison of spontaneous subduction models – towards a free surface: *Phys. Earth Planet. Int.* 171, 198-223.
- [2] Crameri, F., Schmeling, H., Golabek, G. J., Duretz, T., Orendt, R., Buitert, S. J. H., May, D. A., Kaus, B. J. P., Gerya, T. V. and Tackley, P. J. (2012), A comparison of numerical surface topography calculations in geodynamic modelling: an evaluation of the 'sticky air' method. *Geophysical Journal International*, 189: 38–54.
- [3] Crameri, F., P. J. Tackley, I. Meilick, T. V. Gerya, and B. J. P. Kaus (2012), A free plate surface and weak oceanic crust produce single-sided subduction on Earth, *Geophys. Res. Lett.*, 39, L03306.
- [4] Tackley, P. J. (2008): Modelling compressible mantle convection with large viscosity contrasts in a three-dimensional spherical shell using the yin-yang grid. *Phys. Earth Planet. Int.*

P 2.5

Exhumation of HP to UHP-HT rocks during delamination in orogenic settings - distribution of P-T paths from numerical modelling

Ueda Kosuke¹, Gerya Taras¹

¹ *Departement Erdwissenschaften, ETH Zürich, Sonneggstrasse 5, 8050 Zürich*

Geological exposures of HP and UHP rocks in collisional orogens worldwide indicate subduction of continental material to considerable depths before its separation from mantle lithosphere. Numerical models produce exhumation, after continental subduction to depths as large as 200 km, by a variety of mechanisms, but tend to predict cooler P-T paths than observed in geological analogues. In this contribution, we explore the exhumation record predicted from recent thermo-mechanical models of self-consistent subduction-collision-delamination cycles.

UHP/HP exposures are mainly associated with Phanerozoic orogenies operating with lower Moho-temperatures than during the Precambrian. The potential of delamination for exposing deeper subduction-channel rocks and for superimposing HT/LP metamorphism has been principally demonstrated. In addition to the uniformitarian, geodynamic role in accompanying recent subduction-collision tectonics, delamination is also a potential mechanism permitting, protracting, and stabilizing long-lasting sub-crustal vertical tectonics in and after hotter, accretionary orogens during the Precambrian.

Synthetic P-T-t results are presented with a novel perspective: making use of the marker-in-cell technique, markers in surface positions are identified for each time step and then tracked back individually through the evolving temperature and dynamic pressure fields. The approach honors (i) the volatility of the observation reference frame, the surface, through time; (ii) lateral variability in exposed records; (iii) a spread of P-T paths, sampled in large numbers on the marker distribution rather than at isolated arbitrary points. A P-T evolution envelope can be established from the set of predicted P-T paths. In addition, this approach allows better to probe the sensitivity of the predicted range of exhumation records to factors like surface processes or lithostatic pressure assumptions.

Retreating, syn-collisional delamination in orogens, in absence of external forcing, is characterised by three contributions to P-T exposure. In an early stage, HP rocks that originate from the subduction channel are exposed in proximal positions to the suture. They record moderate ($\leq 600^\circ\text{C}$) temperatures, and produce simple and prolate initial P-T loops. Subsequently, an increasing HT overprint results in more complex loops with pronounced near-isobaric heating after isothermal decompression. The respective peak conditions of the separate HP; HT contributions amount to pressures of ca. 3 GPa, and temperatures of ca. 800°C . A third component becomes apparent in late model stages as the exhumation level becomes deeper. Contemporaneous UHP-HT conditions of > 4 GPa and ca. 1000°C reduce to 1 GPa at ca. 800°C on the retrograde path. The appearance of the last component is limited to the region close to the suture in which lower crust reaches the surface late in the evolving model, demonstrating the sensitivity of exposure to the surface evolution of the model.

The conditions and complexity of observed P-T paths are compatible with thermobarometric data from the Mediterranean, in particular the Aegean.

P 2.6

Towards combined modelling of planetary accretion and differentiation

Golabek Gregor^{1,2}, Gerya Taras¹, Morishima Ryuji³, Tackley Paul¹ & Labrosse Stéphane²

¹ Institut für Geophysik, ETH Zürich, Sonneggstrasse 5, CH-8092 Zürich (gregor.golabek@erdw.ethz.ch)

² Laboratoire de Géologie, ENS Lyon, 46 Allée d'Italie, F-69364 Lyon.

³ Department of Earth and Space Sciences, University of California, Los Angeles, 595 Charles Young Drive East, CA 90095-1567

Results of current 1D models on planetesimal accretion yield an onion-like thermal structure with very high internal temperatures due to powerful short-lived radiogenic heating in the planetesimals. These lead to extensive silicate melting in the parent bodies. Yet, magma ocean and impact processes are not considered in these models and core formation is, if taken into account, assumed to be instantaneous with no feedback on the mantle evolution.

It was pointed out that impacts can not only deposit heat deep into the target body, which is later buried by ejecta of further impacts, but also that impacts expose in the crater region originally deep-seated layers, thus cooling the interior. This combination of impact effects becomes even more important when we consider that planetesimals of all masses contribute to planetary accretion. This leads occasionally to collisions between bodies with large ratios between impactor and target mass.

Thus, all these processes can be expected to have a profound effect on the thermal evolution during the epoch of planetary accretion and may have implications for the onset of mantle convection and cannot be described properly in 1D geometry.

Here we present a new methodology, which can be used to simulate the internal evolution of a planetary body during accretion and differentiation: Using the N-body code PKDGRAV we simulate the accretion of planetary embryos from an initial annulus of several thousand planetesimals. The growth history of the largest resulting planetary embryo is used as an input for the thermomechanical 2D code I2ELVIS. The thermomechanical model takes recent parametrizations of impact processes like impact heating and crater excavation into account. The model also includes both long- and short-lived radiogenic isotopes and a more realistic treatment of largely molten silicates.

Results show that late-formed planetesimals do not experience silicate melting and avoid thermal alteration, whereas in early-formed bodies accretion and iron core growth occur almost simultaneously and magma oceans develop in the interior of these bodies. These tend to form first close to the core-mantle boundary and migrate upwards with growing internal pressure.

REFERENCES

- Davies, G.F. 1990: Heat and Mass Transport in the Early Earth, in: *Origin of the Earth*, ed. H.E. Newsom, J.H. Jones, Oxford Univ. Press, 175-194.
- Gerya, T.V and Yuen, D.J. 2007: Robust characteristics method for modelling multiphase visco-elasto-plastic thermo-mechanical problems, *Phys. Earth Planet. Int.*, 163, 83-105.
- Monteux, J., Coltice, N., Dubuffet, F. & Ricard, Y. 2007: Thermo-mechanical adjustment after impacts during planetary growth, *Geophys. Res. Lett.*, 34, L24201.
- Morishima, R., Stadel, J. & Moore, B. 2010: From planetesimals to terrestrial planets: N-body simulations including the effects of nebular gas and giant planets, *Icarus* 207, 517-535.
- Safronov, V.S. 1978: The Heating of the Earth during its Formation, *Icarus*, 33, 3-12.
- Zahnle, K.J., Kasting, J.F. & Pollack, J.B. 1988: Evolution of a steam atmosphere during Earth's accretion, *Icarus*, 74, 62-97.

P 2.7

3D Marker-In-Cell Finite Element based Discretisation for Lithospheric Scale Geodynamics: Theory and Applications

Dave A. May¹

¹ *Department of Earth Sciences, Geophysical Fluid Dynamics, ETH Zürich, Sonneggstrasse 5, CH-8092 Zürich (dave.may@erdw.ethz.ch)*

Developing numerical methods to study long term, 3D lithospheric scale processes requires specialized techniques. Of most importance is that the numerical method should provide the ability to (i) resolve the large deformation of visco-elastic-plastic materials and (ii) robustly solve the inherently non-linear equations describing the evolution of the material and its rheology.

The use of a mixed finite element formulation to discretise Stokes equations, coupled with a particle based Lagrangian representation of the material lithology is a common numerical technique employed within geodynamics to study large deformation processes. The extension of this methodology to enable high-resolution, three-dimensional simulations represents a number of challenges. From a theoretical point of view, there is currently little mathematical analysis to define the accuracy and support the robustness of the numerical solution obtained from such methods. From the computational side, traditional FE implementations are memory intensive. The development of efficient FE methods which are 'light-weight' and can accurately and robustly solve linear and non-linear problems, and furthermore are performant on multi-core, massively parallel computational hardware is an on going research challenge.

Here I describe the developments of a hybrid finite element (FE) discretisation, coupled with a particle based Lagrangian representation of the material lithology to study geodynamic processes. The development of the method includes both a theoretical analysis of the discretisation errors, and a computationally 'cheap' and efficient numerical implementation utilizing the mixed element Q2-P1. With this new methodology, we intend to study 3D geodynamic processes associated with subduction, rifting and folding.

The key to the efficient implementation is as follows: 1) Always pose the discrete problem in defect-correction form; 2) Utilise a mixture of assembled and matrix-free operations to evaluate the non-linear residual and apply the operators and smoothers required to define the multi-level preconditioner for the Jacobian.

The performance characteristics of the matrix-free, multi-level preconditioning strategy is demonstrated by considering several 3D visco-plastic models. The robustness of the preconditioner and non-linear solver with respect to the viscosity contrast and the topology of the viscosity field, together with the parallel scalability is demonstrated.

P 2.8

3D FEM modeling of fold nappe formation in the Western Swiss Alps

von Tschärner Marina & Schmalholz Stefan

Université de Lausanne, Institut de géologie et paléontologie, Quartier UNIL-Dorigny, Bâtiment Anthropole, CH-1015 Lausanne, (marina.vontschärner@unil.ch)

Fold nappes are recumbent folds with amplitudes usually exceeding 10 km and they have been presumably formed by ductile shearing. They often exhibit a constant sense of shearing and a non-linear increase of shear strain towards their overturned limb.

The fold axes of the Morcles fold nappe in western Switzerland plunges to the ENE whereas the fold axes in the more eastern Doldenhorn nappe plunges to the WSW. These opposite plunge directions characterize the Wildstrubel depression (Rawil depression, Ramsay, 1981). The Morcles nappe is mainly the result of layer parallel contraction and shearing (Ramsay, 1981).

During the compression the massive limestones were more competent than the surrounding marls and shales, which led to the buckling characteristics of the Morcles nappe, especially in the north-dipping normal limb. The Doldenhorn nappe exhibits only a minor overturned fold limb.

There are still no 3D numerical studies which investigate the fundamental dynamics of the formation of the large-scale 3D structure including the Morcles and Doldenhorn nappes and the related Wildstrubel depression. Such studies require a numerical algorithm that can accurately track material interfaces for large differences in material properties (e.g. between limestone and shale) and for large deformations.

The applied numerical algorithm is based on the finite element method (FEM) and can simulate 3D fluid flow for a power-law viscous rheology. Our FEM code combines a numerical marker technique and a deformable Lagrangian mesh with re-meshing (Poliakov and Podladchikov, 1992). With this combined method it is possible to follow the initial material contours with the FEM mesh to accurately resolve the initial buckling instabilities.

Two 2D models represent simple end-member scenarios for the Morcles and the Doldenhorn domain (Fig. 1 and 2). The models consider a sediment filled half graben within a basement block. Within the sediments are two layers with a 50 times larger reference viscosity than the surrounding sediments. These layers are sheared over the basement due to overall pure shear shortening and form a fold nappe with an overturned limb (Fig. 1 and 2).

The two models differ in the initial sedimentary thickness below the stiff layers representing the general situation of the pre-shortening Morcles (thicker) and Doldenhorn (thinner) domain. Thicker sediments yield a larger amplitude fold nappe with a significant overturned limb (Fig. 2) whereas thinner sediments yield a smaller amplitude fold with a minor overturned limb. For both models a cusp (mullion) forms at the basement-sediment contact.

The two end-member models are combined in a full 3D model where the sedimentary thickness is laterally increasing (Fig. 3). The 3D model is used to study the 3D deformation and the geometry resulting from the laterally varying style of folding and shearing due to laterally varying sediments thickness.

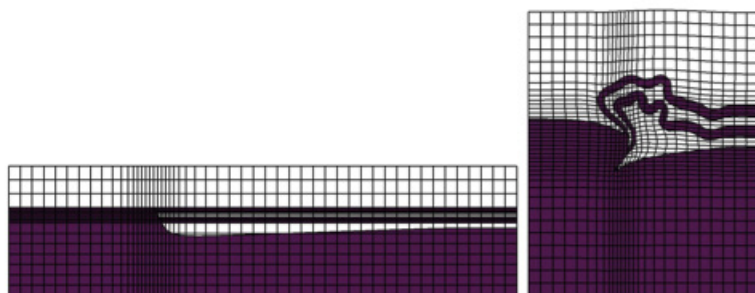


Figure 1: 2D results for an initial graben depth of 30% of the total basement thickness before (left) and after 55% (right) shortening.

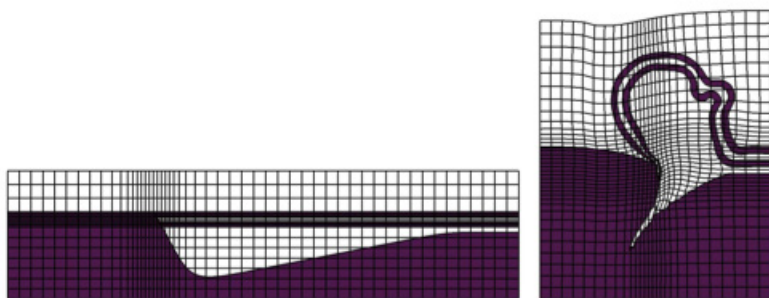


Figure 2: 2D results for an initial graben depth of 60% of the total basement thickness before (left) and after 55% (right) shortening.

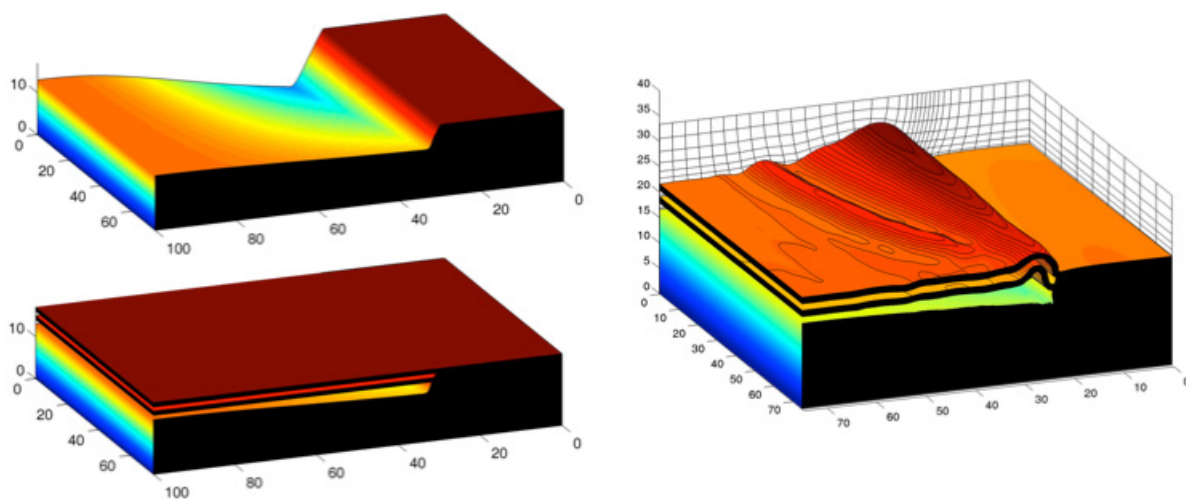


Figure 3: Geometry of the initial 3D model for the basement (top left) and for the whole geometry before (bottom left) and after 25% shortening (right, first results for low resolution). The basement depth is laterally increasing. Color plot represent the topography.

REFERENCE

- Poliakov, A. and Podladchikov, Y., 1992: Diapirism and topography. *Geophysical Journal International*, 109, 553-564
- Ramsay, J. G., 1981: *Tectonics of the Helvetic Nappes, Thrust and Nappe Tectonics*. The Geological Society of London, 293-309 .

P 2.9

Do foliation refraction patterns around buckle folds represent finite strain?

Marcel Frehner¹ and Ulrike Exner²

¹Geological Institute, ETH Zurich, Switzerland (marcel.frehner@erdw.ethz.ch)

²Natural History Museum, Vienna, Austria

Axial plane foliation associated with geological folds may exhibit a divergent or convergent fan. To test the hypothesis that the foliation orientation coincides with the major principal finite strain, numerical finite-element (FE) simulations of single-layer buckle folding are performed (Figure 1; Frehner & Exner, *subm.*). Four different strain measures are considered: (1) finite strain (recording the entire strain history), (2) infinitesimal strain (current strain), (3) incremental strain (recording the strain history from a certain shortening value until the end of a simulation), and (4) initially layer-perpendicular passive marker lines.

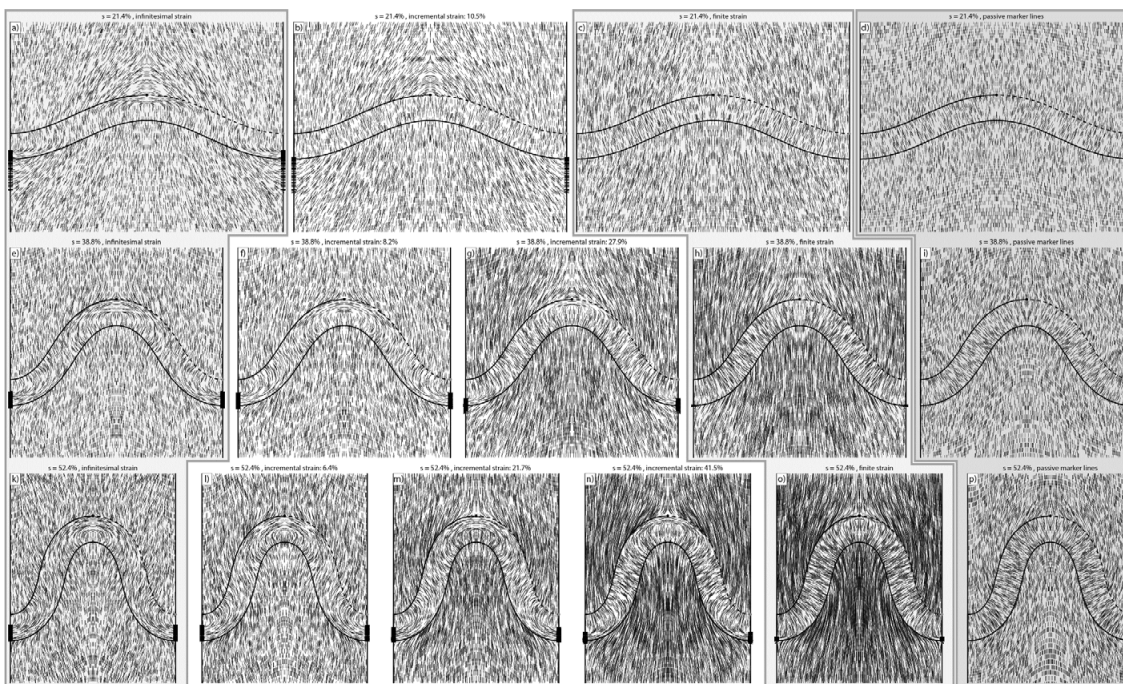


Figure 1: Snapshots of a FE simulation of a single-layer buckle fold with a viscosity ratio of 100 between the folding layer and the surrounding matrix. Top to bottom represents increasing shortening. Lines represent the orientation and magnitude (indicated by line length) of the major principal strain for the infinitesimal (a, e, and k), finite (c, h, and o) and incremental strain measures (b, f, g, l, m, and n). The amount of strain recorded by the later strain measure is indicated above the respective snapshots. d, i) and p) show the orientation of initially vertical passive marker lines.

Since all strain measures result in similar divergent fan patterns in the matrix at the outer arc of the fold (Figure 2), these patterns do not necessarily reflect the finite strain. In the stronger layer differences of the convergent fans between the different strain measures are identified. The main difference is associated with a 90° major principal strain rotation from a layer-perpendicular to a layer-parallel orientation at the outer arc, which was also observed in one of the studied natural folds (Figure 3). However, because in natural folds a bedding-parallel foliation is challenging to identify as it may coincide with sedimentary structures, also the convergent foliation fan pattern in natural folds is not very well suited for strain estimates.

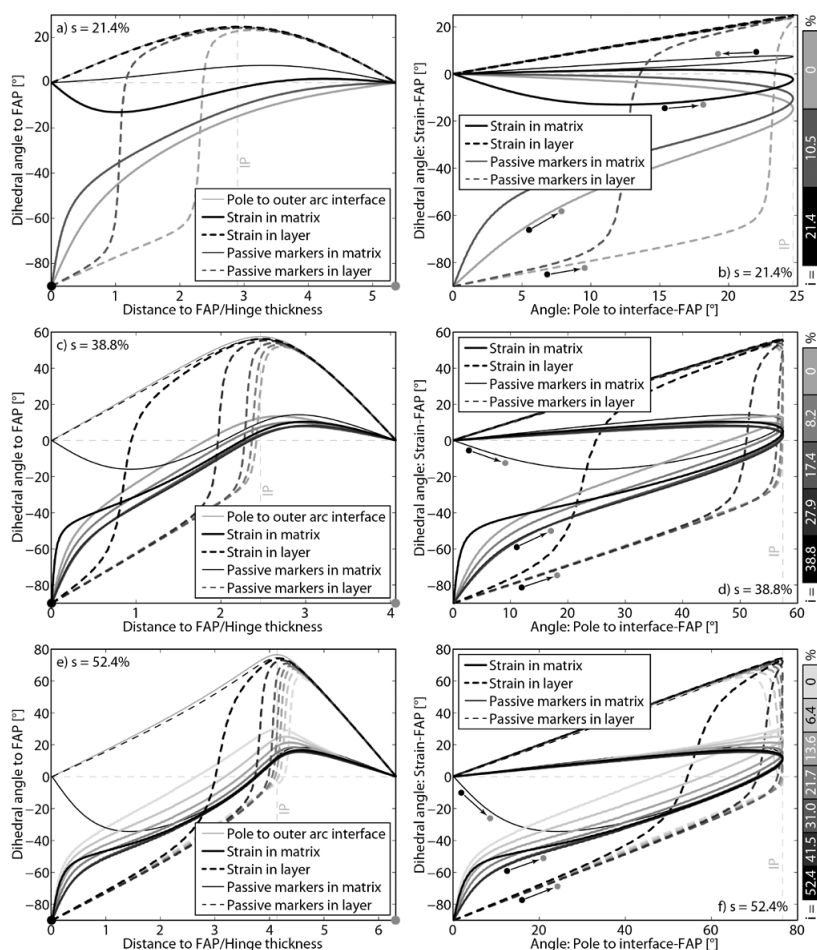


Figure 2. Strain and fold interface orientation data for the simulation in Figure 1. Line gray levels represent different strain measures (black: finite strain, lightest gray: infinitesimal strain, intermediate gray: different incremental strains). Positive values indicate a convergent fan; negative values a divergent fan. IP: Inflection point. a), c), e) Angle between major principal strains and fold axial plane (FAP) plotted versus normalized distance from FAP. b), d), f) Angle between major principal strains and FAP plotted versus angle between pole to fold interface and FAP. Arrows indicate the direction from antiform to synform.

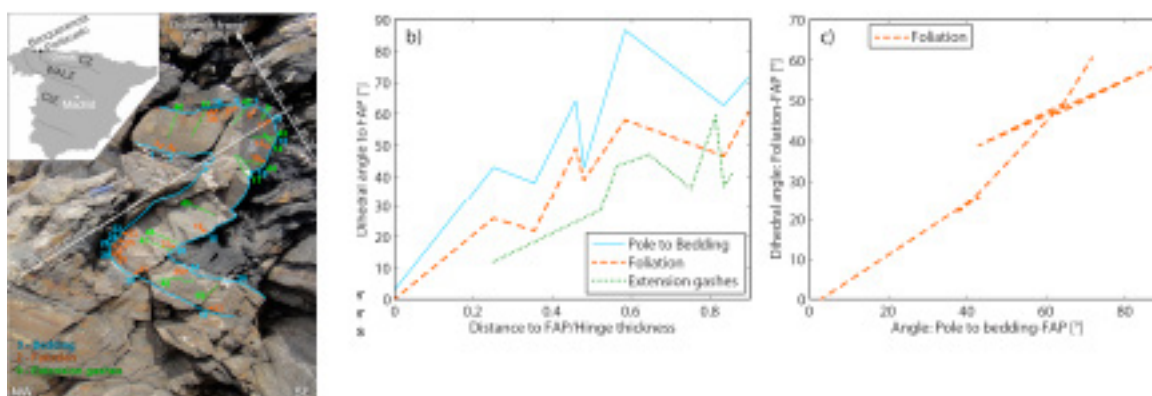


Figure 3. a) Outcrop at Portizuelo, NW Spain. Orientation of bedding, foliation, and extension gashes (b and c) were measured at the positions indicated by numbers in a) within the sandstone and plotted in the same way (b and c) as in Figure 2.

REFERENCE

Frehner, M. & Exner, U. submitted: Do foliation refraction patterns around buckle folds represent finite strain?
Geological Society Special Publications

P 2.10

Modeling interactions between tectonic and surface processes in the Zagros Mountain, Iran.

Collignon Marine¹, Kaus Boris², Frehner Marcel¹, Fernandez Naiara², Castellort Sébastien³, Simpson Guy³ & Burg Jean-Pierre¹.

¹ Geological Institute ETH Zurich, Sonneggstrasse 5, 8092 Zurich, (marine.collignon@erdw.ethz.ch)

² Institut für Geowissenschaften, Johannes Gutenberg-Universität, Mainz, Germany.

³ Section of Earth and environmental Sciences, University of Geneva, Switzerland

Introduction

Fold and thrust belts record a variety of landscape forms (e.g. wind/water gaps, diverted rivers), and sedimentary features (e.g. alluvial fans, growth strata), reflecting the competition between tectonics and surface processes. Moreover, this competition plays a key role in the distribution and behavior of fluvial systems and thus affects both the transport and the deposition of sediments from mountains to basins.

Over the past decades, numerous models have been developed to study interactions between tectonics erosion, sedimentation and deformation. However, only a few models are using a fully 3D mechanical representation of the deformation and many issues remain unsolved. For instance, what control does an array of growing folds exert on drainage network development and, conversely, how does river incision influences growing structures? Which physical parameters are essential in predicting and interpreting wind gaps and diverted river features?

Landscape evolution model

The approach taken here is based on Simpsons and Schlunegger (2003) and uses a nonlinear diffusion formulation, which is the simplest mathematical formulation to model erosional processes taking both hillslope and channel processes into account by assuming that the sediment discharge qs is given by

$$qs = k_0 S + cq^n S \quad (1)$$

where k_0 is the hillslope diffusivity, c the fluvial transport coefficient, and n a power law exponent relating the sediment transport to the fluid discharge. qs , and q are the sediment and surface water discharges, respectively, and $S (= |\nabla h|)$ is the local slope.

Governing equations:

The model is governed by a system of two equations with the two unknowns $h(x,y,t)$ and $q(x,y,t)$, the topography and the magnitude of surface fluid discharge, respectively. The masses of moving sediments and surface water are conserved, which yields:

$$\partial h / \partial t = - \nabla \cdot (\mathbf{n}qs) \quad (2) \quad \text{and} \quad \nabla \cdot (\mathbf{n}q) = \alpha \quad (3)$$

where $\mathbf{n} (= -\nabla h / S)$ is a unit vector directed down the surface, and α the effective rainfall. Substituting equation (1) into equation (2), the system can be written as

$$\partial h / \partial t = \nabla \cdot ((k_0 + cq^n) \nabla h) \quad (4), \quad \text{where } k_0 + cq^n \text{ has the dimensions of a diffusion coefficient and } \nabla \cdot (\nabla h / |\nabla h|) = -\alpha \quad (5)$$

The system is solved by the finite element method on an irregular triangle mesh. Equation (4) is discretized on 3 nodes triangle using linear shape functions, and equation (5) is solved using a discrete water flow routing algorithm (also called D8 method). This method consists on routing progressively both sediment and fluid down the computed drainage area between discrete neighbors from the highest to the lowest elevation. This algorithm is computationally efficient but suffers from significant grid dependency.

Preliminary results

Velocities in z-direction, obtained from a 3D multilayer folding simulation of the thermo-mechanical code LaMEM were used as uplift rates in the landscape evolution model (Figure 1), to simulate the effect of more realistic uplift rates on erosion, without feedback of erosion to deformation.

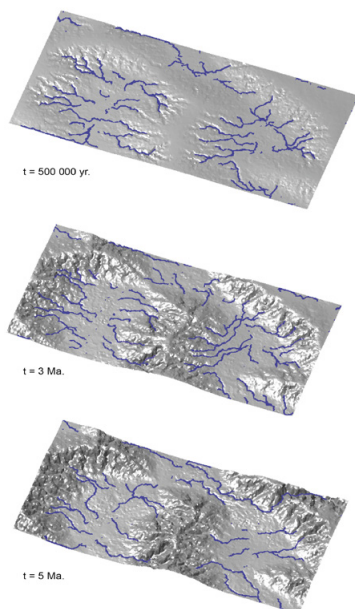


Figure1

REFERENCES

Simpson, G. & Schlunegger, F. 2003: Topographic evolution and morphology of surfaces evolving in response to coupled fluvial and hillslope sediment transport, *Journal of geophysical research*, 108, 7-1 – 7-16

P 2.11

Kinematic Investigation of the Central Alborz Mountain belt

Bahiraie Sareh¹, Abbasi Mohamadreza²

¹ Science and Research Branch Islamic Azad University. Earth Science Department, Hesarak, Tehran, Iran; P.O. Box 1477/893855 (sara_bahiraee@yahoo.com)

² International Institute of Earthquake Engineering and Seismology. Farmanie St. Dibaji shomali Ave, Arghavan Alley, No 21, P.O. Box 3913/19395

The compressional faults and overturned anticlines with East-West trend are the most important structural features in the Alborz Mountain belt. One of the major reverse faults which plays an important role in the evolution of the Alborz is the Mosha fault. It locates in the southern part of the Alborz mountain belt. The Mosha fault separates Paleozoic successions in the North from the southern Cenozoic deposits. The Kinematic history of the Mosha fault is investigated as a representative of the central part of the Alborz. More than 200 fault planes included striations are measured over of the Mosha fault along two transverse river valleys and one parallel outcrop (figure 1). These field observations are used to obtain the occurred stress fields by using inversion method. The field observations are processed all at once and also separately for each measured sections. The result of both ways of investigations implies two distinct stress fields with different trends (NW-SE and NE-SW) (figure 2). Furthermore, the spatial direction of stress vectors (δ_1 and δ_3) are obtained for each stress fields. On the basis of the result, the southern part of the Alborz Mountain belt experienced two major stress fields which probably driven by different tectonic events. Indeed, the spatial location of the δ_1 is rotated clock wise through the geological time. The Mosha fault displacement mechanism is changed from right-lateral reverse (dextral) fault to left-lateral reverse (sinistral). These stress directions appear in transpiration tectonic, and they overcome compression regime to strike slip regime. The ages of stress changes are determined by using the cross cutting relations of individual fault planes. The dextral system is occurred as a result of the movement of the Arabian plate toward the North. This age is determined to be Miocene and probably older. The sinistral system originates from structural transition of Alborz Mountain because of the progressive deformation in Alborz. At present, most of the movements on the Mosha fault show a contribution of sinistral and reverse faulting.

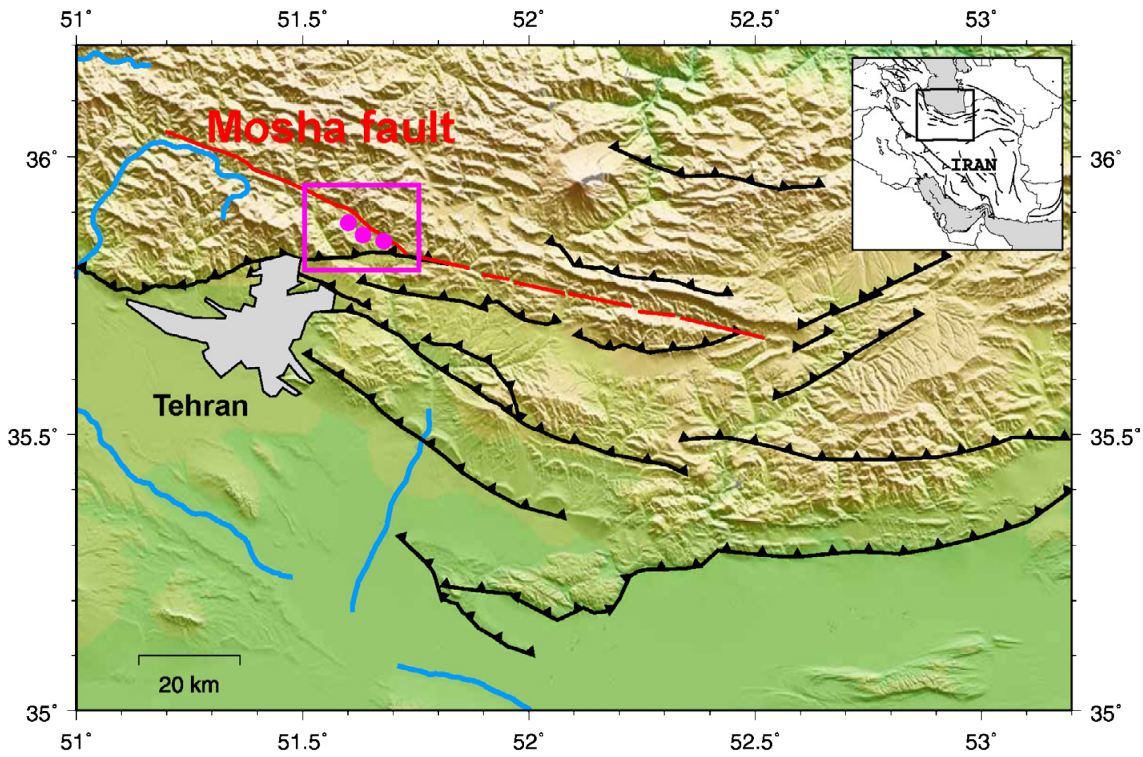


Figure 1: The digital elevation map combined with major faults. The Masha fault is shown in red, the studied area and three investigated sections are shown in pink.

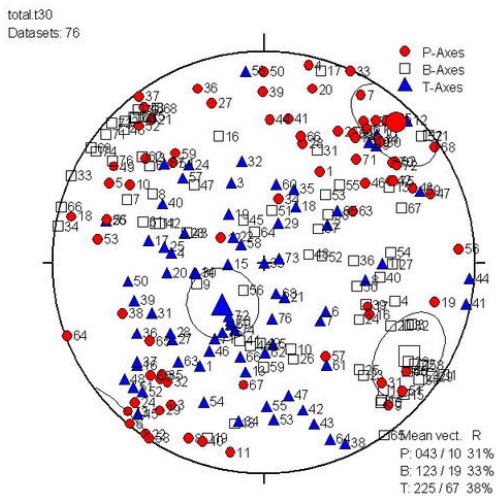


Figure 2: Two distinct stress fields with different trends

REFERENCES

- Angelier, J. 1994: Fault slip analysis and paleostress reconstruction in Hancock, Continental deformation, pergamon press, Oxford, p.53-100.
- Axen, G. J. 2001: Exhumation of the west-central Alborz mountain, Iran, caspian subsidence, and collision-related tectonics. Geol V.29 ; no.6 ; 559-562 Geological map, 1995, east of Tehran, scale: 1:100000, GSI
- Fry, N. 2003, A geometric test for possible Andersonian stress using striated faults. Journal of structural geol, 25, 897.
- Tatar, M. et al. 2012: Microseismicity and seismotectonics around the Masha fault (Central Alborz, Iran). Tectonophysics 544-545; 50-59.

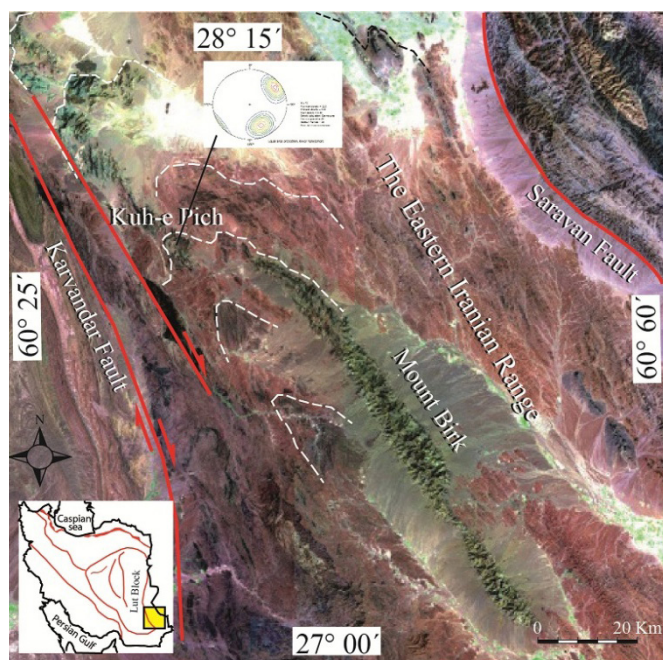
P 2.12

Cenozoic deformation of Mount Birk: A key to restoring of Iranian Baluchestan tectonic history

Bagheri Sasan¹, Damani Gul Shamsoddin¹ & Jafari Safieh¹

¹Department of Geology, University of Sistan and Baluchestan, Zahedan, Iran

Mount Birk is a continental ribbon composed of platform deposits mainly late Cretaceous in age is situated through the Eocene deep-water siliclastic turbidites, the eastern flysch, about 100 km in the north-west direction in Iranian Baluchestan (Fig. 1). There is not any consensus on the origin of Mount Birk. A group of researchers considers this outcrop as the deeper parts of the flysch basin, another group consider as the eastern continuation of the Sanandaj-Sirjan Zone, others believe in a separate microcontinent (McCall, 2002), and finally, the rest attributes to a suspect terrane. Here, we try to use some of structural evidences inside and around of Mount Birk to restoring its previous position may be helping to shed light on the tectonic history of the southeastern Iran. Our structural studies including field works as well as satellite image observations show that the northwestern continuation of Mount Birk discontinuously exposes again in Kuh-e Pich, where its trend completely turns back toward south and makes a closed upright to inclined plunging anticlinorium. The same and parallel curved structures can be observed both toward south of Kuh-e Pich in the ophiolitic mélangé of east of Iranshahr, and in direction of northwest near west of Khash in the crystallized limestone with probable age of Permian. This huge curved structure was geometrically appeared such as a similar macrofold which at its axial surface there are several mesofolds and refolding structures confined to the west by the Karvandar right-lateral strike-slip shear zone and from east to the Saravan fault. We think such huge structure could not have been constructed by simple folding during closure of the eastern flysch basin. The dome-and-basin structures distributed in this zone demonstrates at least two periods of folding with perpendicular axial surfaces have occurred since the late Cretaceous time. Exploration of Middle Eocene fossiliferous shallow-water limestone exotic blocks inside a serpentine matrix at slopes of Mount Birk yields a late Eocene to Oligocene age for the most robust episode of mélangé generation. We propose this curved structure which occupied more than half of the Eastern Iranian Range wideness could have been formed during the anti-clockwise rotation of the Central-East Iranian Microplate around a vertical axis relative to preliminary position of the subduction zone south of the Eurasian margin. This rotation which is confirmed by few old paleomagnetic reports (e.g. Conrad et al., 1982) was happened synchronous with the India-Eurasia collision event (Bagheri, 2008) when the Central Afghanistan Block westwardly escaped



and pushed the accretionary prisms away toward the margin of the Lut Block and rotated them in a wedge-shaped basin with a sharp nose toward north probably in a clockwise direction. Since the stratigraphy of the Mount Birk is similar to the Lut Block at the Nehbandan area, few hundred kilometers toward north, we suggest during this amalgamation incident it may narrow ribbons of the Lut Block were detached from its eastern edge along the right lateral strike-slip faults such as the West Neh Fault, incorporated into the accretionary prisms and squeezed and folded between two large blocks of Lut and Central Afghanistan. By this model we may be able to explain why the wideness of the Eastern Iranian Range gets larger toward south. Afterwards, the effects of Iran-Arabia plate collision in this area were reactivity of the Karvandar shear zone and shaving of the southwestern limb of the mentioned curved structure as well as distribution of minor conjugate strike-slip faults and folding of continental Neogene beds.

Figure 1: Satellite image of Mount Birk and distribution of the structural trends around it.

REFERENCES:

- Bagheri, S., 2008, Anticlockwise rotation of the Central-East Iranian Microcontinent and the Eurasian-Indian collision, STT-06 Marine and Continental fold and thrust belts, The 33rd International Geological Congress, Oslo, Norway.
- Conrad, G., Montigny, R., Thuizat, R. and Westphal, M., 1982. Dynamique cénozoïque de "Bloc du Lut" (Iran) d'après les données paléomagnétiques, isotopiques et structurales. *Géologie Méditerranéenne*, IX, n° 1: 23-32.
- McCall, G.J.H., 2002. A Summary of the Geology of the Iranian Makran. In: P.D. Clift, D. Kroon, C. Gaedicke and J. Craig (Eds.), *The tectonic and climatic evolution of the Arabian Sea Region*. Geological Society, London, Special Publication, pp. 147-204.

P 2.13

Sandstone detrital mode and heavy mineral study in the Makran accretionary wedge, southeast Iran: implication for the tectonic setting

Mohammadi Ali, Winkler Wilfried & Burg Jean-Pierre

*Geological Institute, ETH-Zentrum, Sonneggstrasse 5, 8092 Zurich, Switzerland
(ali.mohammadi@erdw.ethz.ch)*

The Makran accretionary prism results from the convergence between the Arabian and Eurasian plates, which was initiated during the Late Cretaceous. Today, the system is characterized by great sediment thickness (> 7 km) in the foreland of the Oman Sea and a wedge width of > 500 km, > 300 km of which are exposed onshore. The clastic sedimentary record is useful for monitoring the long lasting history of the supplying Makran chain. Provenance analysis of sediments is aimed at reconstructing the parent-rock assemblages of sediments and the tectonic setting conditions under which sediments formed.

Samples collected from different units span the regional stratigraphy from Upper Cretaceous to Miocene. Point counts of 25 sandstone thin sections were performed following the Gazzi-Dickinson method (e.g. Dickinson & Suzek 1979). 300-400 points were counted in each thin section. For heavy mineral study we selected 17 samples. 200-300 grain were identified and counted in each sample.

The sandstones are classified as feldspathic litharenites and litharenites. In majority feldspar is plagioclase (> 90%) with minor amounts of K-feldspar. Most quartz grains (75%) are mono-crystalline but poly-crystalline quartz (maximum 25%) and minor amounts of foliated tectonic quartz occur. Rock fragments are represented by sedimentary, volcanic and metamorphic grains. Volcanic grains mostly are andesites and glasses. Extrabasinal sedimentary lithic grains are mostly sandstone, siltstone, limestone and dolomite. Metamorphic lithic grains are generally low-grade schists and phyllite. In various compositional ternary diagrams, the sources of the sandstones plot in the transitional to dissected arc and recycled orogenic fields. These preliminary detrital mode analysis show that the Makran sandstones were supplied from mixed source terranes including older orogenic basement and presumable continental arc rock series.

Heavy mineral suites show a highly variable composition (Fig. 1) including (1) a group of ultrastable minerals (zircon, monazite, tourmaline, rutile, brookite, anatas and sphene) deriveable from shallow granitic continental crust, (2) metastable minerals delivered from variable metamorphic-grade source rocks (epidote group, garnet, staurolite, chloritoid, kyanite, andalusite, blue amphibole), (3) chromian spinel from ultrabasic (serpentinite) rock sources, (4) common hornblende either supplied from metamorphic or igneous series, and (5) a local pyroxene-rich source in the basal sandstone formation overlying pillow lavas (Fig. 2). It is worth noting that in several samples 5-20% of blue amphiboles occur, which indicate the presence of high-p/low-T metamorphic rocks in the detrital source areas.

The Makran area is critical with regard to the Himalayan orogeny. Earlier works (e.g. Critelli et al. 1990) suggested that pre-Miocene sediments in the Pakistanian Makran were supplied from the Himalaya, whereas Miocene to Recent deposits were formed by reworking (canibalism) of older sediments of the accretionary wedge. Our present data would not support this idea. We instead find subduction-related detrital sources in older orogenic basement and a continental volcanic arc (U-Pb dating of detrital zircons in progress). In addition, an other portion of the clastic material most-likely has been derived from the blueschist-bearing Makran ophiolitic belt.

REFERENCES

- Critelli, S., De Rosa, R., Platt, J.P. 1990: Sandstone detrital modes in Makran accretionary wedge, southwest Pakistan: implication for tectonic setting and long-distance turbidite transportation. *Sedimentary Geology*, Vol. 68. Pp 241-260
- Dickinson, W.R., Suzek, C.A. 1979: Plate tectonics and sandstone compositions. *American Association of Petroleum Geologist*, 63, 2164-2182.

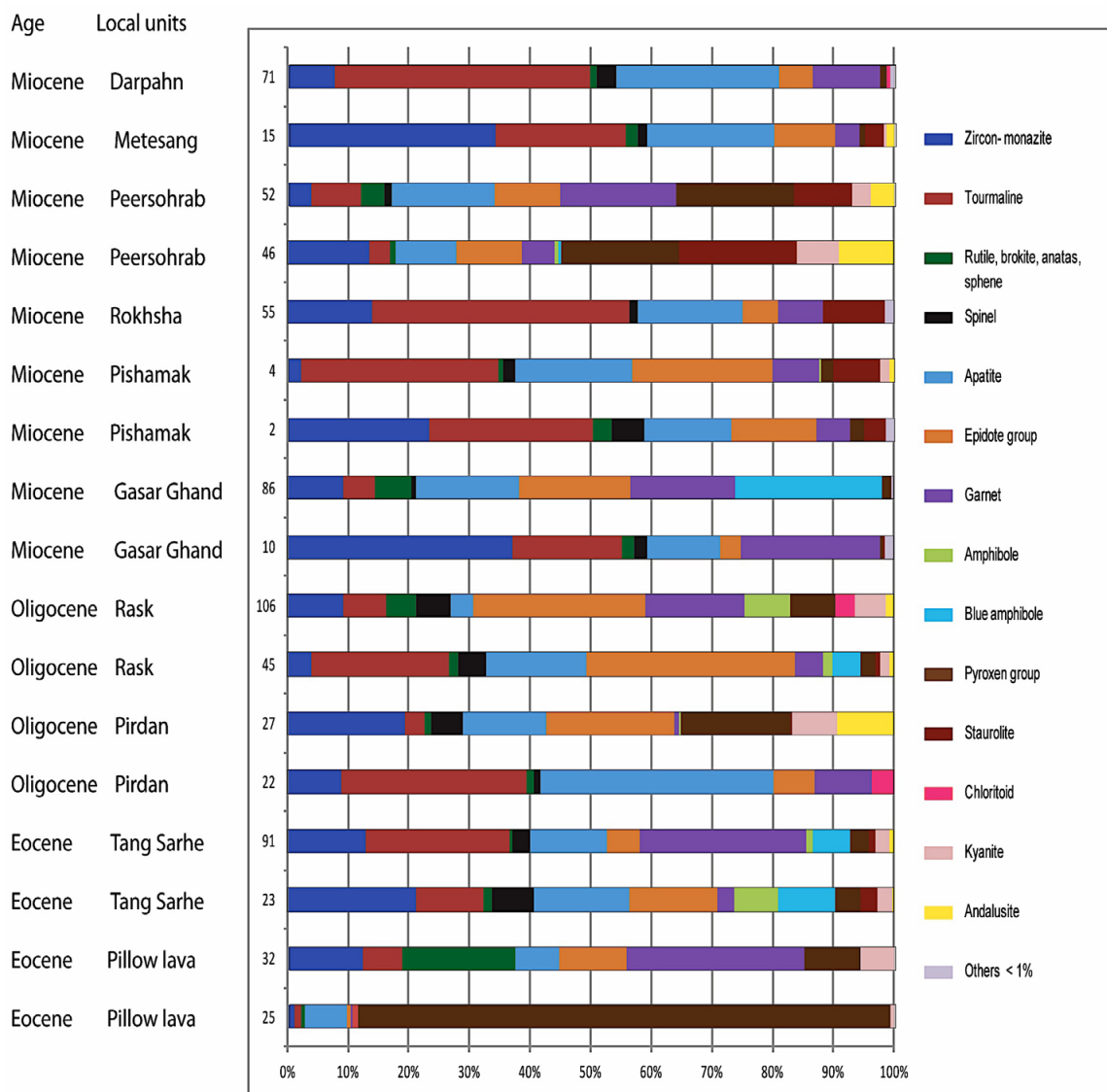


Fig. 1: Heavy minerals distribution in Eocene to Miocene units of Makran accretionary wedge. The work is supported by the Swiss National Science Foundation project no.2-77644-09.

P 2.14

The Cretaceous-Palaeogene (K/Pg) boundary: cyclostratigraphic and U-Pb zircon geochronological constraints

Ben D. Heredia¹, Frits Hilgen², Jon R. Gaylor³, Klaudia Kuiper² & Klaus Mezger¹

¹*Institute of Geological Sciences, University of Bern, Baltzerstrasse 1+3, CH-3012 Bern (benjamin.heredia@geo.unibe.ch)*

²*Faculty of Geosciences, University of Utrecht, Utrecht*

³*University Paris-Sud Laboratory IDES, University Paris-Sud, Paris.*

The boundary between the uppermost Maastrichtian and lowermost Danian has been in constant debate. This is because its closest relation to a large asteroid impact at Chicxulub, Mexico, which may be the cause for the latest mass extinction. However, since the impact discovery and subsequent definition at the base of the boundary clay at El Kef, Tunisia, several attempts have been made to constraint its age. Uncertainties in the computation of Earth's orbital parameters beyond 40 Ma (including a gap in the astronomical tuning for the Eocene) and radiometric age constraints by Ar-Ar dating (and its limited accuracy) have led to a widespread of studies with geochronological tie-points and derivative age models that are different and of variable quality.

We have here derived with an unprecedented study combining independent numerical dating techniques for the boundary, aiming to contribute with the tuning of such an important event in Earth's history.

The uppermost part of the Horseshoe Canyon Formation in southern Canada, shows well-preserved cyclic alternations of organic material, silt and sandy horizons, in which altered volcanic ash-layers are abundant. Rationale is that if the deposition of these alternations was controlled by sea-level changes, it will be possible to "pin-down" the astronomical imprint and we would be able to tie it in with radiometric age constraints. After decomposing the stratigraphy into the time-frequency space by wavelet analysis, it has been observed that the section has a strong precession-frequency signal, matching the observations in the field. A thick volcanic ash-layer containing zircon grains was found ~30 cm above the K-Pg boundary, which in the area is placed at the bottom of a thick coal seam (Coal nr. 13 or Nevis Coal). 11 zircon grains have been dated from this ash-layer using isotope dilution-thermal ionisation mass spectrometry (ID-TIMS). Single grains and grain fragments ²⁰⁶Pb/²³⁸U dates range from 65.69 to 66.27 Myr with 2σ uncertainties of 0.16 to 0.3%. 6 analyses have a weighted mean of 65.74±0.03 Ma with a mean square of the weighted deviates (MSWD) that satisfies the null-hypothesis, when analysing the distribution of ages by weighted mean statistics. We therefore suggest this age as the age for the boundary.

This research has been funded by the European Community's Seventh Framework Program (FP7/2007-2013), under agreement no. 215458.

P 2.15

The breccias of Sambosan Accretionary Complex (southwestern Japan): tectonic vs depositional origin

Peybernes Camille¹, Martini Rossana¹, Chablais Jérôme²

¹ University of Geneva, Department of Geology and Paleontology, Rue des Maraîchers 13, CH-1205 Geneva, Switzerland-
Camille.Peybernes@unige.ch

² Geneva Petroleum Consultants International, CH-1211 Geneva 1, Switzerland

The Sambosan Accretionary Complex (SAC) is a Late Jurassic to Early Cretaceous subduction-generated accretionary complex that crops out in southwestern Japan (Honshu, Shikoku and Kyushu) and in the Ryukyu Islands. In Shikoku and Kyushu the SAC is composed of several units of limestone, basalt, breccia, chert, and mudstone. These units are interpreted as atoll-type limestones, intra oceanic seamount basalts, seamount flank deposits, pelagic siliceous sediments and trench-fill sediments respectively. According to the Ocean Plate Stratigraphy concept (Wakita & Metcalfe 2005), most of these units represent accreted remains of panthalassic seamounts capped by Upper Triassic atoll-type carbonates.

In March 2012, we visited 9 localities along the Sambosan Accretionary Complex in Shikoku and Kyushu. In each locality various polygenic breccias composed of clasts of basalt and/or limestone and/or chert in a volcanoclastic or chert matrix occur.

Several studies provide a theoretical frame for description and interpretation of SAC breccias. For example, according to the size and distribution of clasts, some breccias are considered to be debris flows (granule to pebble size clasts) or debris avalanches (pebble to boulder size) deposited at the toe of seamount flanks.

Although origin of some breccias is quite well known, more particularly in Kyushu (Onoue & Stanley 2008, Chablais et al. 2010), others breccia features remain puzzling. Indeed, in the Wajiki area (eastern Shikoku), a breccia complex exhibiting reefal limestone clasts floating in a microbrecciated chert matrix lacks reliable interpretation.

To explain breccia formation two hypotheses are generally considered: (1) a tectonic origin, related to the subduction/accretion of the seamount (Okamura 1991, Sano & Kanmera 1991); (2) collapse of the atoll-type carbonate platform, including predominantly reefal limestones on the seamount flanks before the subduction event (Onoue & Stanley 2008). The former correspond to non-depositional breccias, the second to depositional breccias.

In the SAC, geological units are often chaotically associated due to accretional processes. Therefore, this geological frame makes difficult the recognition of depositional or tectonic breccias.

To improve our understanding of seamounts history, we want to test these two hypotheses for the breccias found in Shikoku. In order to achieve this objective, a detailed classification of the different kinds of breccia based on fabrics, clast facies and matrix composition is needed. Therefore, field observations, mapping and thin section analysis will be performed on breccia outcrops including samples on both the matrix and clasts.

The first observations show that clasts exhibit similar facies and fauna in different breccia outcrops, today located hundred kilometers from each other (e.g. typical *Peronidella* sponge reefal clasts).

It is important to be noticed that in the SAC, limestones are often strongly recrystallized. However, in breccias, limestone clasts are relatively well preserved. This enhanced preservation improves facies analysis and thereby, could allow more accurate reconstruction of the paleoenvironments of panthalassic seamounts during the Triassic.

REFERENCES

- Chablais, J., Martini, R., and T. Onoue. 2010: Aulotortus friedli from the Upper Triassic gravitational flow deposits of the Kumagawa River (Kyushu, Southwest Japan), *Paleontol Res*, 14, 151-160.
- Onoue, T., and G. D. Stanley. 2008: Sedimentary facies from Upper Triassic reefal limestone of the Sambosan accretionary complex in Japan: mid-ocean patch reef development in the Panthalassa Ocean, *Facies*, 54, 529-547.
- Sano, H., Kanmera, K. 1991: Collapse of ancient oceanic reef complex- What happened during collision of Akiyoshi reef complex?- Sequence of collisional collapse and generation of collapse products, *Journal of the Geological Society of Japan*, 97, 631-644.
- Wakita, K., Metcalfe, I. 2005: Ocean Plate Stratigraphy in East and Southeast Asia, *J Asian Earth Sci*, 24, 679-702.
- Okamura, Y. 1991: Large-Scale Melange Formation Due to Seamount Subduction: An Example from the Mesozoic Accretionary Complex in Central Japan, *The Journal of Geology*, 99, 661-674.

P 2.16

Investigation of deep geological structures in the north-west part of Canton of Neuchatel using a combination of gravity and 3D geological model

Abdelfettah Yassine¹, Mauri Guillaume¹, Pascal Kuhn¹, Schill Eva¹ & Vuataz Francois-David¹

¹ Centre for Hydrogeology and Geothermics (CHYN), University of Neuchâtel, Emile-Argand 11, CH-2000 Neuchâtel (yassine.abdelfettah@unine.ch)

Pioneer work on the Atlas of gravimetry (Klingelé & Olivier, 1980) has allowed the scientific community to discover that the underground structure of Switzerland was affected by significant gravity variation within the Jura Mountain, and in the Molassic plateau. While some of the gravity decreases are clearly associated to sedimentary deposit during the post-Mesozoic period, source of decrease of gravity in other part cannot be explained using the existent knowledge on current geophysical and geological information. More recent work on reinterpretation of seismic profiles within the frame of the Seismic Atlas of Switzerland (Sommaruga et al., 2012) has shown the existence in some area of permo-carboniferous graben below the Mesozoic sedimentary pile. These grabens are also highlighted using gravity exploration in the 80-ties by Klingelé and Schwendener (1984), in the northern part of Switzerland.

The study presented here investigates the possibility of permo-carboniferous graben within the Jura Mountain in the north-west part of canton of Neuchâtel. The investigated area go from the French border in the west, to west of La Chaux-de-Fonds. To better understand the origin of deep geological structures, a new gravity data set has been collected along a profile overlapping one of the seismic profiles, which come from the Seismic atlas of Switzerland.

Gravity has been collected with a sampling step of 200 m and the data set has been combined with the gravity database of the gravimetry Atlas of Switzerland. A gravity data set from the BRGM was also used to cover the French area. Special considerations were taken in account to merge both Swiss and the French database. Two techniques were used to validate this compilation; i) using a geostatistical approach, and ii) using the means value of the neighboring measurements within a specified radius. In the end, a complete Bouguer anomaly computed at the same ellipsoid is obtained for the whole studied area. As this Bouguer anomaly is strongly dominated by the regional trend, caused by the sedimentary layer and by the deepening of the cristallin basement, a Betterworth filter (Abdelfettah and Schill, 2012) using different wavelength is applied to get a residual anomalies which are ready to be interpreted.

In order to explain the large negative anomaly observed in the center of the interesting area, a 3D geological model has been build using available information (e.g. Sammaruga, 1997). However, due to limited information in this area, uncertainties remain on the depth of the deep structure. In order to investigate the crystalline basement and determine the possibility of a permo-carboniferous graben, a simplification of the sedimentary formation of the Mesozoic period has been done by grouping them into a fewer number of units. This simplification is justified by the important size of the geological model which reach ~65x50 km. The obtained 3D geological model has then been used to calculate the theoretical gravity response by doing a 3D forward modeling.

Gravity survey results confirm the existence of decrease of ~8 mGal in the south of Le Locle (NE), which was previously highlighted in the gravimetry Atlas of Switzerland. The general regional trend is well recovered by the geological model, although that the dynamic of the computed Bouguer anomaly remain smaller than the observed Bouguer anomaly. A constrained inversion is achieved on the basis of the geological model and a density values, which minimize the misfit between the observed and the computed Bouguer anomalies, is recovered. This misfit remains important especially in the center of the model. A stripping of the known structures is achieved and the gravity effect for each unit is removed. In the end, we show that the observed residual anomaly cannot be explained without using a permo-carboniferous graben in the basement, where this negative anomaly remains unresolved.

REFERENCES

- Abdelfettah Y. & Schill E., 2012. Delineation of geothermally relevant Paleozoic graben structures in the crystalline basement of Switzerland using gravity. Submitted to Society of Exploration Geophysics meeting, Istanbul, 2012.
- Klingelé, E. and Olivier, R., 1980. Die neue Schwere-Karte der Schweiz (Bouguer- Anomalien), Bern.
- Klingelé, E. & Schwendener H., 1984. Geophysikalisches Untersuchungsprogramm Nordschweiz: Gravimetrische Messungen 81/82, Nagra, Baden.
- Sommaruga, A., 1997. Geology of the central Jura and the molasse basin: New insight into an evaporite-based foreland fold and thrust belt. Dissertation. Univ. Neuchâtel.
- Sommaruga A., Eichenberger U. & Marillier F., 2012. Seismic Atlas of the Swiss Molasse Basin. 24 Tafeln. ISBN 978-3-302-40064-8.

P 2.17

The Born Engelberg Anticline (Eastern Jura Mountains): New insights from balanced cross sections and 3D modelling

Arndt Dirk¹, Jordan Peter¹ & Madritsch Herfried²

¹Böhringer AG, Mühlegasse 10, CH-4104 Oberwil (dirk.arndt@boe-ag.ch)

²Nationale Genossenschaft für die Lagerung radioaktiver Abfälle, Hardstrasse 73, CH-5430 Wettingen

The Born-Engelberg-Anticline is one of the most distinctive structures of the Eastern Jura-fold-and-thrust belt, characterized by an isolated location in the Molasse basin to the south of the main Jura Mountain range (Fig.1). The internal structure of the anticline and its kinematic significance during the formation of the Jura fold-and-thrust belt has been discussed controversially (e.g. Bitterli 1979; Ziegler et al. 1995) and is still unrevealed (Jordan et al. 2011).

The wide anticlinal arch of the Born-Engelberg is built up by Upper Jurassic limestones. In the hinge zone it reaches an elevation of more than 1000m above the lateral projection of the presumed decollement level within Mid-Triassic evaporites. A straight forward depth extrapolation of the structure based on outcrop data thus leads to volumetric problems in the core of the anticline. Ziegler et al. (1995) suggested a crystalline horst structure to solve this problem and as consequence argued against the distant-push hypothesis (Laubscher 1961). Bitterli (1979) postulated Muschelkalk imbrications in combination with a moderate basement high.

Another important aspect regards the formation timing of the Born-Engelberg Anticline. The watergap of the Aare-Klus and several higher located and hence presumably older windgaps are antecedent with respect to the anticline's axis. Considering the regional drainage system evolution this could possibly point toward a comparatively young formation age

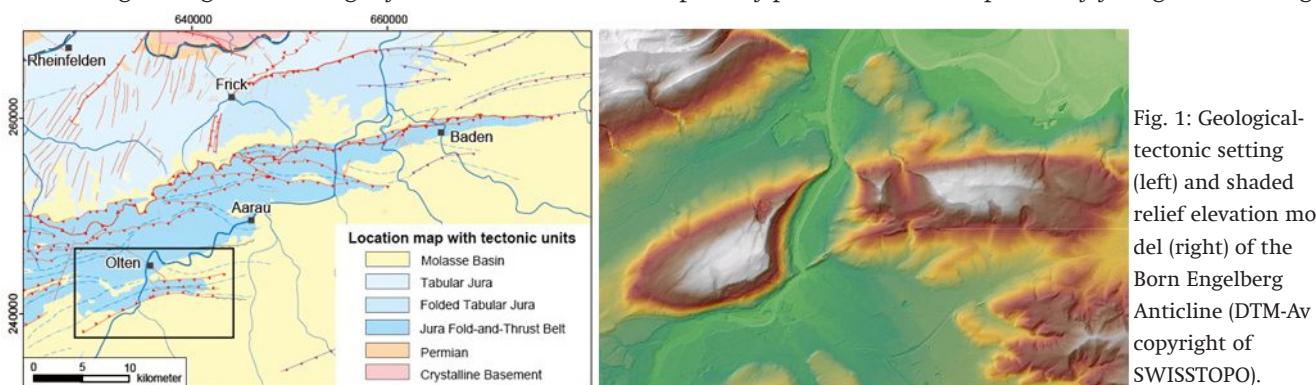


Fig. 1: Geological-tectonic setting (left) and shaded relief elevation model (right) of the Born Engelberg Anticline (DTM-Av copyright of SWISSTOPO).

The open scientific questions outlined above and the close vicinity of the Born-Engelberg Anticline to one of the potential siting regions for a deep geological repository proposed by Nagra led to a tectonic re-investigation of the structure applying state of the art structural geological analysis tools. Based on newly available high resolution geological maps (Jordan et al. 2011) and reprocessed, depth migrated reflection seismic data balanced cross sections were constructed using the Move-software suite (Midland Valley). Together with additional geological information from boreholes, structural geological field measurements and recently acquired new seismic data the sections were used to develop a structural geological 3D model of this area, using the GOCAD software (Paradigm). The 3D-compilation of these different data was then used to check the 2D- cross sections on coherence and revise them if necessary.

The 3D model provides a coherent big picture for the Born-Engelberg-Anticline avoiding isolated 2D-interpretations that often lack lateral coherency. As a next step, it is anticipated to perform forward modelling of the lateral coherent cross sections to learn more about the kinematics of the Born-Engelberg structure. Together, the results make a significant contribution for a better understanding of the kinematic processes in this area during the orogenesis of the Jura fold-and-thrust belt.

REFERENCES

- Bitterli, P. 1979: Standortgebiet Born, Strukturanalyse der Born-Antiklinale, Nagra, Interner Bericht.
- Jordan, P., Graf H.R., Eberhard, M., Jost, J., Kälin, D. & Bitterli-Dreher, P.H. 2011: Blatt 1089 Aarau. Geol. Atlas Schweiz 1:25 000
- Laubscher, H. 1961: Die Fernschubhypothese der Jurafaltung, *Eclogae Geol. Helv.*, 54, 222 – 282.
- Ziegler, P.A., Cloetingh, S., & van Wees, J-D. 1995: Dynamics of Intra-plate Compressional Deformation: The Alpine Foreland and other Examples. *Tectonophysics* 252: 7–59.
- Ziegler, P.A. & Fraefel, M. 2009: Response of drainage systems to Neogene evolution of the Jura fold-thrust belt and Upper Rhine Graben. *Swiss Journal of Geosciences* 102: 57–75.

P 2.18

To what extent have inherited normal faults influenced thrust propagation at the front of the easternmost Jura fold-and-thrust belt?

Malz Alexander¹, Madritsch Herfried², Meier Beat³, Heuberger Stefan⁴, Navabpour Payman¹ & Kley Jonas⁵

¹ Friedrich-Schiller-Universität Jena, Institut für Geowissenschaften, Burgweg 11, D-07749 Jena (alexander.malz@uni-jena.de)

² Nagra, Hardstraße 73, CH-5430 Wettingen

³ Interoil E&P Switzerland AG; Seefeldstraße 287, CH-8008 Zürich

⁴ geosfer-ag, Büro für angewandte Geologie, Glockengasse 4. CH-9000 St.Gallen

⁵ Georg-August-Universität Göttingen, Geowissenschaftliches Zentrum, Goldschmidtstr. 3, D-37077 Göttingen

The formation of the Jura fold-and-thrust belt in the foreland of the Central Alps is widely accepted to be caused by thin-skinned deformation (Laubscher, 1961). The major structures of the range are considered to have been formed in Late Miocene times as in-sequence thrust faults over a subhorizontal basal detachment (décollement) located within evaporites of the Middle Muschelkalk Formation (Lower Triassic) while the basement underneath the basal detachment was not involved in deformation. In northern Switzerland the basement underlying the easternmost Jura fold-and-thrust belt is dissected by a deep trough system of Carboniferous to Permian age that is documented by several deep wells and seismic reflection data. The Oligocene to Early Miocene reactivation of normal faults bounding the trough system is clearly documented by normal offsets within the Tertiary Molasse sediments (Laubscher, 1986). It is suspected that the deep trough system could also have been reactivated in a compressional/transpressional manner in the course of the later formation of the Jura fold-and-thrust belt, which would mark a change from thin-skinned to thick-skinned tectonics (e.g. Ustaszewski and Schmid, 2007).

Here we present selected new interpretations of recently reprocessed and depth migrated seismic reflection profiles, which are verified by classical balancing methods of equal bed length and constant area and conceptual kinematic considerations. A focus was laid on the reinterpretation of the most external structures north of the Jura main thrust that interfere with the Permocarboniferous trough system and are thus ideal to test thin- vs. thick-skinned interpretation approaches.

Our results confirm the hypothesis that the deformation of the easternmost Jura fold-and-thrust belt is mostly thin-skinned. The interpretation of thick-skinned deformation is possible in some areas but is most often more ambiguous. Key issues to clarify before a thin- or thick-skinned interpretation are the seismic identification of the décollement and the precise picking of the base Mesozoic reflector. Despite the availability of high quality seismic reflection data both tasks are often very difficult to accomplish. For this reason the development of conceptual models for pre-Jura folding scenarios are essential. The models developed out of our balanced cross sections constrain Mesozoic and Cenozoic normal fault reactivation along the Permocarboniferous trough boundaries resulting in stratigraphic thickness variations. Moreover, the analyses indicate that an offset of the main décollement by pre-existing normal faults potentially favours the presence of basement thrusts in the eastern Jura fold-and-thrust belt. We conclude that even if thin-skinned deformation explains the overall structure, the possibility of thick-skinned thrusting cannot be disregarded as a component of Jura deformation.

REFERENCES:

Laubscher, H. 1961: Die Fernschubhypothese der Jurafaltung, *Eclogae Geol. Helv.*, 54, 222 – 282.

Laubscher, H. 1986: The eastern Jura: Relations between thin-skinned and basement tectonics, local and regional, *Geol. Rundsch.*, 75, 535–553.

Ustaszewski K. & Schmid, S.M. 2007: Latest Pliocene to recent thick-skinned tectonics at the Upper Rhine Graben – Jura Mountains junction, *Swiss J. Geosci.*, 100, 293 – 312.

P 2.19

Deep geothermal exploration of low enthalpy reservoir in the Neuchâtel Jura (GeoNE project) – Use of gravity survey to validate and improve 3D geological models.

Mauri Guillaume¹, Negro Francois¹, Abdelfettah Yassine¹, Schill Eva¹, Vuataz Francois-David¹

¹ *Laboratory for Geothermics (CREGE), Centre for Hydrogeology and Geothermics (CHYN), University of Neuchâtel, Emile-Argand 11, CH-2000 Neuchâtel (guillaume.mauri@unine.ch)*

Within the frame of the GeoNE project, different areas of Neuchâtel canton have been explored to investigate the geothermal potential of deep aquifer. The aim of the GeoNE project is to determine, which areas are more suitable for deep geothermal district heating in the main populated areas of the canton. Supported by the authorities of the canton of Neuchâtel, three regions in the canton have been investigated; the work presented here focus, on the region of Neuchâtel – St-Blaise and the Region of Boudry - Auvernier, which are both along the Lake of Neuchâtel in the southern part of Neuchâtel canton.

In context of sedimentary mountain range, like the Jura mountains, deep geothermal exploration is traditionally done through a combination of geological model and seismic reflection survey, however, this geophysical method is still very expensive and require a heavy organization plan. In order to obtain reliable information on the geology structure at depth with a limited budget, the GeoNE project use extensive gravity surveys combined with geological model based on available data.

The study presented here focusses along the north shore of the lake Neuchâtel, where the geology characterizes the south border to the Jura Range and present relatively complex structures. The structure of the Neuchâtel Jura is composed of thrust-related folds which are crosscut by several strike-slip fault systems. These folds are composed of Mesozoic to Cenozoic cover rocks detached from their pre-Triassic basement. Bedrocks are mainly composed of limestones and marls, which can reach a thickness of several hundred meters. The three main deep aquifers investigated in this area, from the shallowest (≤ 400 m below surface) to deepest (< 2000 m), are the upper Malm, the Dogger and the Muschelkalk.

The present study is based on gravimetry surveys, 3D geological models and 3D gravimetry models to best characterize the underground structures and to find areas where the rock properties would be favourable to geothermal exploitation. This means targets are geological structures (i.e., fault and fractured zone) where permeability and porosity are high in the potential aquifers, allowing a significant flow at the future production wells.

The results indicate that 3D geological models are able to reproduce the expected geological structures with thrust-related folds and which are overcut by strike-slip fault systems and secondary faulting events.

Validation of the 3D geological models has been done through the comparison of forward gravity models with the residual gravity anomaly maps. The comparison indicate that the forward gravity model reproduce quite well the main measured gravity structures, which allow us to validate the 3D geological model.

P 2.20

Exploration of deep low enthalpy geothermal reservoirs in the Neuchâtel Jura (GeoNE project) – 3D geological and thermal modeling of potential aquifers.

Negro François, Mauri Guillaume, Vuataz Francois-David, Schill Eva

*Centre d'Hydrogéologie et de Géothermie (CHYN), Université de Neuchâtel, Emile-Argand 11, CH-2000 Neuchâtel
(francois.negro@unine.ch)*

Within the frame of the GeoNE project, different zones of Neuchâtel canton have been explored to investigate the geothermal potential of deep aquifers using a multi-disciplinary approach. In this context, 3D geological and thermal modeling has been performed in order to select potential drilling sites for geothermal exploitation in the canton.

The canton of Neuchâtel is located in the central part of the Jura fold and thrust belt at the north-western limit of the Molasse basin. The structure of this part of the Jura is a succession of thrust-related folds, composed of Mesozoic to Cenozoic cover rocks detached from their pre-Triassic basement, and limited by several major tear faults. Three main aquifers, representing potential geothermal reservoirs, are recognised within the cover series in this area. These are from top to bottom: the upper Malm, the Dogger and the upper Muschelkalk.

In order to constrain the geometry of these three aquifers at depth, 3D geological modelling has been performed using 3D Geomodeller software (BRGM, Intrepid Geophysics). Two large models have been realised, a first one in the lake Neuchâtel area, between Neuchâtel and Saint-Blaise, and a second one, in the northern part of the canton, between Le Locle and la Chaux de Fonds. More detailed models have also been realised with further details on the geology and tectonic features, in the zones of potential exploitation of deep geothermal energy. These models have then been used to perform 3D thermal modelling and estimate temperatures in the different aquifers, taking into account the possible effect of cold water circulations in karstic aquifers.

We present the different 3D models and discuss the implications for the potential exploitation of geothermal energy in the Neuchâtel Jura.

P 2.21

Permeable Fault Detection in Deep Geothermal Aquifer Exploration by Soil Gas Measurement

Giroud Niels¹, Vuataz François-David¹ & Schill Eva¹

¹ Centre for Hydrogeology and Geothermics (CHYN), University of Neuchâtel, Emile-Argand 11, CH-2000 Neuchâtel (niels.giroud@gmail.com)

The two key focus points in the exploration for deep geothermal fluids are the inferred temperature and productivity. These two parameters define whether the resource will be economic or not. The productivity is dependent on the permeability of the reservoir, and turns out to be the main factor limiting the number of fully successful geothermal projects in deep aquifers of Switzerland. To improve the capacity to exploit the resources available under our feet, the exploration campaigns aim at localizing fault zones, in which the fracture density naturally enhances the circulation of water. However, traditional methods used to detect fractured zones, either geological or geophysical, give no information on the permeability of the fractures.

The measurement of volatile species in soils has been widely used for detection of ore deposits, and contaminants monitoring, but also for active fault detection and geothermal reservoir localization. Some of the main soil gases used in exploration are CO₂, He and Rn, which all have a specific source. Carbon dioxide is a major gas in soils and groundwater, and is mainly produced by biologic activity and equilibrium with carbonate minerals. However, part of the CO₂ can also originate from mantle degassing or metamorphic processes. Sources of He are the mantle, radiogenic decay in the crust, and the atmosphere, where its concentration is considered homogenous, at 5.24 ppm.

High He fluxes are often found in tectonically active zones, where seismic activity tends to maintain a high permeability in active fractures. These fractures act as preferential conduits for gases trapped in the mantle or the crust, leading to gas concentration anomalies in soils close to the intersection of the fractures with the surface (Baubron et al., 2002). In the framework of an exploration campaign for heat production from deep geothermal aquifers in the canton of Neuchâtel, numerous faults have been detected and localized by geological and geophysical methods. Helium and CO₂ were measured in soil gases along two ~ 800 m long profiles across the fault of St-Blaise, which is one of the major known faults in the prospected area. The gases were sampled through a 10 mm diameter copper tube inserted at ~ 90 cm depth in the soil. The gas was pumped and analyzed for CO₂, together with O₂ and CH₄, by a portable gas analyzer, and gas samples were taken to the lab to be analyzed for He on a mass-spectrometer (leak-detector) on a semi-daily basis. Radon was not considered in this study.

Soil gas concentrations are highly sensitive to meteorological conditions and environmental factors like soil moisture and biological activity (Hinkle, 1994). During the sampling campaign of this study, the meteorological conditions varied from very humid spring weather to dry and warm summer weather.

Along the two profiles, CO₂ and O₂ values showed important variations depending on the type of soil, and a strong negative correlation between the two gases suggesting a biological origin of these variations. Methane was never detected during this campaign. Helium data show a positive correlation with CO₂ in most measuring stations, but still remain mostly within ± 0.2 ppm of the concentration in the atmosphere. On the first profile, a small positive anomaly was observed in three to four stations located above one of the main outcropping fractures. On the second profile, a large anomaly of small amplitude (about 0.2 ppm) was observed at the beginning of July just a few meters east of the main branch of the St-Blaise fault. However, this anomaly was not observed after a second sampling three weeks later. Between the two sampling trips the soil moisture had dramatically decreased, from near saturated to dry and cracked. The possible explanation of this discrepancy is the trapping of deep sourced He under the humid clay-rich soil, and its release after some weeks of dry weather.

The use of soil gases for the detection of permeable faults in geothermal exploration is well established in some geological settings. At the Jura mountain foothills, this study shows that more measurements are needed to better understand, and account for, variations due to meteorological conditions.

REFERENCES

- Baubron, J. C., Rigo, A., & Toutain, J.-P. 2002: Soil gas profiles as a tool to characterize active tectonic areas: the Jaut Pass example (Pyrenees, France). *Earth and Planetary Science Letters*, 196, 69–81.
- Hinkle, M.E. 1994: Environmental conditions affecting concentrations of He, CO₂, O₂ and N₂ in soil gases. *Applied Geochemistry*, 9, 53–63.

P 2.22

Cross-correlation and location error assessment of nano-earthquakes on the Fribourg Lineament - Switzerland

Abednego Martinus¹, Vouillamoz Naomi^{1,2}, Deichmann Nicolas², Husen Stephan², Wust-Bloch Hillel Gilles³, Mosar Jon¹

¹ University of Fribourg, Departement of Geosciences, Earth Sciences, Chemin du Musée 6, CH-1700 Fribourg, Switzerland
(martinus.abednego@unifr.ch, naomi.vouillamoz@unifr.ch, jon.mosar@unifr.ch.)

² Schweiz. Erdbebendienst (SED), Sonneggstrasse 5, CH-8092 Zürich, Switzerland

³ Tel Aviv University, Department of Geophysics and Planetary Sciences, P.O.B. 39040, Tel Aviv, 69978, Israel

As part of two joint PhD projects, we study the low-magnitude seismicity in the Fribourg area (Switzerland) with special focus on the Fribourg Lineament (KASTRUP et al., 2007) (Figure 1). Since the beginning of 2010, the Fribourg Lineament has been monitored by two seismic navigating systems (SNS), consisting each of one central 3D sensor surrounded by three 1D sensors in a tripartite array of about 100 m radius (JOSWIG, 2008). The two SNS complement recordings of the three permanent stations of the Swiss Seismological Service (SED) in the area (SCOU, STAF and TORNY in Figure 1).

Event detection is done daily with SonoView (GeophysSuite software – nano.geophys.uni-stuttgart.de) for the two SNS and the three SED stations. Sonoview displays seismic traces in form of sonograms which are spectrograms based on power spectral density (PSD) matrix, noise adapted, muted and prewhitened (SICK, 2012). Special features of sonograms allow extraction and recognition of earthquake signals near to 0 dB SNR by visual pattern recognition. Detected events are then located using HypoLine, a software especially suited for SNS records but applicable to all kinds of networks. Event location in HypoLine is done interactively in a sense that every onset change induces immediate simulation updates in the affected parameter space. This conveniently takes into account geological knowledge of the area in the manifold of possible location choices (JOSWIG, 2008). Depending on data quality and solution consistency, a location quality factor is assigned to each event. Densification of the seismic network in the Fribourg area together with event detection on SonoView permitted to lower the detection threshold relative to that of the Earthquake Catalog of Switzerland (ECOS) by one order of magnitude on the Fribourg Lineament, and thus multiplied by about a factor of ten the earthquakes detected on the Lineament after 2010. However, a large part of the detected events with local magnitude lower than 1-1.5 were recorded only by a few stations and/or SNS (sometimes only by one). Accurate location of such events remains a difficult task. Moreover, signal to noise ratios can be very low, rendering phase picking and hence the location more imprecise.

Signal cross-correlation has shown that most of the recorded earthquakes detected only by one station and/or SNS show good correlation ($cc > 0.7$) with other well-located higher magnitude events. Several families of events have been identified in this manner on the Lineament. In order to corroborate location solutions of master events obtained with HypoLine, the location software (NonLinLoc) and 3-D velocity model routinely employed by SED are used for event relocations (with same phase picking data). NonLinLoc gives hypocenter solutions in the form of a probability density function that holds information on X, Y, Z hypocenter uncertainties (LOMAX et al., 2009). First results show that HypoLine locations are consistent with NonLinLoc solutions (HypoLine location are situated in NonLinLoc X,Y,Z error bars of the respective event). Quantitative errors on location need now to be determined with more accuracy by defining phase picking error consistently (DIEHL et al., 2009) and the influence of the station distribution relative to the Lineament must be evaluated (LOMAX et al, 2009).

REFERENCES

- Joswig, M., 2008. Nanoseismic monitoring fills the gap between microseismic networks and passive seismic, *First Break*, 26, 2008.
- Kastrup, U., Deichmann, N., Fröhlich, A., Giardini, D., 2007. Evidence for an active fault below the northwestern Alpine foreland of Switzerland, *Geophys. J. Int.* (2007) 169, 1273-1288.
- Mosar, J. et al., 2011. Du Jura central aux Préalpes romandes – Une tectonique active dans l'avant-pays des Alpes, *Géochroniques* n°117, Mars 2011, p.52-55.
- Sick, B., 2012. NanoseismicSuite manual; <http://www.nanoseismic.net> last consulted on 23.08.2012.
- Diehl, T., Kissling, E., Husen, S and Aldersons, F., 2012. Consistent phase picking for regional tomography models: application to the greater Alpine region, *Geophys. J. Int.*, 2009, 176, 542-554.
- Lomax, A., A. Michelini, A. Curtis, 2009. Earthquake Location, Direct, Global-Search Methods, Complexity In *Encyclopedia of Complexity and System Science*, Part 5, Springer, New York, pp. 2449-2473.

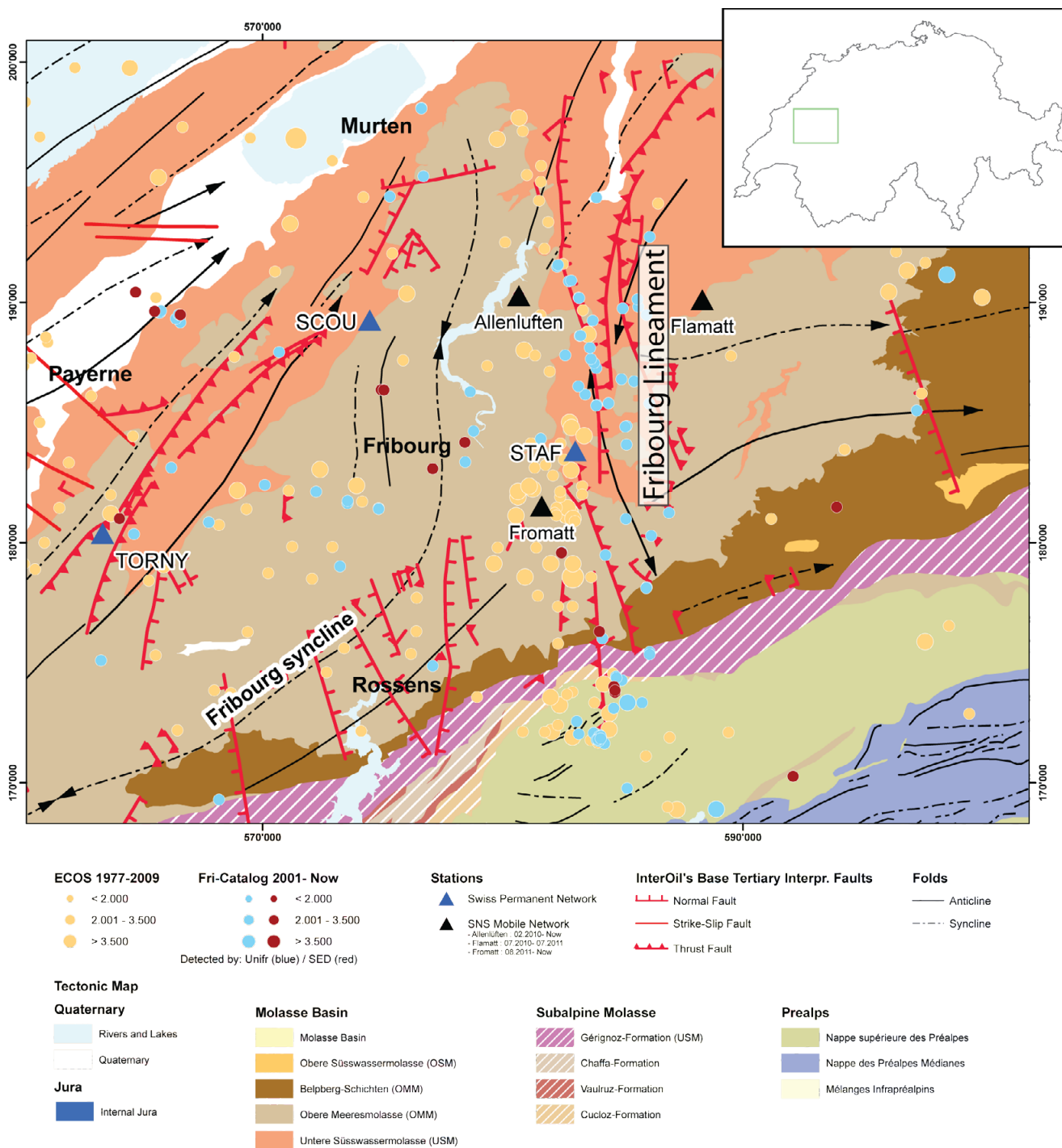


Figure 1: Tectonic Map of the Fribourg Zone showing location of detected earthquakes

P 2.23

The application of titanium-in-quartz geothermometry in recrystallized quartz - a methodological discussion

Peters Max¹, Weber Christian²

¹Institute of Geological Sciences, University of Bern, Baltzerstrasse 1+3, CH-3012 Bern (max.peters@geo.unibe.ch)

²Clay and Interface Mineralogy, RWTH Aachen University, Bunsenstrasse 8, D-52072 Aachen (christian.weber@cim.rwth-aachen.de)

In rocks deformed under intermediate-grade metamorphic conditions, the precise determination of deformation temperatures (and pressures) becomes particularly challenging due to the absence of neocrystallized phases in the case of quartz mylonites. The characterization of distinctive deformation processes in rock-forming minerals, such as the three dislocation creep regimes for dynamically recrystallized Qtz, only yields qualitative temperature estimates, for instance. In contrast, direct temperature measurements based on geothermometry promise more accurate temperature estimations. Recently, the titanium-in-quartz geothermometer (TitaniQ) was applied to dynamically recrystallized Qtz (Kohn & Northrup, 2009) and exercised in various studies.

In this study, TitaniQ measurements were performed in dynamically recrystallized Qtz from (i) weakly deformed host rocks and (ii) monomineralic Qtz veins in granitic or mylonitic rocks of the Aar massif (Swiss external massif). Ti concentrations measured by means of laser-ablation ICP-MS reveal low Ti concentrations in dynamically recrystallized Qtz (sub- $\mu\text{g/g}$ to $\mu\text{g/g}$ -range).

(i) The TitaniQ temperatures of weakly deformed and mylonitic samples show a temperature range between ca. 160°C to 585°C. This range in temperatures indicates leaching of Ti, caused by pervasive fluid activity, which has modified igneous Ti concentrations, but did not lead to Ti re-equilibration in Qtz during subgrain rotation recrystallization.

(ii) In contrast, synkinematically recrystallized Qtz (SGR) veins in weakly deformed host rocks reveal temperatures between around 450°C and 350°C in ultramylonites. High-temperature recrystallized veins are interpreted as veins that initially formed during the cooling of the pluton, which later recrystallized under peak-greenschist metamorphic conditions (450°C). Samples from ultramylonitic shear zones indicate latest stage strain localization in ductile shear zones at lower temperatures at around 350°C in the Aar massif. Both recrystallized vein generations indicate synkinematic reequilibration of Ti from pervasively penetrating (Ti-oversaturated) fluids during subgrain rotation recrystallization, which lead to a readjustment of the Ti concentrations.

Furthermore, a comparison of three different available TitaniQ calibrations (Wark & Watson, 2006; Thomas et al., 2011; Huang & Audétat, 2012) was performed by student's t-tests. The limitations of TitaniQ calculations in a rutile-absent system were taken into consideration by consistently propagating the error on the activity of Ti in Qtz as $a(\text{TiO}_2)=0.8\pm 0.2$ (Ghent & Stout, 1984; Kohn & Northrup, 2009).

The two-tailed t-test distributions indicate that TitaniQ calculations gained by the calibrations of Wark & Watson (2006) and Huang & Audétat (2012) do not significantly differ (within the 2s confidence interval). Moreover, TitaniQ temperatures calculated by the calibration of Thomas et al. (2011) significantly differ from the above-mentioned calibrations, which apparently result in lower temperatures. Temperatures obtained by the Thomas et al. (2011) calibration are not in line with the microstructural record, emphasizing the importance of good constraints on the pressure conditions during deformation and the activity of Ti in Qtz in rutile-absent rocks.

REFERENCES

- Ghent, E.D. & Stout, M.Z. 1984: TiO_2 activity in metamorphosed pelitic and basic rocks, principles and applications to metamorphism in southeastern Canadian Cordillera. *Contributions to Mineralogy and Petrology*, 86, 248-255.
- Huang, R. & Audétat 2012: The titanium-in-quartz (TitaniQ) thermobarometer: A critical examination and re-calibration. *Geochimica et Cosmochimica Acta* 84, 75-89.
- Kohn, M.J. and Northrup, C.J. 2009: Taking mylonites' temperatures. *Geology*, 37, 47-50.
- Thomas, J.B., Watson, E.B., Spear, F.S., Shemella, Nayak, S.K. & Lanzirotti, A. 2010: TitaniQ under pressure: the effect of pressure and temperature on the solubility of Ti in quartz. *Contributions to Mineralogy and Petrology*, 160, 743-759.
- Wark, D.A. & Watson, E.B. 2006: Titanium-in-quartz geothermometer. *Contributions to Mineralogy and Petrology*, 152, 745-754.

P 2.24

Role of brittle deformation and fluid-rock interactions on the formation of ductile shear zones under blueschist facies metamorphic conditions: example in the Roffna metarhyolite (Suretta nappe, eastern central Alps).

Poilvet Jean-Charles¹, Goncalves Philippe¹, Olliot Emilien² & Marquer Didier¹

¹ UMR CNRS 6249 Chrono-Environnement, Université de Franche-Comté, 16 route de Gray 25030 Besançon Cedex, France

² UMR CNRS 7516 Institut de Physique du Globe de Strasbourg, 1 rue Blessig, 67084 Strasbourg Cedex, France

Although ductile shear zones are known to be preferential pathways for fluid and therefore the loci of metamorphic and metasomatic reactions, the impact of fluid-rock interactions on shear zone formation is still poorly understood. The formation of shear zones in a homogeneous granitic host-rock may be subdivided into two distinct stages; (1) nucleation on a new or pre-existing brittle structure and (2) lateral widening during ductile deformation (e.g. Mancktelow & Pennacchioni, 2005). The aim of this study is to describe and identify the consequence of fluid-rock interactions in both stages.

The studied shear zones are located in the Roffna metarhyolite from the Suretta nappe (Penninic domain, eastern central Alps). This early Permian massif intruded a Variscan basement at ca 268 Ma (Marquer et al., 1998) and was affected by Alpine tectonics under blueschist facies conditions (450 °C, 1 GPa) at ca 45 Ma (Challandes et al., 2003). The ductile deformation is characterized by a network of precursor brittle fractures and shear zones from millimetric to plurimetric scale. The symmetrical development of angular micrometric quartz crystals without any crystallographic preferred <c> axes orientations to either side of the shear fracture is interpreted as a cataclastic flow. Epidote, biotite and phengite nucleate in the intracrystalline porosity of the cataclastic quartz layer. The mineralogical assemblage and the highly substituted white micas (Si = 3.6 cations p.f.u.) suggest that the initiation of this shear zone occurred during a stage of brittle deformation (shear fracture and cataclastic flow) already under blueschist facies conditions. High resolution X-ray mapping of the brittle precursor indicates that the brittle deformation is accompanied with a gain of MgO and a total loss of Na₂O.

With increasing strain, the discrete zone broadens and new quartz grains become plastically deformed simultaneously with crystallization of metamorphic epidote, biotite and phengite at the expense of magmatic K-feldspar and plagioclase. More developed strain gradient, from centimeter to meter scale, shows the same large mass transfers that consists of MgO gains (up to 500%) and complete leaching of Na₂O.

It appears that fluid-rock interactions (chemical mass transfer and metamorphic reactions) are identical from the nucleation stage to the widening stage of the shear zone, which is consistent with the development of the shear (initial fracturing and ductile widening) at the same P-T-fluid conditions (i.e. blueschist facies conditions). This isobaric/isothermal coeval development of brittle and ductile structures challenges the temperature-dependent concept of brittle-ductile transition. We also suggest that the widening of the shear zone is driven and controlled by the kinetics of the equilibration of the metastable host-rock at the P-T-fluid conditions of the deformation. Using a suite of PT and chemical potential computed phase diagrams, we are able to model the reaction path involved during the equilibration process from the host rock to the highest strained zone.

REFERENCES

- Challandes N., Marquer D. & Villa I.M. (2003) Dating the evolution of C-S microstructures: a combined ³⁹Ar-⁴⁰Ar step-heating and UV laserprobe analysis of the Alpine Roffna shear zone. *Chemical Geology* 197,1-4, 3-19.
- Mancktelow N.S. & Pennacchioni G. (2005) The control of precursor brittle fracture and fluid-rock interaction on the development of single and paired ductile shear zones. *Journal of Structural Geology* 27, 4, 645-661.
- Marquer D., Challandes N. & Schaltegger U. (1998) Early Permian magmatism in Briançonnais terranes: the Truzzo granite and Roffna rhyolite (Eastern Penninic nappes, Swiss and Italian Alps). *Schweiz. Mineral. Petrogr. Mitt.* 78, 397-415.

P 2.25

Transient Temperature and Pressure variations in crustal shear zones – numerical modelling using local-thermodynamic equilibrium and a conservative approach

Evangelos Moulas¹, Yuri Podladchikov², Johannes Vrijmoed², Lucie Tajcmanova¹, Nina Simon³ and Jean-Pierre Burg¹

¹Department of Earth Sciences, ETH-Zurich, Sonneggstrasse 05, CH-8092 Zurich, Switzerland (evangelos.moulas@erdw.ethz.ch)

²Faculty of Geosciences and Environment, University of Lausanne, CH-1015 Lausanne, Switzerland

³Department of Environmental Technology, Institute for Energy Technology, 2027 Kjeller, Norway

Crustal shear zones can accumulate considerable displacements, therefore the mechanical energy released in shear zones is an important factor that contributes to significant and transient perturbations of the temperature and the pressure (P-T) fields. The P-T estimates from metamorphic phase equilibria is the main source of information available on the conditions of the middle and lower crust. Interpretations of these estimates commonly assume spatial homogeneity and steady-state conditions.

Direct numerical simulations assuming only local-thermodynamic equilibrium are free of the aforementioned assumptions. More specifically, we develop a non-Boussinesq (compressible) approach, to be used for the investigation of geodynamic scenarios, assuming local thermodynamic equilibrium, conservation of mass, energy and momentum. This allows the investigation of problems where density changes are important without violating the conservation of mass. In addition, our approach considers the conservation of total energy of which, mechanical energy is an important contributor. In this formulation, shear heating follows as a natural consequence of the conservation of energy rather being an additional fitting parameter.

P 2.26

Chemical zoning and ductility of natural garnet at lower crustal conditions: An example from the Rhodope Massif

Evangelos Moulas¹, Jean-Pierre Burg¹, Dimitrios Kostopoulos² & Filippo Schenker¹

¹Department of Earth Sciences, ETH-Zurich, Sonneggstrasse 05, CH-8092 Zurich (evangelos.moulas@erdw.ethz.ch)

²Department of Geology and Geoenvironment, University of Athens, Panepistimioupoli Zographou, GR-15784 Athens

The Kesebir-Kardamos gneiss dome in the Rhodope Massif (northern Greece – southern Bulgaria) is a late orogenic extensional structure that deformed an Alpine, synmetamorphic nappe complex containing high-pressure (HP) metamorphic rocks. Microdiamond inclusions in garnet of quartzofeldspathic rocks from one of the thrust sheets suggests equilibration at ultrahigh-pressure metamorphic conditions ($P > 2.5$ GPa). This study aims at delimiting the P-T conditions of the metamorphic evolution experienced by these rocks.

Garnets (10-15% vol, pyrope: 15% grossular:10% almandine:65%) from the aforementioned quartzofeldspathic rocks are chemically zoned. Biotite and kyanite are other major phases of the rock paragenesis. Garnet-biotite-plagioclase-quartz geobarometry and garnet-biotite geothermometry confine the recorded peak conditions at ca 1.0 ± 0.1 GPa and 690 ± 50 °C in the stability field of kyanite. The consistency of these results with the metamorphic overprint of HP-metapelites from central Rhodope indicates that the low-pressure (1GPa) metamorphic overprinting event has a regional significance. The lensoid shapes of the chemically zoned garnet crystals place recrystallisation of this mineral phase before the extensional evolution of the Kesebir-Kardamos gneiss dome. Furthermore, the shapes of garnet grains indicate that the ductile deformation of natural garnet crystals is not restricted to ultrahigh-temperature conditions.

P 2.27

Fission-track constraints on the thermal evolution of the Serbo-Macedonian Massif (south Serbia, southwest Bulgaria and east Macedonia)

Antić Milorad¹, Kounov Alexandre¹, Trivić Branislav², Peytcheva Irena³, von Quadt Albrecht⁴ & Gerdjikov Ianko⁵

¹ *Geologisch-Paläontologisches Institut, Universität Basel, 4056 Basel, Switzerland. (m.antic@unibas.ch)*

² *Faculty of Mining and Geology, University of Belgrade, 11000 Belgrade, Serbia*

³ *Geological Institute, Bulgarian Academy of Sciences, 1113 Sofia, Bulgaria*

⁴ *Institute of Geochemistry and Petrology, ETH-Zürich, 8092 Zürich, Switzerland*

⁵ *Faculty of Geology and Geography, St. Kl. Ohridski University of Sofia, 1504 Sofia, Bulgaria*

Serbo-Macedonian massif (SMM) is a crystalline terrane situated between the two diverging branches of the Eastern Mediterranean Alpine orogenic system, the northeast-vergent Carpatho-Balkanides and the southwest-vergent Dinarides and the Hellenides. It is outcropping from the Pannonian basin to the Aegean Sea in central and southeastern Serbia, southwestern Bulgaria, eastern Macedonia and central Greece. It's affiliation to European or African plate basement is still questionable due to the lack of reliable geochronological dating and detailed structural investigation along its boundaries. The massif is also a key area to understand the bipolarity of the Alpine orogenic system, as well as the interaction of the Pannonian and Aegean back-arc extension during the Cenozoic time.

SMM is generally considered to be comprised of an Upper (low-grade) and a Lower (medium to high-grade) complex (Dimitrijević 1959). The protoliths of both units are reported as volcano-sedimentary successions, which have later been intruded by magmatic rocks during several pulses.

We have applied fission-track analysis on both, apatites and zircons from the rocks of the SMM in order to reveal its low-temperature evolution. Two distinct phases of cooling have been discerned in the study area. The region west of Južna Morava river experienced relatively fast cooling through zircon and apatite closure temperatures (300° - 60°C) during the late Cretaceous (100 - 67 Ma). This event is interpreted as a post-orogenic collapse following the regional nappe-stacking event ("Austrian" phase). In the rest of the study area, same late Cretaceous cooling was recorded by the zircon data, whereas the apatite suggests a heating event at temperatures higher than 120°C (but lower than 200°C) prior to the late Eocene (43 - 32 Ma) extension and post-magmatic cooling. Within the Crnook dome however, both zircon and apatite fission-track data reveal a late Eocene (45 - 33 Ma) cooling event related to the extension and the exhumation of the dome itself. For the first time the Crnook dome was recognised as continuation of the Osogovo-Lisets extensional complex in Serbia.

REFERENCES

Dimitrijević, M. D. 1959: Osnovne karakteristike stuba Srpsko-makedonske mase. (Basic characteristics of the column of the Serbo-Macedonian Mass). First symposium of the SGD, Abstracts.

P 2.28

The Eastern Pelagonian metamorphic core complex: insight from the $^{40}\text{Ar}/^{39}\text{Ar}$ dating of white micas

Schenker Filippo Luca¹, Forster Marnie² & Burg Jean-Pierre¹

¹ ETHZ, Department of Earth Sciences, Sonneggstrasse 5, CH-8092 Zürich
(filippo.schenker@erdw.ethz.ch)

² Research School of Earth Sciences, The Australian National University, Mills Road, Acton, Canberra, ACT 0200, Australia

The Pelagonian Zone in continental Greece constitutes a pre-alpine gneissic block trending approximately NNW-SSE between two domains with oceanic affinity: the Pindos in the west and the Vardar zone in the east. In the eastern Pelagonian zone we recognized a denuded metamorphic dome extending about 20 x 15 km with the long axis trending NNW-SSE. The main lithologies (gneiss, marbles and amphibolites) display a shallow-dipping foliation whose up-arch defines the structural dome. The metamorphic conditions decrease from upper-amphibolite in the core to greenschist metamorphic conditions in the flanks of the dome. Aligned micas and amphiboles and elongated quartz and feldspar grains define a prominent lineation trending SW-NE. Asymmetric structures in the XZ plane of finite strain record two regional senses of shear: (i) everywhere, top-to-the-SW sense of shear (direction: $252^\circ \pm 30$; plunge: $8^\circ \pm 25$) is associated with strain gradients from protomylonite to ultramylonite and recumbent, isoclinal and occasional sheath folds; (ii) top-to-the-E sense of shear (direction: $88^\circ \pm 24$; plunge: $11^\circ \pm 12$) is localized into narrow (0.1 to 100 m), low-angle shear zones on the eastern flanks of sub-domes.

The $^{40}\text{Ar}/^{39}\text{Ar}$ step-heating dating technique has been applied to micas from orthogneisses sampled from the core to the flanks of the dome. The micas have been separated with acoustical shockwaves produced in the SELFRAG apparatus, with the advantage to liberate morphologically intact grains. The liberated grains were sieved at different grain-sizes (between 100 and 300 μm) according to the microstructures recognized in thin-sections. Results show "plateau"-ages at ca. 100-120 Ma, 80 Ma and 50 Ma. The 100-160 μm fraction of white micas in mylonitic orthogneisses yielded slightly younger ages than the 160-300 μm fraction. This difference sets the discussion between neo-crystallization age of the smaller grain fraction and cooling age with multiple diffusion domains of the larger fraction. The latter hypothesis is tested with modeling of Ar-diffusion along Pressure-Temperature-time histories using the MacArgon program. These new ages are consistent with ages published on the southern Pelagonian, demonstrating major tectonic and metamorphic activity during early Cretaceous and Eocene times.

P 2.29

Inversion tectonique d'une zone de relais extensive adjacente à un diapir salifère: terminaison orientale du Dj. Chambi (Atlas central tunisien).

Ladeb M.F. ^{1,2}, Zargouni F.²

¹ Department of the Earth Science, Faculty of Sciences of Sfax, ladebmf@gmail.com

² Department of Geology, Faculty of Sciences of Tunis, fouadzargouni@yahoo.fr

Actuellement, dans les travaux de terrain, de sismique réflexion ou encore expérimentaux l'inversion tectonique d'un relais de failles normales à un relais transpressif demeure peu documentée. Ce processus au quelle peut être associé une tectonique salifère est mis en évidence à partir des données de terrain de la terminaison E du Chambi (Tunisie centrale). Ainsi à l'Aptien, cette terminaison apparait comme une zone de relais en extension correspondant à une rampe de relais de direction ENE-WSW affectée par deux structures monoclinales de même direction et à vergence S. Cette rampe de relais est limitée par deux failles de transfert (NW-SE) : faille de la laverie E et W dont la dernière relie la faille de Kasserine à celle du Chambi (faille normale probable à vergence N). Au droit de cette dernière (partie haute de la rampe) se développe un diapir salifère asymétrique. L'inversion de cette zone de relais extensive en zone de relais transpressive lors de l'orogène alpin (fin crétacé-oligocène), s'effectue par la concentration de la déformation au niveau de ce diapir qui facilite la formation des failles en short cut et favorise la propagation de la déformation sur la rampe de relais au niveau de la quelle se développe une mégastructure en fleur positive d'inversion. Cette dernière est associée aux décrochevauchements en short-cut et des rétrochevauchements qui s'incurvent ensemble vers la surface dans la couverture.

P 2.30

$^{40}\text{Ar}/^{39}\text{Ar}$ dating of Alpine shear zones in the Mont Blanc area

Egli Daniel¹, Mancktelow Neil¹ & Spikings Richard²

¹ Geologisches Institut, ETH-Zürich, Sonneggstrasse 5, CH-8092 Zürich (daniel.egli@erdw.ethz.ch)

² Département de Minéralogie, Université de Genève, Rue de Maraîchère 13, CH-1205 Genève

Timing of deformation in the Mont Blanc area is crucial for the understanding of its structural evolution, especially with regard to its recent exhumation and the tectonic evolution of this area, where the major bend of the western occurs. Ductile deformation in the Mont Blanc region lasted from Oligocene to Upper Miocene, resulting in the development of the Helvetic nappe stack, with the Mont Blanc massif (MB) forming the core of its lowermost structural unit, the Morcles nappe. The general NW-directed kinematics interacts with dextral transcurrent movements along the Rhône-Simplon fault, which finds its continuation both in the Chamonix valley and the Val Ferret on the internal side of MB. Shearing along the nappe contacts (e.g. Diablerets thrust, Morcles thrust) lasted over a timespan of ~15 Ma and is supposed to end in mid-Miocene times (Kirschner et al., 1996), possibly related to increased influence of movements on the Rhône-Simplon fault. However, ongoing NW-SE compression as well as dextral transcurrent movements promoted localized shearing on either side of the massif. This study presents $^{40}\text{Ar}/^{39}\text{Ar}$ age data of white micas from shear zones in key areas of the Mont Blanc region. The sampled shear zones are low-grade mylonites and phyllonites and the ages obtained are interpreted to reflect neocrystallization of synkinematically grown minerals. In the Mont Chétif basement slice on the eastern side of Mont Blanc, dextral + E-side up oblique-slip to transcurrent movements dominate, with a tendency toward a stronger strike-slip component with time. The youngest sample from the Mont Chétif yields an Upper Miocene age, suggesting that subsequent folding that overprints the shear zone must have taken place after 9.5 Ma. Samples from the eastern margin of the Aiguilles Rouges massif (AR) in the Chamonix zone indicate top-NW directed shear around 20 Ma and subsequent uplift of AR relative to MB at ~15 Ma subsequent to shear along the Morcles thrust. This suggests a NW-migration of the deformation zone and possible tectonic extrusion of AR after ~16 Ma. One age spectrum from Col de la Seigne of 28-35 Ma fits well with Oligocene activity along the Penninic Front. A NW-verging shear zone between the MB granite and MB paragneiss, close to Champex-Lac and coinciding with the Faille du Midi, yields ages between 15-20 Ma. The age results are used to provide time constraints on a model for the structural and temporal evolution of the Mont Blanc area in Neogene times.

REFERENCES

Kirschner, D. L., Cosca, M. A., Masson, H. & Hunziker, J. C. 1996: Staircase $^{40}\text{Ar}/^{39}\text{Ar}$ spectra of fine-grained white mica: Timing and duration of deformation and empirical constraints on argon diffusion, *Geology*, 24(8), 747-750.

P 2.31

Structural and $^{40}\text{Ar}/^{39}\text{Ar}$ geochronological data from different mylonite belts along the Canavese Fault

Pleuger Jan¹, Mancktelow Neil¹ & Spikings Richard²

¹ Geologisches Institut, ETH Zürich, Sonneggstrasse 5, CH-8092 Zürich (jan.pleuger@erdw.ethz.ch)

² Département de Minéralogie, University of Geneva, Rue de Maraîchère 13, CH-1205 Genève

The Canavese Fault (CF), i.e. the Insubric Fault west of Lago Maggiore, accounts for the uplift of the relatively high-grade Penninic Alps with respect to the Southern Alps and a poorly constrained amount of dextral displacement.

Between Lago Maggiore and Valle d'Ossola, the CF comprises two several hundred metres thick, partly overlapping greenschist-facies mylonite belts. N(W)-side-up mylonites (Belt 1) are developed mostly within the Sesia Zone (SZ) immediately N(W) of the CF. Dextral mylonites, locally with a considerable S(E)-side-up component (Belt 2), are developed mostly within the Southern Alpine rocks (see also Schmid et al. 1987). The foliation of Belt 1 is the axial planar foliation S_{n+1} of generally NW-vergent F_{n+1} folds which overprint the "pre-Insubric" foliation S_n . In moderately sheared domains, F_{n+1} folds are open and L_{n+1} is a generally subhorizontal intersection lineation of S_{n+1} and S_n parallel to F_{n+1} axes. In highly sheared domains, F_{n+1} folds are tight to nearly isoclinal with axes parallel to the steeply plunging stretching lineation L_{n+1} . Close to the boundary between the SZ and the Southern Alps, the Belt 1 mylonites are locally refolded by F_{n+2} folds. F_{n+2} folds developed during shearing and ongoing mylonitisation of Belt 2.

Belt 2 can be traced toward the W until Valle Strona where it finally ends in a brittle fault. Belt 1 also becomes thinner toward the W, being restricted in Valle Mastallone to a few hundred metres of the SZ. Outside Belt 1, the shear sense in the SZ is SE-side-up. $^{40}\text{Ar}/^{39}\text{Ar}$ data obtained from recrystallised white mica from these SE-side-up mylonites (UTM32 5084144/436441) yield a weighted plateau age of 37.45 ± 0.61 Ma which we interpret as the time of the mylonitisation. These mylonites are thus considerably older than shearing in Belt 1 which started at ca. 32 Ma. $^{40}\text{Ar}/^{39}\text{Ar}$ weighted plateau ages of 34.07 ± 0.43 Ma and 33.70 ± 0.59 Ma obtained from pseudotachylyte samples (5084356/437405 and 5084360/437415) collected immediately S of the protolith boundary in the Ivrea Zone (IZ) probably date brittle faulting at the onset of the N(W)-side-up shearing.

A second belt of dextral plus SE-side-up mylonites (Belt 3) parallels the CF inside the IZ in Valle Sermenza and Valle Sesia. In a section along the Dolca river, the same shear sense is observed in augengneiss mylonites occurring between the SZ and basic rocks of the IZ. The mylonites are crosscut by post-kinematic andesitic dykes which were probably emplaced coevally with the ca. 30-33-Ma-old Biella and Miagliano Plutons (Kapferer et al. 2012; Carraro & Ferrara 1968). Therefore, Belt 3 is older than Belt 2. The SZ rocks are affected by a lower greenschist-facies ductile to brittle belt with a NW-side-up plus sinistral displacement sense (Belt 4). South of Dolca river, Belt 4 is covered by ca. 33-Ma-old (Kapferer et al. 2012) andesitic volcanites. These volcanites often contain xenoliths derived from the SZ and rest on top of Sesia-derived conglomerates which in turn were deposited onto the SZ basement. In most places, the succession from the SZ basement into the volcanites is not faulted. A largely brittle fault accommodated the relative uplift of the IZ with respect to the volcanites. In Valle Sessera, this fault is represented by kakirites and a fault breccia containing mylonite fragments. $^{40}\text{Ar}/^{39}\text{Ar}$ on white mica from such a fragment (5057936/427188) gave a weighted plateau age of 53.82 ± 0.78 Ma.

South of Valle Sessera, shear zones observed along the protolith boundary between the SZ and the Southern Alps are commonly only a few metres thick and subordinate to fault breccia. Since the displacement sense of these shear zones is variable and the CF is poorly exposed, the observed structures cannot be integrated into a regional pattern.

From the Serra d'Ivrea towards south, the CF splits into two branches, the Internal (ICF) and External Canavese Faults (ECF), which frame the Canavese Zone to the (S)E and (N)W, respectively. The ECF is dominated by brittle fault rocks and only rheologically weak rocks such as serpentinite and calcschist were mylonitised. From a W-side-up calcschist mylonite (5030790/397670), we obtained a $^{40}\text{Ar}/^{39}\text{Ar}$ white mica weighted plateau age of 28.93 ± 1.50 Ma. The displacement senses of low-grade mylonites at the ICF are mostly dextral plus E-side-up and thus in line with a relative uplift of the IZ postdating the emplacement of the Miagliano Pluton further north.

The distribution and timing of the mylonite belts observed along the CF show that coherent N(W)-side-up (Belt 1) and dextral (Belt 2) mylonite belts of Oligocene age are only present between Lago Maggiore and Valle Sesia. Therefore, large amounts of dextral "Insubric", i.e. Oligocene, displacement in the order of 100 km or more (e.g. Schmid & Kissling 2000) cannot have been accommodated along the CF itself. Either there was a transfer of dextral shearing into the Penninic nappe stack (e.g. Handy et al. 2005) or a smaller amount of dextral displacement must be assumed.

REFERENCES

- Carraro, F. & Ferrara, G. 1968: Alpine "Tonalite" at Miagliano, Biella (Zona Diorito-kinzigitica) A preliminary note. *Schweiz. Mineral. Petrogr. Mitt.* 48, 75-80.
- Handy, M.R., Babist, J., Wagner, R., Rosenberg, C.L. & Konrad, M. 2005: Decoupling and its relation to strain partitioning in continental lithosphere - insight from the Periadriatic Fault system (European Alps). In: *Deformation mechanisms, rheology and tectonics: From minerals to the lithosphere* (Ed. by Gapais, D., Brun, J.P. & Cobbold, P.R.). *Geol. Soc. London Spec. Publ.* 243, 249–276.
- Kapferer, N., Mercolli, I., Berger, A., Ovtcharova, M. & Fügenschuh, B. 2009: Dating emplacement and evolution of the orogenic magmatism in the internal Western Alps: 2. The Biella Volcanic Suite. *Swiss J. Geosci.* 105, 67-85.
- Schmid S. M. & Kissling, E. 2000: The arc of the western Alps in the light of geophysical data on deep crustal structure. *Tectonics* 19, 62-85.
- Schmid, S.M., Aebli, H.R., Heller, F. & Zingg, A. 1989: The role of the Periadriatic Line in the tectonic evolution of the Alps. In: *Alpine Tectonics* (Ed. by Coward, M. P., Dietrich, D. & Park, R.G.). *Geol. Soc. London Spec. Publ.* 45, 153-171.
- Schmid, S.M., Zingg, A. & Handy, M. 1987: The kinematics of movements along the Insubric line and the emplacement of the Ivrea Zone. *Tectonophysics* 135, 47-66.

P 2.32

Basement lithostratigraphy of the Adula nappe: implications for alpine kinematics

Mattia Cavargna-Sani, Jean-Luc Epard, François Bussy & Alex Ulianov¹

¹ Institut des sciences de la Terre, Université de Lausanne, 1015 Lausanne (mattia.cavargna@unil.ch)

The Adula nappe is the uppermost Alpine basement nappe of the Lower Penninic nappe stack in the Lepontine Dome. The basement consists of strongly folded and sheared gneisses of various types; a minor amount of rocks from the cover series is also present. Based on detailed field investigations, U-Pb zircon geochronology and geochemical analysis, we propose a new lithostratigraphic sequence of the northern Adula nappe basement:

- Cambrian clastic metasediments with abundant carbonate lenses and minor manifestations of bimodal magmatism;
- Cambro-Ordovician metapelites with amphibolite boudins containing abundant eclogite relicts and representing oceanic metabasalts;
- Ordovician metagranites of a peraluminous calc-alkaline affinity related to a continental collision scenario;
- Ordovician metamorphic volcano-sedimentary deposits;
- Lower Permian post-collisional granites recording the Alpine deformation and metamorphism only.

The Adula basement, composed of pre-variscan polyorogenic rocks and post-Variscan intrusions, represents a complete Palaeozoic geodynamic cycle from Cambrian to Permian, also recognized in other Alpine basements. The Alpine cover shows also a coherent and uniform Triassic sedimentary series (Galster et al. 2012). This coherency proves that the Adula nappe was a single entity before the Tertiary collision and was not an accretion of different units related to subduction. This entity was already moulded before the Alpine collision. However, the Adula nappe was not subducted and exhumed as a huge block, the strong internal deformation suggests that the whole nappe operated as a major deformation plane during the Alpine nappe stack emplacement.

REFERENCES

Galster, F., M. Cavargna-Sani, J. L. Epard, and H. Masson, 2012, New stratigraphic data from the Lower Penninic between the Adula nappe and the Gotthard massif and consequences for the tectonics and the paleogeography of the Central Alps. Tectonophysics. Available online 15 June 2012.

P 2.33

Distribution and inferred ages of exfoliation joints in the Aar Granite (Central Alps, Switzerland)

Ziegler Martin¹, Loew Simon¹, Moore Jeffrey R.¹

¹Geological Institute, ETH Zurich, Sonneggstrasse 5, CH-8092 Zurich (martin.ziegler@erdw.ethz.ch)

Exfoliation joints are well-known natural fractures limited to the near ground surface. Relatively few details, however, are known about their distribution and age in the Swiss Alps. Exfoliation joints follow the landscape surface at the time of their formation. The age of the landscape then provides a minimum age of exfoliation joint formation. While landscape forms can change through time, exfoliation joints may preserve elements of former landscape morphologies by their undisturbed orientations.

The Grimsel region of the Central Swiss Alps is well-suited for analyzing the impact of erosional episodes, and accompanying stress changes, on exfoliation joint formation. Our study area exhibits some of the most well-developed exfoliation joints in granitic rocks in Europe, as well as numerous glacial and fluvial landscape features of different age. In situ and remote mapping above and below ground revealed that exfoliation joints are widespread, and occur over an elevation range of more than 1.5 km within different geomorphological settings: inner and hanging trough valleys, gently-inclined linear slopes above the trough valleys, inner valley gorges, steep V-shaped side gullies, glacial cirques and steep mountain crests. Upper valley slopes are thought to mimic a former landscape surface that developed predominantly by fluvial erosion prior to the glacial incision of the trough valley (Ivy-Ochs 1996). The prominent U-shaped cross-profile of the upper Hasli valley is likely to have been established during the Middle Pleistocene after intensified glacial activity in MIS 22 (0.87 Ma) (e.g. Muttoni et al. 2007; Haeuselmann et al. 2007). Prominent cirques and hanging valleys likely formed during the same period. Glacial erosion during the LGM (Last Glacial Maximum) is thought to be relatively minor, not decisively changing the overall shape of the main valley (e.g. Florineth 1998).

Three exfoliation joint types have been distinguished in the study area: joints oriented distinctly parallel to the present-day ground surface (type C), joints that are nearly parallel ($< 10^\circ$ difference in orientation with respect to the today's ground surface) (type B), and joints that are not parallel (type A). These types may represent different generations. Joint orientation, curvature, and spacing indicate that the bulk of mapped type A joints along slopes of the inner U-shaped valley, hanging valleys, and V-shaped gullies most likely belong to one generation. This exfoliation generation reveals areas that likely experienced considerable glacial incision after joint formation. We suggest that these type A joints formed prior to or during an early stage of Middle Pleistocene trough valley erosion. Type B joints, which (nearly) parallel the present-day landscape, are interpreted to have a minimum age dating to about the LGM. Less widespread type C joints occur almost exclusively within the extent of Late Glacial ice margins and are most likely of LGM or post-LGM age.

REFERENCES

- Florineth, D. 1998: Geometry of the Last Glacial Maximum (LGM) in the Swiss Alps and its paleoclimatological significance, Dissertation, 128 pp., Bern.
- Haeuselmann, P., Granger, D. E., Jeannin, P.-Y. & Lauritzen, S.-E. 2007: Abrupt glacial valley incision at 0.8 Ma dated from cave deposits in Switzerland, *Geology* 35: 143-146.
- Ivy-Ochs, S. 1996: The dating of rock surfaces using in situ produced ^{10}Be , ^{26}Al and ^{36}Cl , with examples from Antarctica and the Swiss Alps, Dissertation, 196 pp., Zürich.
- Muttoni, G., Ravazzi, C., Breda, M., Pini, R., Laj, C., Kissel, C., Mazaud, A. & Garzanti, E. 2007: Magnetostratigraphic dating of an intensification of glacial activity in the southern Italian Alps during Marine Isotope Stage 22, *Quaternary Research* 67, 161-173.

P 2.34

Seismic properties and anisotropy in melt-generating metapelites

Almqvist Bjarne S. G.¹, Misra Santanu¹¹ ETH Zurich, Institute of Geological Sciences, Sonneggstrasse 5, CH-8092 Zurich
(bjarne.almqvist@erdw.ethz.ch; santanu.misra@erdw.ethz.ch)

Small amounts of melt have a profound influence on mechanical properties and deformation of rocks. However, the understanding of processes by which melt generates and distribute in rocks remains incomplete. We present new experimental findings that track the compaction, partial melting and neo-crystallization of minerals in parent rocks representative of mid-crustal conditions. The samples used consist of a mixture of quartz and muscovite powders, each mineral phase in equal volume proportion. These powders were consolidated to synthetic rocks in two steps, 1) by cold uniaxial compaction (200 MPa differential stress) followed by 2) hot isostatic compaction (580° C, 160 MPa confining pressure). Three specimens were drilled from the synthetic rock, parallel, perpendicular and at 45° to the compaction axis. The initial porosity in the specimens ranged from 24 - 26 %, and initial microstructural images indicated an overall uniform microstructural arrangement (Figure 1a). After specimen preparation we used a Paterson gas-medium apparatus, equipped for ultrasonic wave measurements, in order to observe the dynamic compaction and melting. Static peak experimental conditions were kept at 300 MPa confining pressure and 750 °C for six hours, with measurements of the ultrasonic velocity at regular intervals (Figure 1e). From these measurements we infer that the rock initially becomes elastically stiffer with significant accompanying acoustic anisotropy. This hardening is followed by elastic softening, marking the onset of dehydration melting and formation of semi-connected melt lenses (i.e., Figure 1b). In addition to lowering the overall acoustic velocity (i.e., the mean velocity of the three specimens investigated), the elastic wave anisotropy is significantly reduced and approaches isotropy, because of preferential melting of the highly anisotropic muscovite. The initial microstructural anisotropy of the sample dictates compaction and the geometrical distribution of generated melt. Upon cooling, after six hours at peak experimental conditions, crystallization of new phases and notable development of a foliation are evident, (Figure 1c, d). Crystallization of new minerals, including potassium feldspar, biotite, spinel and sillimanite is accompanied with the re-introduction of strong acoustic anisotropy. Although no active deformation was imposed at peak experimental conditions, the results provide useful insight on the seismic properties and anisotropy in weakly deforming rocks, at the onset of melting and with small volumes of melt. Our results imply that regions in the Earth's crust where dehydration melting takes place, consuming the most anisotropic minerals such as muscovite, biotite and amphibole, may effectively become seismically less anisotropic than regions where these minerals remain intact, or where crystallization of new phases has taken place.

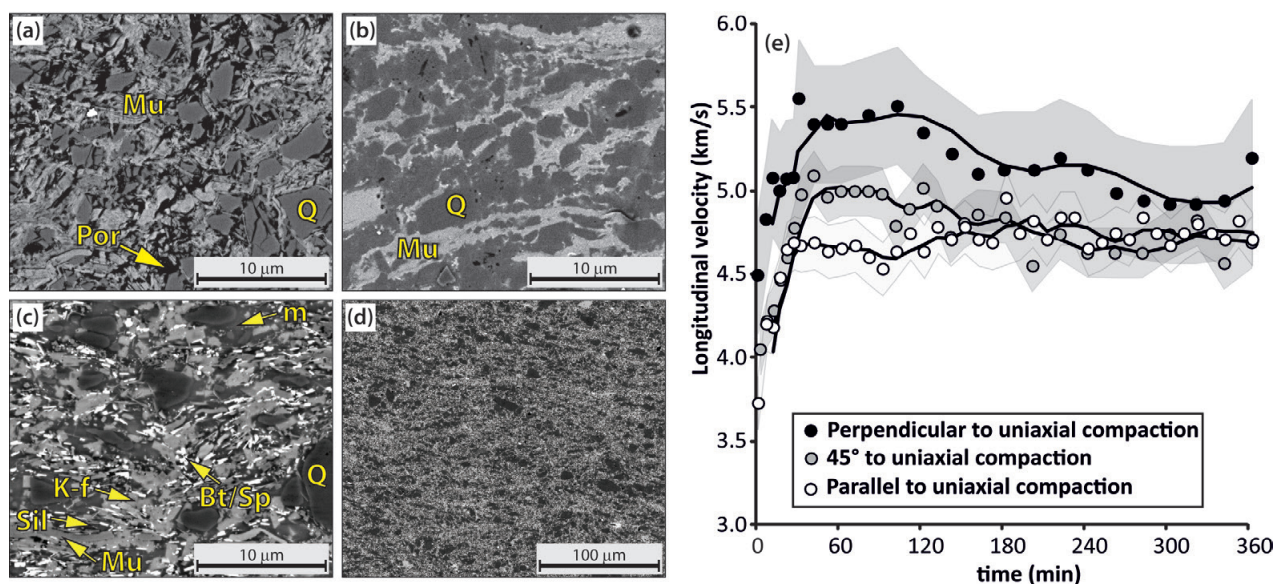


Figure 1. Scanning Electron Microscopy images (BSE mode) illustrating the sequence of compaction, melting and crystallization discussed in this article; (a) starting material of quartz (Q, dark grey) and muscovite (Mu, light gray) with pores (Por, black). Muscovite defines a foliation; (b) compacted sample after ca. 1 hour at 750 °C and 300 MPa. Pores have collapsed; (c) after 6 hours melt (m) and new crystals of k-feldspar (K-f), biotite (Bt), spinel (Sp) and sillimanite (Sil) along with quartz (Q) and muscovite (Mu) as restites; (d) a low magnification image of same stage of figure (c) showing that the pseudo-foliation, in terms of both mechanical and compositional anisotropy, of the initial sample is retained. The composition, and thus the density, of the sample changed due to chemical reaction at 750 °C; (e) Longitudinal wave velocity, measured at 0.1 MHz, as a function of experimental duration (shown in minutes), for three specimen orientations. The line represents the fit of a 3-point running average, to the velocity data points. The shaded area surrounding the three sets of data points represents the uncertainty in velocity, resulting from the error in picking first arrival of the ultrasonic wave.

P 2.35

AlpArray – the next generation seismology initiative

György Hetényi¹, Edi Kissling², Stephan Husen¹, John Clinton¹ & the AlpArray Working Group³

¹Swiss Seismological Service (SED), ETH Zürich, Sonneggstrasse 5, CH-8092 Zürich (gyorgy.hetenyi@sed.ethz.ch)

²Institute of Geophysics, Department of Earth Sciences, Sonneggstrasse 5, CH-8092 Zürich

³www.seismo.ethz.ch/alparray

AlpArray is a new initiative to study the greater Alpine area with a large-scale broadband seismological network. The interested parties (currently 57 institutes in 16 countries) plan to combine their existing infrastructures into an all-out transnational effort that includes data acquisition, processing, imaging and interpretation. The experiment will encompass the greater Alpine area from the Black Forest and the Bohemian Massif in the north to the Northern Apennines in the south and from the Pannonian Basin in the east to the French Massif Central in the west. We aim to cover this region with a high-quality broadband seismometer backbone by combining the ca. 220 existing permanent stations with additional 300-340 instruments from mobile pools, all of them to be deployed between August 2014 and August 2016. In this way, we plan to achieve homogeneous and high resolution coverage (ca. 40 km average station spacing). Furthermore, we also plan to deploy a few densely spaced targeted networks along swaths across – and in regions of – key parts of the Alpine chain on shorter time scales. These efforts on land will be combined with deployments of ca. 40-45 ocean bottom seismometers in the Mediterranean Sea. We also aim to implement the best practice for synchronizing mobile pool operation procedures and data handling: common data centre and data management procedure, free access to data to participants as soon as possible through EIDA. Data will be open to the public 3 years after the experiment ends.

The main scientific goal of AlpArray is to investigate the structure and evolution of the lithosphere beneath the Alps. A primary target is the geometry and configuration of subducting slabs and their polarity switch beneath the arc. Numerous regional questions such as seismic hazard will be tackled. Targets will be imaged at several depths (e.g., from near-surface structure down to upper mantle anisotropy), scales (e.g., from local seismicity to mantle transition zone thickness variations), using different methodologies in the sub-regions of interest. An overview of these targets and the methodologies intended to be applied in connection with the seismological measurements will be presented. The geodynamic interpretation of the acquired data will be complemented by other Earth Science disciplines such as state-of-the-art numerical and analogue modelling, gravity and magneto-telluric measurements, as well as structural geology. In conclusion, we hope to turn the strong community interest into a truly interdisciplinary and collaborative project in the key region for seismotectonic activity and dynamics of Europe.

At this poster we welcome anybody who is interested to hear more on the project, who would like share their experience with similar large-scale field experiment(s), and/or who has scientific, practical or funding advice, especially in connection to Switzerland.

P 2.36

Deformation of flat areas by using InSAR. Application to the Geneva (CH) and la Faute-sur-mer (FR) areas

Nicolas Houlié

ETG GGL

InSAR is today commonly used to map the surface deformation induced by volcanic or seismic events. However, small deformation detected (less than a fringe) over soft or “changing” areas (ice, sand, rockfalls) is still challenging. Such limitations are due to difficulties in during modeling InSAR phase over complex surface textures. Also, troposphere phase delays affecting accuracy of the surface topography change between two seasons or vegetation coverage that affect coherence of every scene are the most known of these issues. Additionally, flat topography challenges also the correlation between scenes. We explore the potential use of InSAR to two areas where the topography is smooth or quasi-flat: Geneva and La Faute-sur-mer. We show in both cases, that InSAR studies can be completed.

